A
MAJOR PROJECT

ON

Elasto-plastic Load-Settlement Analysis of a Strip Footing

Submitted in partial fulfillment
of the requirement for award of the degree of

Master of engineering
In
Civil engineering
(**Structural Engineering**)

Submitted By
MANISH KUMAR JHA
(Roll No. 3208)

Under the guidance of

Dr. A.K. GUPTA
Assistant Professor
Department of Civil & Environmental Engineering
Delhi College of Engineering

Department of civil & environmental engineering
Delhi College of engineering
University of Delhi
2007

DECLARATION

I here by declare that the work which is embodied in this major project entitled **'Elasto-Plastic Load-Settlement Analysis of a Strip Footing'** is an authentic record of my own work carried out in partial fulfillment of the requirements for the award of Master of Civil Engineering (Structural Engineering) under the guidance of Dr. A.K. Gupta, Asst. Professor, Delhi College of Engineering, New Delhi. The matter embodied in this dissertation has not been submitted for the award of any other degree or diploma.

MANISH KUMAR JHA

Roll No: 3208

University of Delhi

Date:

Place: New Delhi

This is certified that above statement made by the student is correct to the best of my knowledge.

Dr. A.K. GUPTA

Asst. Professor

Department of Civil Engineering

Delhi College of Engineering

New Delhi – 110042

Date:

Place: New Delhi

ACKNOWLEDGEMENT

I wish to express my deep sense of gratitude to my erudite project guide **Dr. A.K. Gupta** Assistant Professor, Department of Civil Engineering, Delhi College of Engineering, New Delhi. I owe his overwhelming debt for helping me plan the content of this project and discussing important points of this project. His ideas, stimulating comments, interpretations and suggestions increased my cognitive awareness and helped considerably in the fruitation of my objective. I remain obliged to him for his help and able guidance through all stages of this project. His constant inspiration and encouragement of our effort shall always be acknowledged. His observation and comments were highly enlightening.

I would like to acknowledge Prof. S.K. Singh, Head, department of Civil Engineering for his encouragement through out the work. Without books and references completing any academic work is not possible, I would like thank Mr. R. K. Shukla Librarian Delhi College of Engineering and Mr. N. Kulkarni, In-charge computer centre, Delhi College of Engineering for giving facility to use library and access internet.

I would like to acknowledge all the faculty member of civil engineering department for their suggestion. In the end I would like to thank all my friends who constantly helped me to completion the work.

Manish Kumar Jha
M.E. II
Structural Engineering
Delhi College of Engineering
New Delhi - 110042

ABSTRACT

For any type of structure a foundation is required and hence soil-structure interaction is an inevitable problem, which has to be tackled. Most often for the analysis, as well as design purpose the linear soil-structure interaction is employed. But it is far away from reality. The actual situation seldom provides such as easy problem.

In the present, work, the soil structure interaction has been studied taking the nonlinear behavior of soil. For this purpose, the Von Mises yield criteria has been employed. The foundation taken for the study is a footing of width (B=2.0 m) resting on the surface of clay in an undrained state subjected to centrally inclined loading. The finite element problem has been taken as a plane strain problem.

The iteration for load settlement has been performed by a program written using MATLAB.

The shallow foundation may be subjected to eccentric inclined load. For designing and proportioning such type of foundations, the main criteria to be considered are bearing capacity, settlement, tilt and horizontal displacement.

Since soil behavior is usually nonlinear, the nonlinear constitutive laws are commonly employed. For this, the material parameters depend upon the state of stress. To encounter this, an incremental approach is often used, which requires a separate solution process for each increment of load.

In the present investigation, analysis and study of the behavior of strip footing, resting on the surface of uniform clay in an undrained state subjected to centrally-inclined load with the finite element analysis has been carried out by using incremental theory of plasticity. The yield criteria which is employed is Von Mises Criteria.

Pressure versus vertical settlement curves for strip footing (B=2.0 m), resting on various type of clays have been obtained for values of load inclination **i** = 0^0, 10^0, 20^0, 30^0. All the pressure-settlement characteristics display an initial linear elastic behavior followed by inelastic behavior till failure during which large settlements occur for every successive pressure increment. It has been found that ultimate bearing capacity is significant in the high consistency range of clay.

Similar to the pressure vertical settlement characteristics, the change of average, horizontal displacement is less at low- pressure but as the pressure increases and approaches the failure, the horizontal displacements increases rapidly. It can be seen also that as the inclination of load increases, the horizontal displacements at the failure also increase.

The bearing capacity factor, N_c value, decreases with the increase of load inclination. The N_c values from finite element analysis have been compared with experimental results of Agrawal (1986), and these values are somewhat on the higher side for **i** $>10^0$, and on the lower side when **i** $<10^0$.

CONTENTS

5. CONCLUSIONS

LIST OF FIGURES

LIST OF TABLES

CHAPTER-1
INTRODUCTION

1.1 GENERAL

Shallow foundation is a common type of substructure provided to support the structure constructed above the ground. The foundation may be subjected to eccentric-inclined load, e.g. in the case of the foundation of retaining walls, abutments, columns, stanchions, portal framed buildings etc. For designing and proportioning such foundation, the main criteria to be considered are bearing capacity, settlement, tilt and horizontal displacement.

Deformation behavior of soil is influenced by a number of factors, such as physical structure, porosity, density, stress history, loading characteristics, existence and movement of fluid in pores, and time-dependence of soil skeleton and the pore fluid. These factors render the stress deformation behavior of soil highly complex and nonlinear. No available analytical solution can handle them all. Numerical methods, such as finite element method have proved successful in approximating the effects of many of these factors.

Since soil behavior is usually nonlinear the nonlinear constitutive laws are commonly employed. For this, the material parameters depend upon the state of stress. To encounter this, an incremental approaches often used, which requires a separate solution process for each increment of load.

In the analysis of footing subjected to centrally inclined load in clay soil, several theories presented, model and field tests have been conducted and published. The bearing capacity, load settlement characteristics, non-dimensional factors for bearing capacity have also been produced and published by earlier investigators.

This work tries to analyze and study the behavior of strip footing, resting on the surface of uniform clay in an undrained state. The strip footing –soil system is subjected to centrally –inclined load. Finite element analysis has been carried out by using incremental theory of plasticity. The yield criteria which is employed is Von Mises criteria.

1.2 SOIL-STRUCTURE INTERACTION IN SHALLOW FOUNDATIONS

The term soil-structure interaction usually refers to the mechanics of interaction and interdependence forces between soil-foundation treated as a system and the superstructure as another system. However, when one attempts to study the behavior of the foundation in relation to soil, study of mechanics of interaction and interdependence of forces between the two components, namely soil and the foundation which acts as a structure has to be considered.

The behavior of any foundation in relation to that soil depends upon whether the interface between the two is rough orb smooth. In case the contact is rough, then there is no relative slip between the two and the shear strength at the interface is not overcome. However, if the contact surface is smooth or partially smooth, then there occurs relative slip between any points of the soil mass.

1.3 PROBLEM IDENTIFICATION

In the present work, it is proposed to study:

(i) The pressure settlement characteristics of strip footings under centrally applied inclined loading. This has been attempted on basis of elasto-plastic finite element analysis.

(ii) The elasto-plastic finite element analysis of strip footing to predict the ultimate bearing capacity.

(iii) The elasto-plastic finite element analysis to obtain the value of cohesive bearing capacity factor, $N_{c.}$

1.4 ORGANIZATION OF THESIS

Available pertinent literature on the subject related to this thesis has been reviewed and discussed in chapter 2.This includes the following aspects:

(i) Bearing capacity of footing on sand and for the centrally vertical and inclined loading.

(ii) Pressure settlement characteristics of footings on sand and clay for the centrally vertical and inclined loading.

Chapter 3 deals with the theoretical part and assumptions used in the elasto-plastic finite element analysis of soil. This includes the following aspects:

(i) Yield criteria for soils

(ii) Plastic flow rule

(iii) Elasto-plastic stress-strain matrix

(iv) Elasto-plastic stiffness matrix

(v) Nonlinear solution strategy

(vi) Convergence criterion

(vii) The elasto-plastic finite element analysis software.

The interpretation and discussions of results have been presented in Chapter 4.The thesis has been concluded in chapter 5.All the references, figures have been given at the end of the thesis.

CHAPTER - 2
REVIEW OF LITERATURE

2.1 GENERAL

In this chapter, a brief review of literature pertaining to the behavior of the footing under inclined load is presented. First, some theory and results obtained from model tests and analytical solution for computing bearing capacity of soil under central vertical and inclined load has been discussed, and then the work related to pressure settlement characteristics of footing under central vertical and inclined loads on sand and clay soil has been presented.

2.2 ULTIMATE BEARING CAPACITY

Prandtl (1920) made use of mathematical theory of plasticity in analyzing the plastic failure of metals due to punching. A special case of his solution is applicable to foundations. Prandtl was mainly concerned with the penetration of punches into metals where the movement of the punches was guide. A basic assumption in his solution is that a loaded footing of width B and great length L will sink vertically downward into the underlying material, thereby producing shear failure on both sides of the footing. Further, it was assumed that the base of footing was smooth and the soil is homogeneous, isotropic and weightless.

According to Prandtl's theory, the bearing pressure q_u on the surface is transmitted through the soil wedge and the plastic zone according to Pascal's law in all the directions. His expression for ultimate bearing capacity for clays is as follows:

$$q_u = (\pi + 2)\, c = 5.14\, c \quad \text{---------- (2.1)}$$

where,

q_u = ultimate bearing capacity of clay at the surface.

c = cohesion of soil

Terzaghi (1943) extended Prandtl's theory for c-φ soil for shallow foundations ($D \leq B$) considering base of the footing as rough. Two propounded case of failure were:

(a) General shear failure, when clay is stiff, and

(b) Local shear failure, when clay is soft.

Further, shear strength of soil above the base of the footing was neglected. However, the surcharge has been taken as γD_f. the following equation were proposed:

(a) General Shear Failure:

(i) For strip footing, $q_{nd} = 5.7\ c$ ----------(2.2)

(ii) For circular and square footing $q_{nd} = 7.4\ c$ ---------- (2.3)

(iii) For rectangular footing $q_{nd} = 5.7\ c\ (1 + 0.3\ B/L)$ ----------(2.4)

(b) Local Shear Failure.

(i) for strip footing, $q_{nd} = 3.8\ c$ ---------- (2.5)

(ii) for circular and square footing $q_{nd} = 4.94\ c$ ----------(2.6)

(iii) for rectangular footing $q_{nd} = 3.8\ c\ (1+ 0.3\ B/L)$ ----(2.7)

where,

q_{nd} = net ultimate bearing capacity.

Meyerhof's (1951), further extended the Prandtl's theory and considered the shear strength of the soil above base of the footing as well. It was claimed that his theory was valid for shallow as well as deep foundations. The theoretical results are summarized as follows:

(a) Strip footing

$q_{nd} = c\ N_{cq}$ ---------- (2.8)

Where,

$N_{cq} = 5.14$, for a surface footing.

$= 8.28$, for a smooth shaft and deep footing.

$= 8.85$, for a rough shaft and deep footing.

(b) Circular footing

$q_{nd} = c\ N_{cqr}$ ---------- (2.9)

Where,

N_{cqr} = 6.18, for a surface footing.

= 9.34, for a deep and smooth footing.

= 9.74, for a deep and rough footing.

(c) Square footing

$$q_{nd} = c\, N_{cqs} \quad \text{---------- (2.10)}$$

As stated by Meyerhof (1953) there is no theoretical solution is available for square footing but there is hardly any difference between square and circular footings. Therefore, the bearing capacity factor, N_{cqs} of a square footing can be taken equal to that of circular footing (N_{cqr}).

Saran (1971), developed analytical solution for the bearing capacity of strip footings subjected to oblique loads. The results were presented in the form of bearing capacity factors charts, N_c, N_q, and N_γ, and which depend on the angle of internal friction (φ) and local inclination. (Fig. 2.1, 2.2, 2.3)

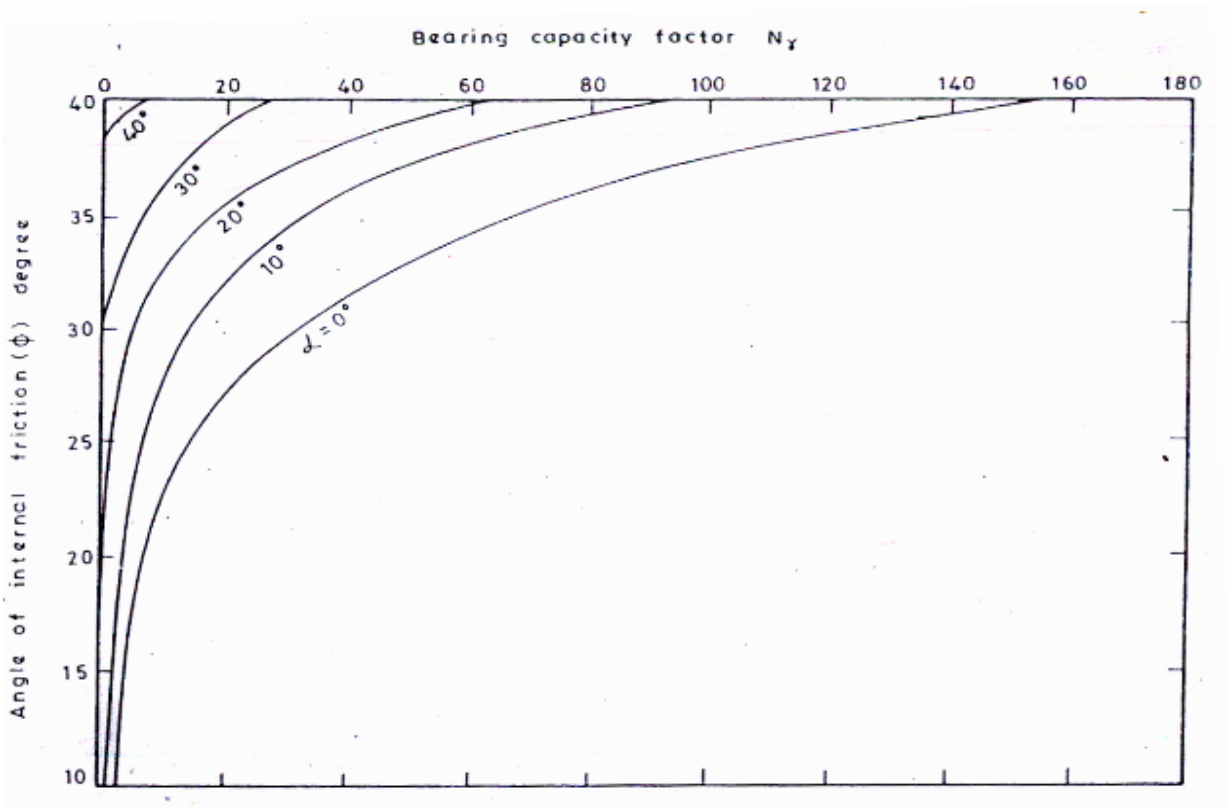

Figure 2.1, N_γ Vs Φ (Saran, 1971)

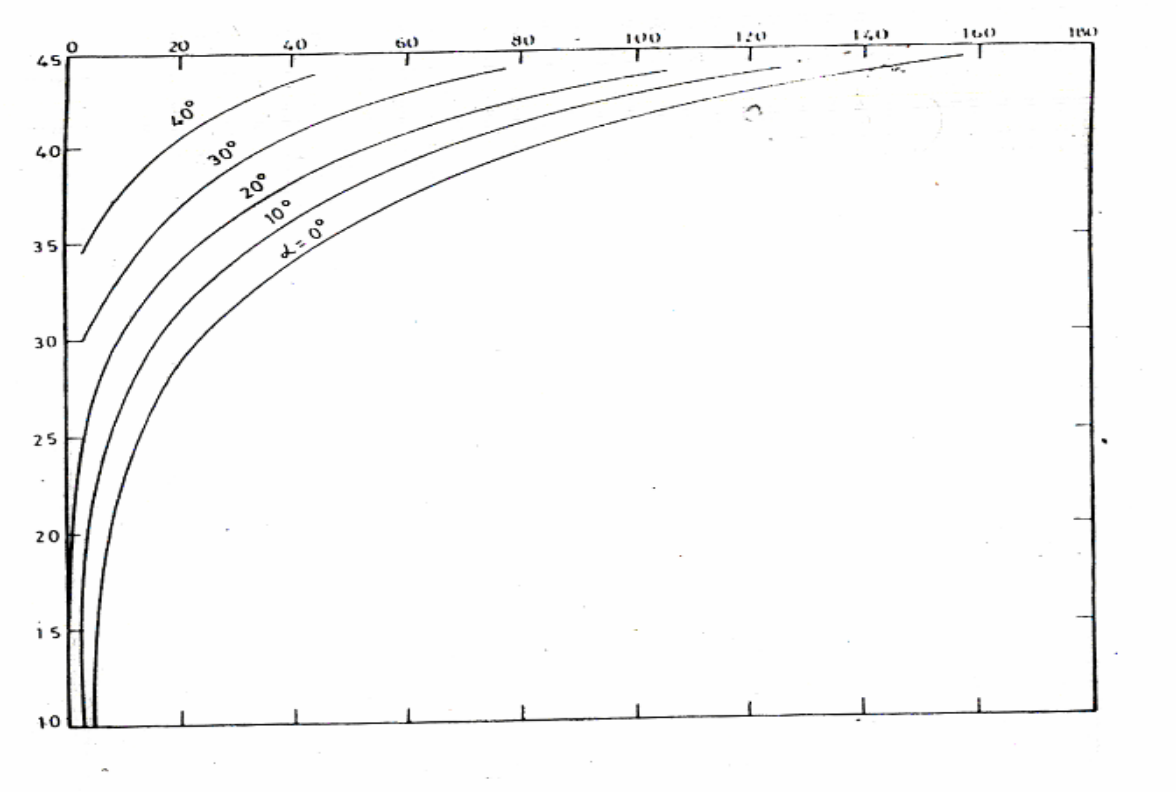

Figure 2.2, N_b Vs Φ (Saran, 1971)

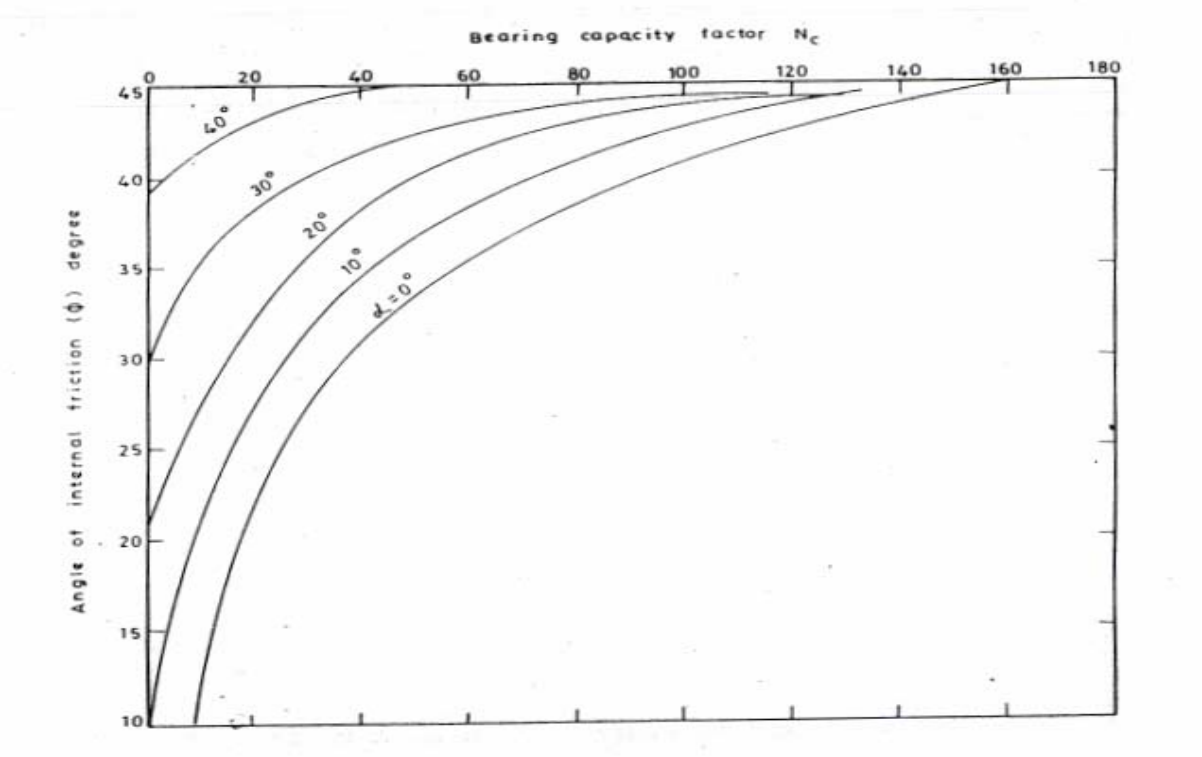

Figure 2.3, N_c Vs Φ (Saran, 1971)

Saran (1971), Prakash and Saran (1971) studied the problem of bearing capacity of eccentrically loaded footings. The results were presented in the form of non- linear factors N_c, N_q, and $N\gamma$, which depend on the angle of internal friction φ and e/B ratio, where e = eccentricity of load and B = width of footing. (Fig 2.4, 2.5, 2.6)

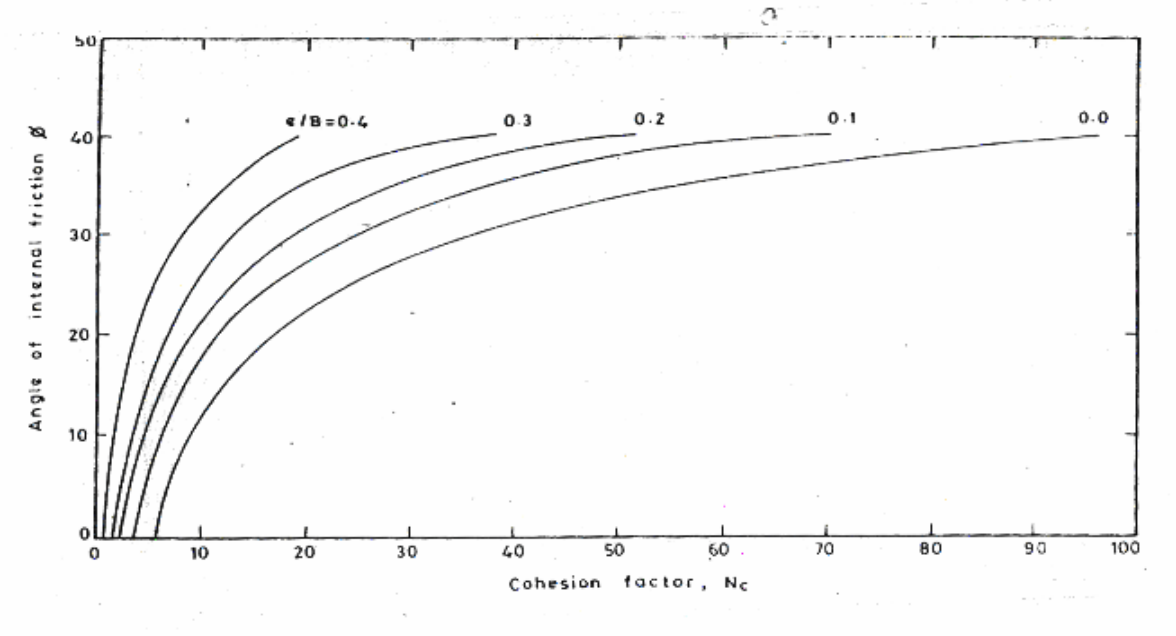

Figure 2.4, N_c Vs Φ for Different Value of e/B (Prakasn & Saran, 1971)

Further, Agrawal (1986) has conducted the model tests for the eccentric-inclined footing. The results have also been verified by analytical solution using nonlinear constitutive laws. The bearing capacity factors were presented in the form of non-dimensional charts factor N_c, N_q, and N_γ, which depend on the angle of internal friction φ and e/B ratio. (Fig. 2.7, 2.8. 2.9)

Some empirical relations have also been suggested by various investigators to obtain the ultimate bearing capacity of footings subjected to central-inclined load, eccentric vertical load and eccentric inclined load.

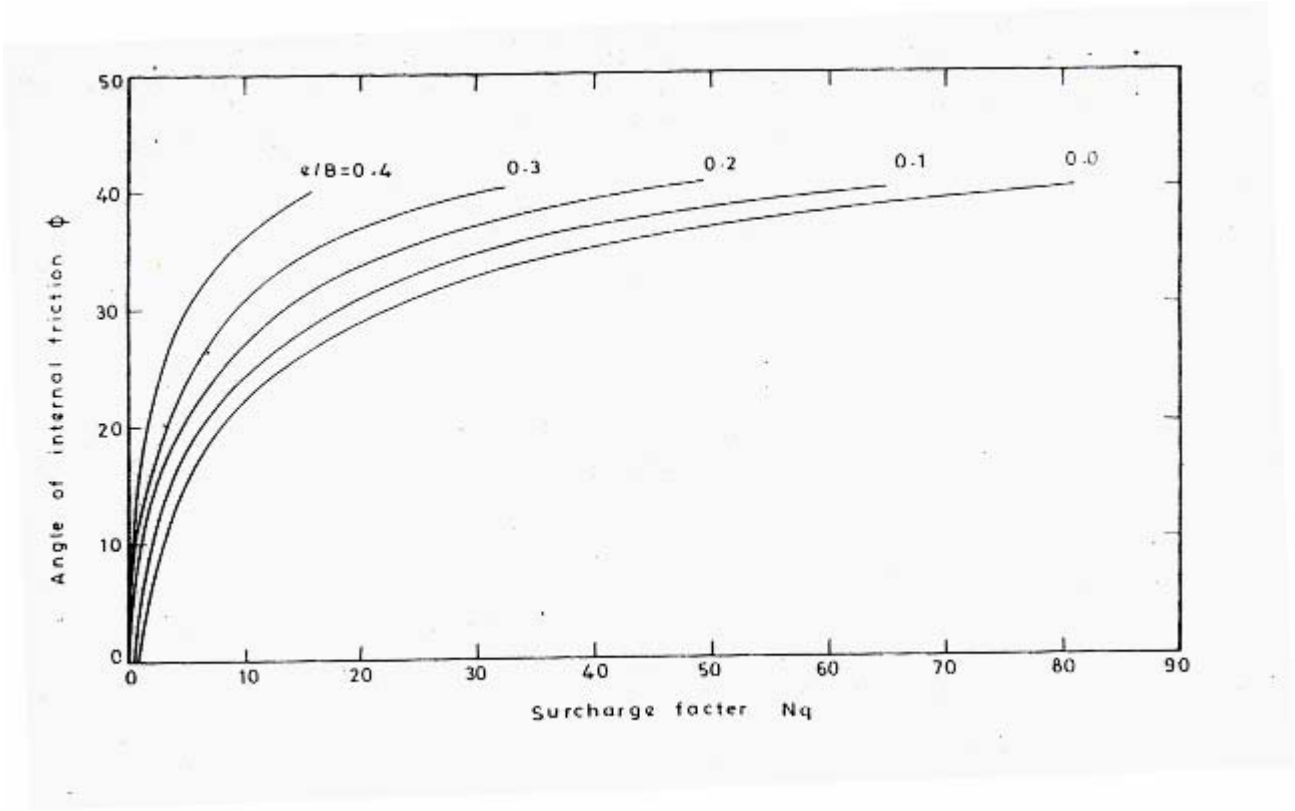

Figure 2.5, N_q vs Φ for Different Value of e/B (Prakasn & Saran, 1971)

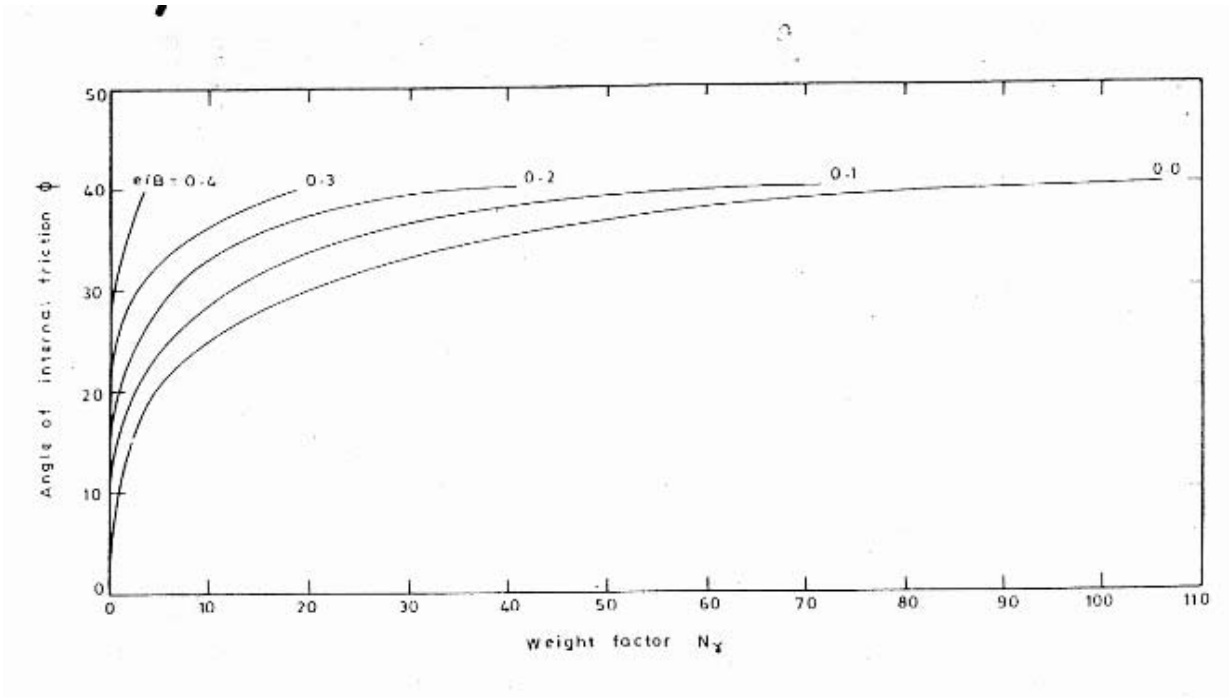

Figure 2.6, N_γ vs Φ for Different Value of e/B (Prakasn & Saran, 1971)

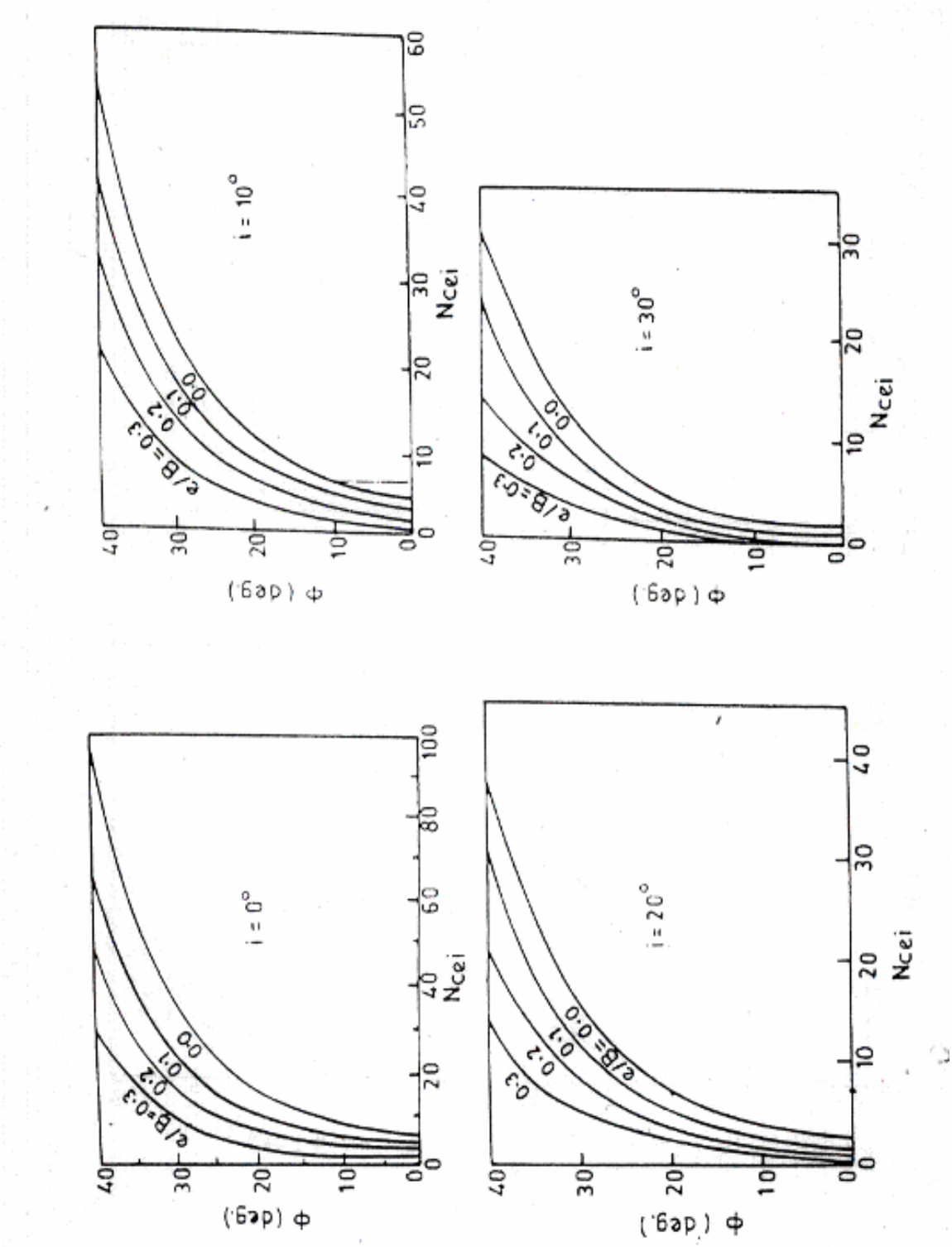

Figure 2.7, N_{cei} vs Φ for different value of e/B (Saran & Agrawal, 1986)

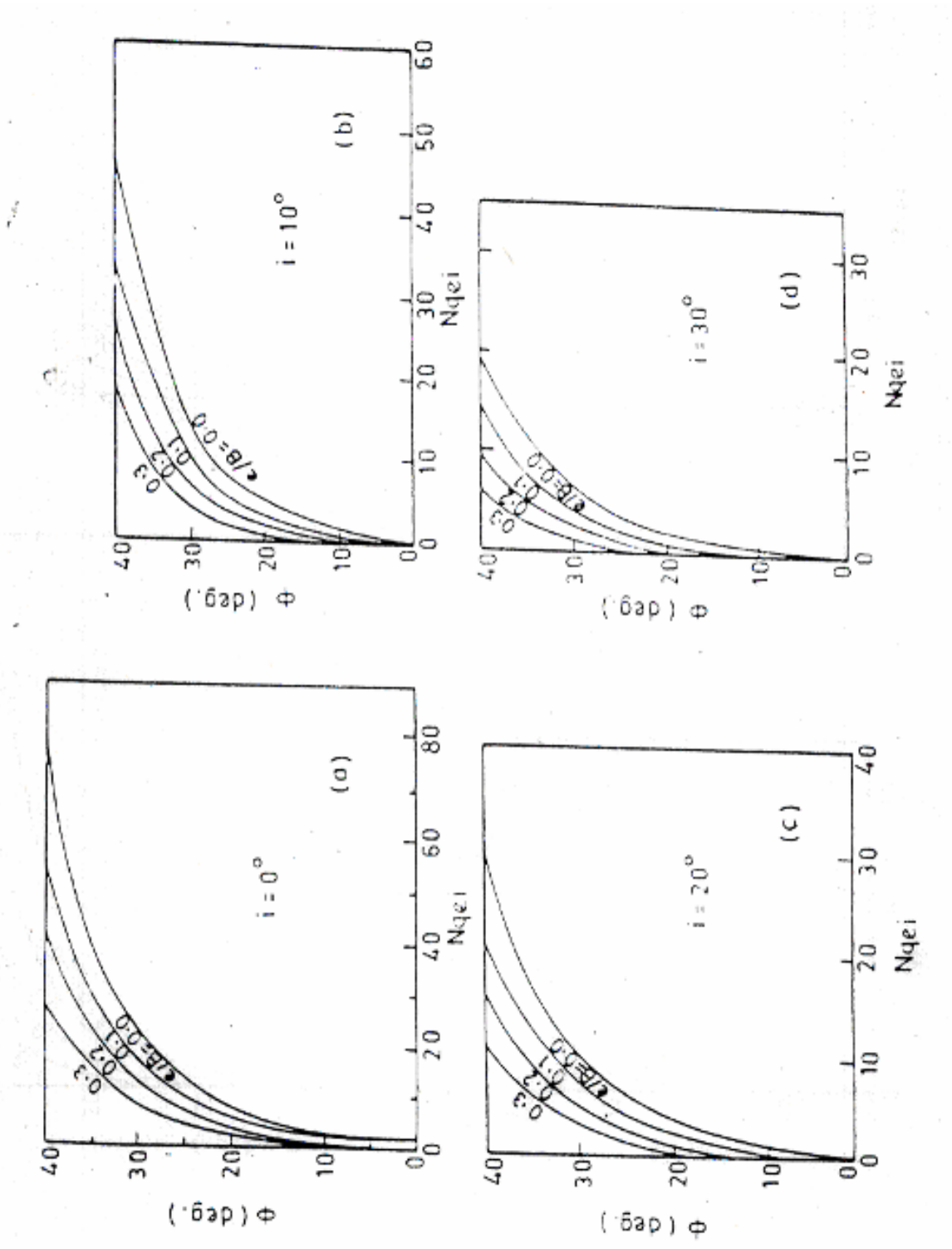

Figure 2.8, N_{qei} vs Φ for different value of e/B (Saran & Agrawal, 1986)

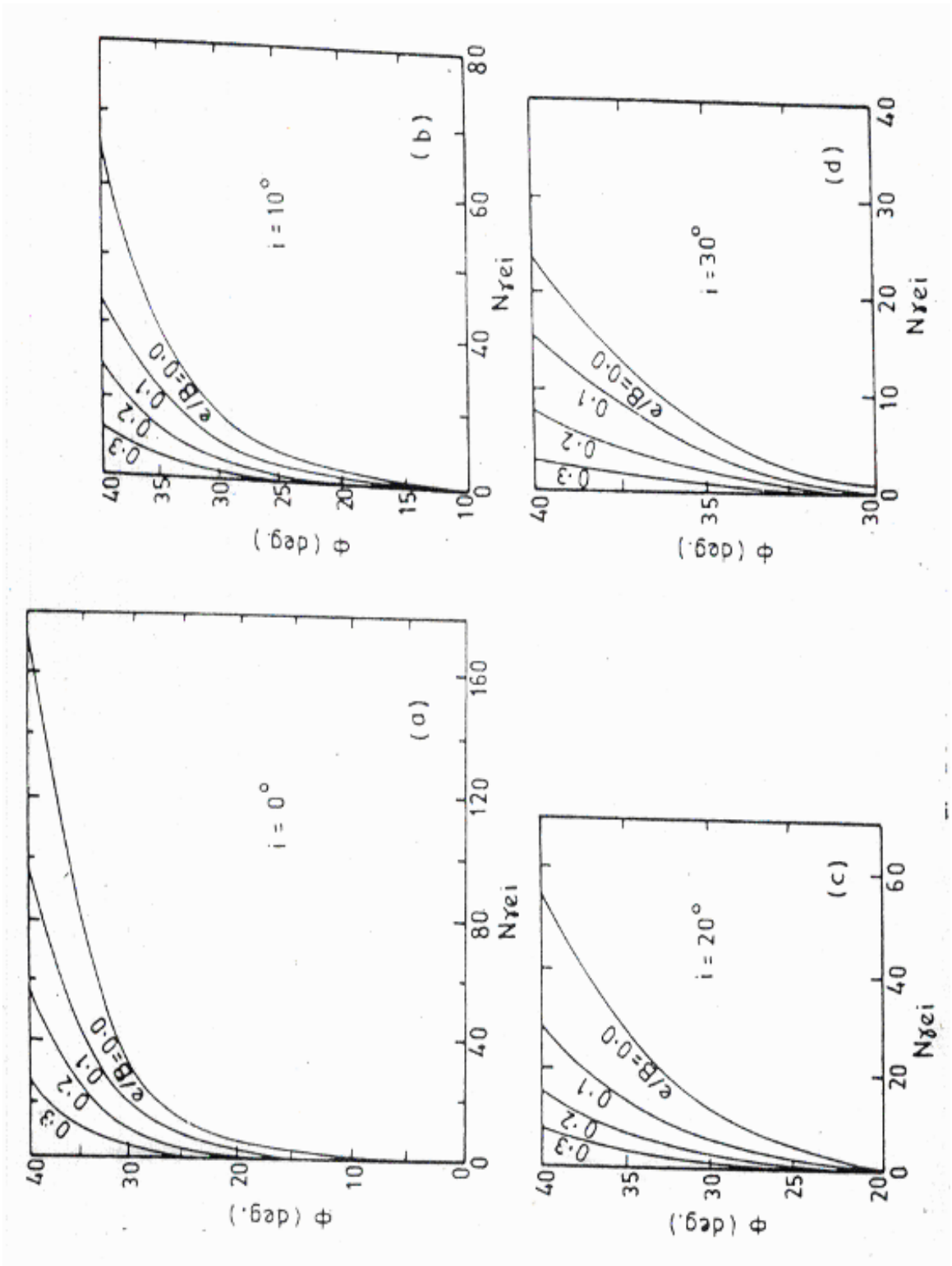

Figure2.9, Nγ vs Φ for different value of e/B (Saran & Agrawal, 1986)

Hansen (1961), proposed to use the general bearing capacity equation with certain correction factors to account for the load inclination. The equations are:

- for granular soil:

$$q_u = \frac{1}{2}\gamma B N_\gamma \left(1-0.3\frac{B}{L}\right)\left(1-1.5\frac{Q_h}{Q_v}\right)^2 + \gamma D_f N_q \left(1+0.1\frac{B}{L}\right)\left(1+0.1\frac{D_f}{B}\right)\left(1-1.5\frac{Q_h}{Q_v}\right) \text{--}$$

(2.11)

- for cohesive equation

$$q_u = 5c\left(1+0.2\frac{B}{L}\right)\left(1+0.2\frac{D_f}{B}\right)\left(1-1.3\frac{Q_h}{Q_v}\right)+\gamma D_f \quad \text{---------- (2.12)}$$

Limitations: $B \leq L$, $D_f \leq 2.5\ B$, $Q_h < 0.4\ Q_v$.

Where,

Q_h = horizontal component of inclined load.

Q_v = vertical component of inclined load.

B = width of footing.

L = length of footing.

D_f = depth of foundation below ground level.

γ = unit weight of soil.

c = unit cohesion.

Mayerhof (1963) also suggested the following empirical relation to get the bearing capacity of footing subjected to inclined load.

$$q_u = cN_C\left(1-\frac{i}{90}\right)^2 + qN_q\left(1-\frac{i}{90}\right)^2 + \frac{1}{2}\gamma B N_\gamma \left(1-\frac{i}{\varphi}\right)^2 \quad \text{---------- (2.13)}$$

Where:

i = load inclination in degrees.

2.3 CONSTITUTIVE LAW OF SOIL

Since the soil behavior is nonlinear, the nonlinear constitutive laws are more commonly employed. To represent the nonlinear stress-strain curve, two methods can be used, i.e. in the form of tabular form or in the of mathematical function.

Kondner (1963) and Kondner and Zelasko (1963) have found that the nonlinear stress-strain behavior of both clay and sand in a triaxial state of stress can be represented by the hyperbolic function. (Fig. 2.10)

$$\frac{\varepsilon}{\sigma_1 - \sigma_3} = a + b\varepsilon \qquad \text{------- (2.14)}$$

or,

$$\varepsilon = \frac{a(\sigma_1 - \sigma_3)}{1 - b(\sigma_1 - \sigma_3)} \qquad \text{---------- (2.15)}$$

Where,

ε = axial strain

a, b = constants of hyperbola.

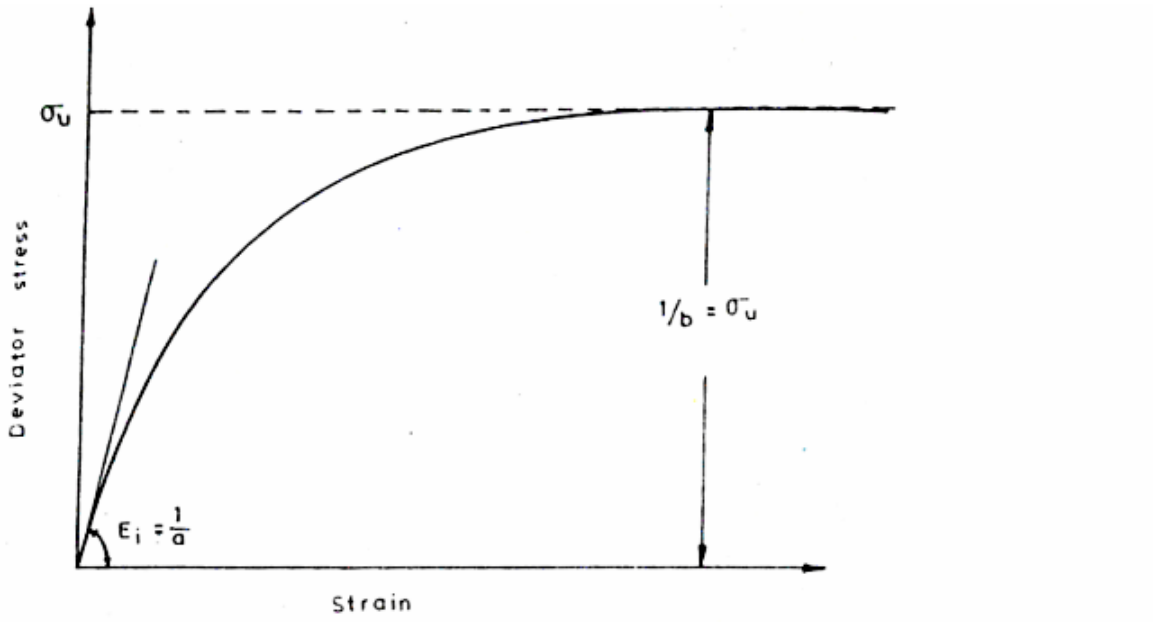

Figure 2.10, Nonlinear Stress-Strain Behavior Represented by the Hyperbolic Function, (Kondner (1963), and Kondner & Zelasko (1963))

Duncan and Chang (1970) have used the hyperbolic form of function to simulate the stress-strain behavior in terms of shear strength and initial tangent modules as given below:

$$E_t = E_t\left[1-\frac{R_f\left(\sigma_1-\sigma_3\right)\left(1-\sin\varphi\right)}{2\sigma_3\sin\varphi+2c\cos\varphi}\right]^2 \quad \text{---------- (2.16)}$$

Where,

E_t = tangent modules.

and

$$R_f=\frac{\left(\sigma_1-\sigma_3\right)_f}{\sigma u}= \text{ failure ratio} \quad \text{---------- (2.17)}$$

The behavior of soil can also be represented as the elasto-plastic material. In this, we can use the linear elastic formulations for the behavior prior to the proportional limit. In the zone of proportional limit and the yield point, the material exhibits nonlinear elastic behavior, and we can employ the piecewise linear approximation,. For this elasto-plastic analysis, we have to describe a yield criterion at which yielding is considered to begin.

We also need a flow rule to explain the post yielding behavior. There are five major yield criteria which are employed in the analysis of soil behavior.

(i) Von Mises criterion

(ii) Tresca criterion

(iii) Mohr-Coulomb criterion

(iv) Drucker- Prager criterion

(v) Critical state model.

(vi) The Mohr-Coulomb criterion for two dimensional state of stress is:

$$f = \frac{1}{2}(\sigma_3 - \sigma_1) - F_1\left[\frac{1}{2}(\sigma_3 - \sigma_1)\right] = 0 \quad \text{---------- (2.18)}$$

Where F_1 is a function of σ_1, σ_3, and φ. The Mohr-Coulomb condition accounts for both the cohesive strength c and the frictional strength φ of the material.

The above review deals with the theoretical aspects of the problem but the practical work carried by the various researchers are as presented below:

- **Professor John Carter et al (2001)**

Experimental investigations of footings on clay under combined loading were led by COFS research fellow **Dr Conleth O'Loughlin** and Associate Professor **Dr Barry Lehane.** In collaboration with visiting scholar **Dr David White** from Cambridge University in the UK, Conleth and Barry have used two recently developed optical methods to measure soil displacement patterns under model footings during loading to failure.

The methods have been used to measure soil displacement patterns for the case of a strip footing founded on dense calcareous clay subject to vertical loading either centrally, or at various eccentricities. The tests were performed in a 700 x 450 x 200 mm plane strain tank with a glass plate at its front face to facilitate the optical measurements.

The first of the methods employed a 'video-extensometer' (Messphysik, 1996) to track the position of the centroid of several discrete target markers on a contrasting background. The

second method used Particle Image Velocimetry (PIV), which is a velocity measurement technique originally developed in experimental fluid mechanics and recently adapted to obtain planar soil deformation measurements by **Dr David White**. A benefit of the PIV method is that it removes the need for discrete target markers by tracking the inherent texture (i.e. spatial variation of brightness) of soil grains through a series of images captured at discrete time intervals using a high resolution digital camera.

Both the monochrome video camera used in the video-extensometer system and the digital camera used for the PIV analysis were securely mounted on a tripod along a common vertical axis displacement vectors at increasing values of applied stress (and hence foundation settlement) facilitate the observance of the soil failure mechanism. Such information allows current constitutive soil models to be rigorously and rationally verified. It is envisaged that during 2003 the optical measurement methods will be employed for centrifuge tests on a variety of foundations subjected to combined vertical, horizontal and moment loading.

.

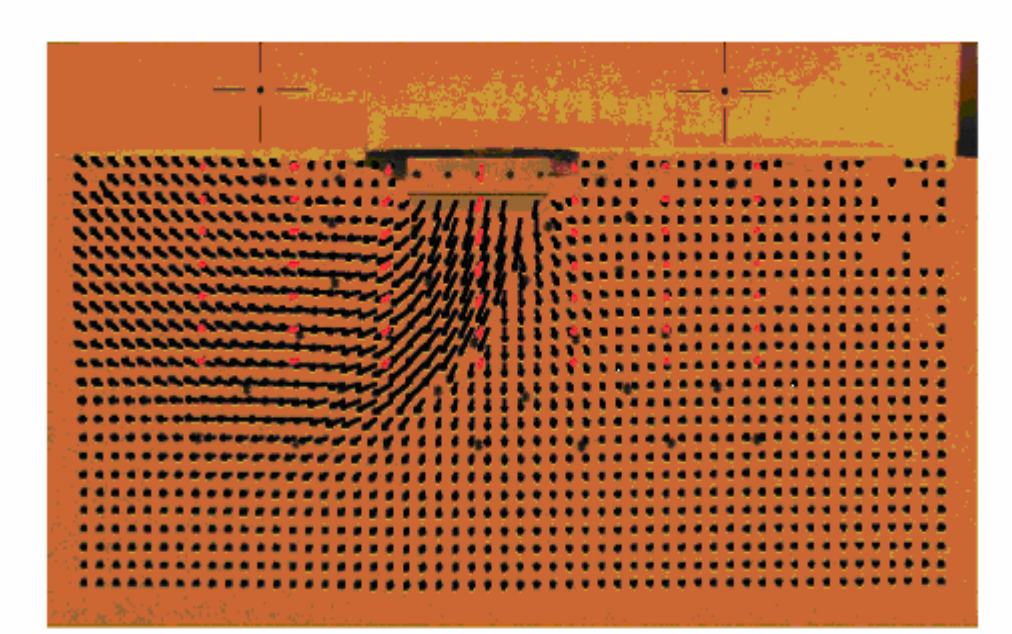

Figure 2.11, Failure Mechanism for an Eccentrically Loaded Strip footing (Carter et al, 2001)

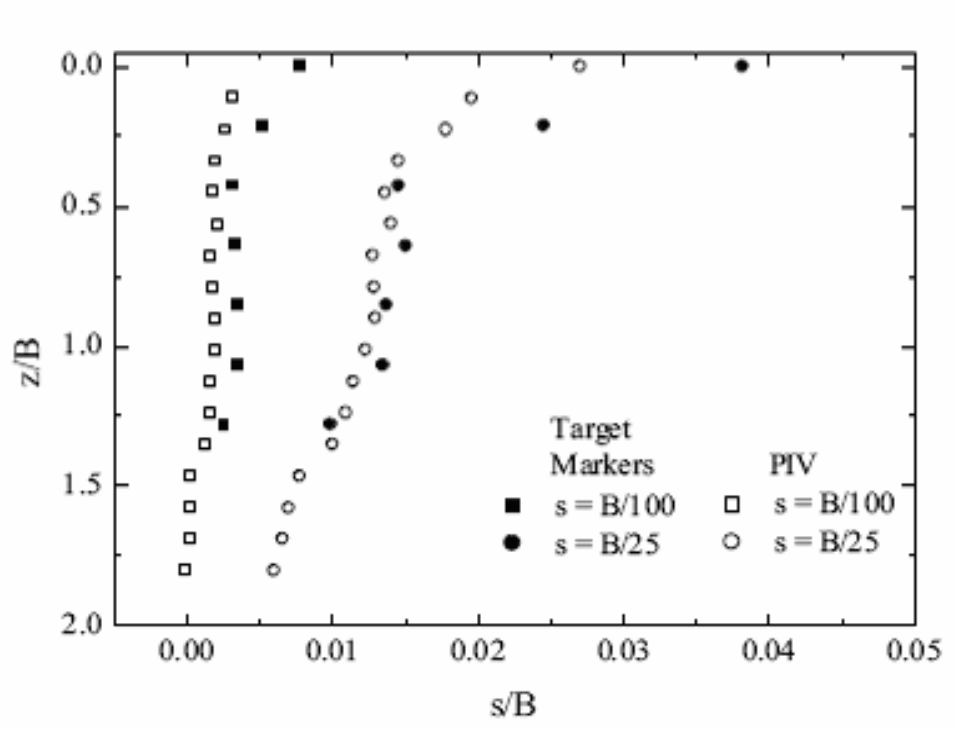

Figure 2.12, Vertical Displacement beneath centrally Loaded Footing (Carter et al, 2001)

- **Bose S.K. and Das S.C. (1995)**

A Nonlinear finite element analysis was carried out by the authors to investigate the stress distribution and load-settlement behavior of footings of absolute rigidity and absolute flexibility. An absolutely rigid footing was modeled by simulating the footing as a rigid body undergoing equal vertical displacements at the contact points. The nonlinearity of the stress-strain curve of soil was taken into account by adopting a "piecewise" linear model. A hyperbolic stress-strain relationship of the soil was assumed, and Mohr-Coulomb yield criterion was chosen for analysis. An analysis was carried out under conditions simulating the experimental setup of the model footing tests, performed on two different types of soil media. Theoretical observations were compared with experimental ones and good agreement between the above two was found. Thus, reasonable predictions of the effect of relative rigidity of footing in the nonlinear range of soil mass could be obtained and a set of conclusions are arrived at from the investigation.

Good agreement of the theoretical and experimental results can lead one to conclude that it is possible to predict the contact stress distribution, stress distribution and deformation characteristics of an absolutely rigid footing in the nonlinear range. The rigidity of footings influences the stress distribution up to a depth of two to three times the loading radius. The contact stress distribution of a perfectly rigid footing is saddle shaped and at different load levels the nature of distribution gets altered

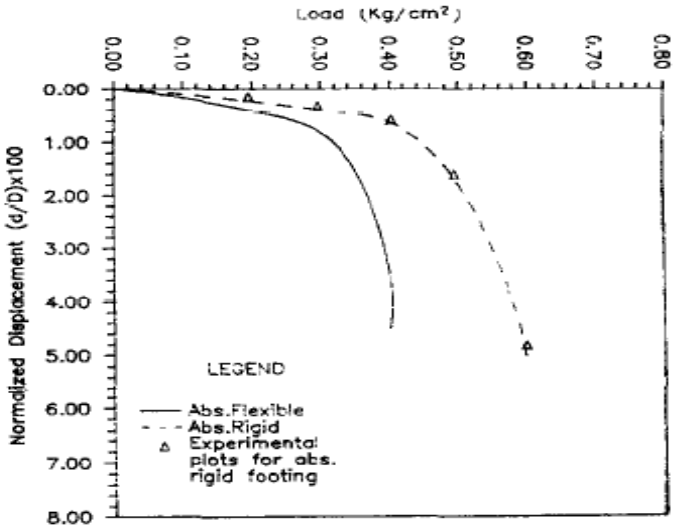

Figure 2.13, Load Settlement Curve of Footing on Kaolin Clay

- **Houlby G.T. & Purzin A.M. (1998)**

They studied various aspects of bearing capacity of strip footing under combined loading and tried to give solution for the problem of its failure on undrained clay subjected to combined vertical moment and horizontal loading. The idea used in this study is that clay which is in contact with the footing is unable to sustain tension, which complicates the problem considerably.

According to authors it is not possible to find the exact bearing capacity of the soil under aforesaid condition, therefore approximate solution is found out using numerical analysis giving solution in a range (between lower bound and upper bound). They said that upper bound and lower bound theorem of plasticity theory are not sufficient to find the solution. They gave certain hypothesis in each theorem to rationalize the solution in which the upper-bound solution does not involve contact-breaking at the soil-footing interface, and the lower-bound solution does not involve tensile stress on the soil-footing interface.

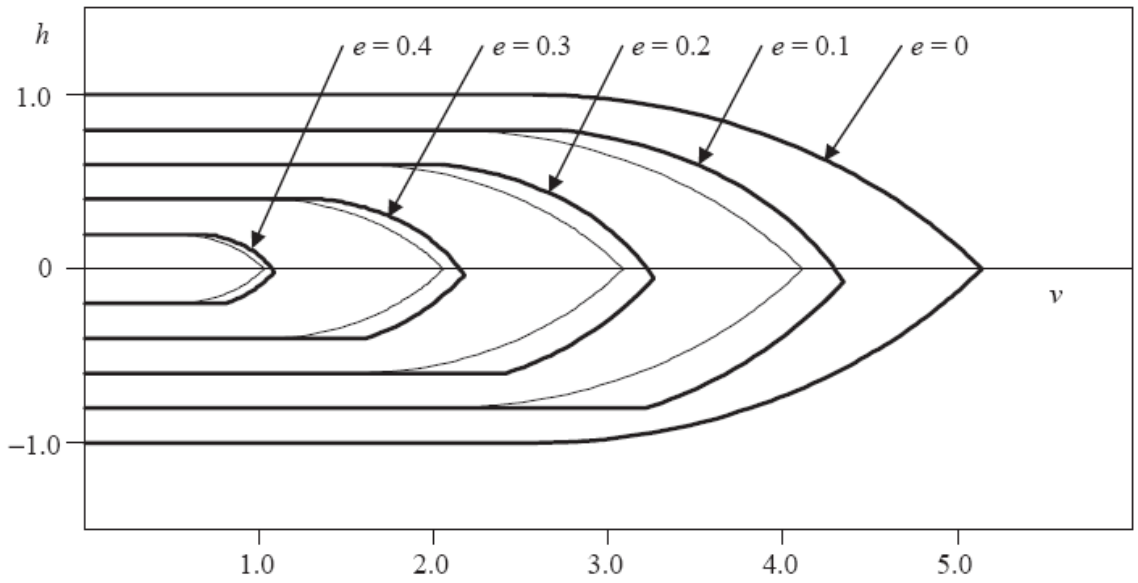

Figure 2.14, Solution Presented as Contours at Constant Eccentricity (Houlby G.T. & Purzin A.M. (1998))

Based on this analysis a solution is presented in the form of contours of constant eccentricity in v-h (vertical horizontal) plane. As shown in Fig.2.14. These contours are derived by intersecting the apparent lower- and apparent upper-bound surfaces by planes containing the h-axis. Apparent lower- and apparent upper-bound estimates coincide on the (m = 0)-plane and along the surfaces derived by scaling or the effective-width concept from solutions for slip along the surface. In these cases, it is reasonable to assume the existence of unique working solutions. For the portions of the surfaces that do not coincide, the bound estimates give a reasonably narrow band for the possible location of the working yield surface.

- **Massin D.Y.A., Hachem E.E. & Soubra A.H. (2005)**

Massih et al determined bearing capacity of strip foundation for inclined load and eccentric load for layered soil consisting of clay and sand. They used upper bound approach of limit analysis theory.

Authors studied failure mechanism of foundation for inclined and eccentric load. For inclined load a translation failure is observed. Fig 2.15 In this mechanism, each radial

surface separating two adjacent rigid blocks consist of two lines inclined at an angle of 'f' to each other in order to respect the normality condition.

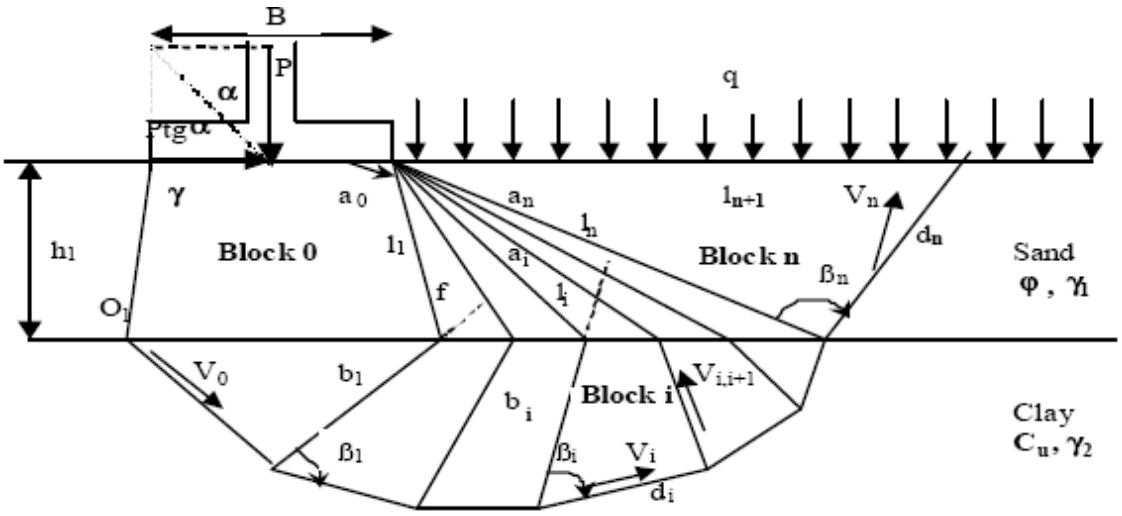

Figure 2.15, Collapse Mechanism for Inclined Load (Massih et al, 2005)

Similarly, for eccentric load a rotational mechanism a rotational mechanism is obtained Fig 2.16. This mechanism is a generalization of the traditional log-spiral mechanism considered in the stability analysis of a homogeneous soil mass. In the present mechanism however, the log-spiral reduces to a circle when its passes through the clay layer.

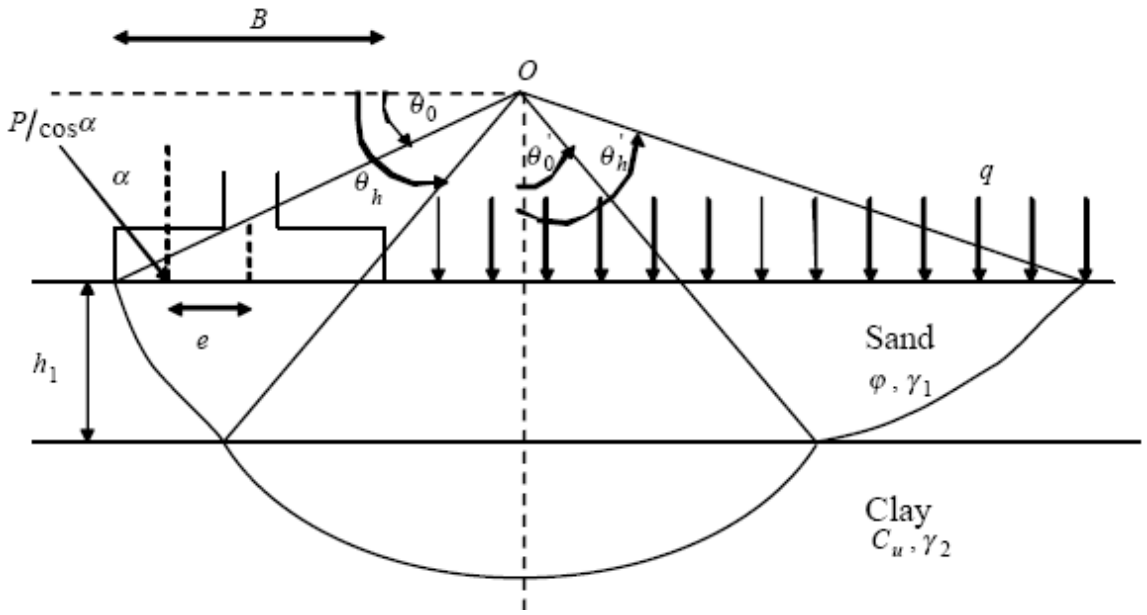

Figure 2.16, Collapse Mechanism for Eccentric Load (Massih et al, 2005)

Further, they equated the rate of energy dissipation to the rate of work done by the external forces for the two mechanisms presented above they obtained work equation as

$$\frac{p_u}{\gamma \cdot B} = \frac{1}{2} \cdot N_\gamma + \frac{q}{\gamma \cdot B} \cdot N_q + \frac{C_u}{\gamma \cdot B} \cdot N_c \quad \text{…….. 2.19}$$

Numerical analysis was done for different angle of inclination and eccentricity and obtained design charts. Fig 2.17 shows design charts for angler of inclination (α) = 5^o and no surcharge (q = 0). The critical depth is accounted for in the charts. As expected, the limit pressure increases with an increase in the depth of the sand layer. It also increases with the clay strength. For most cases, the limit pressure reaches a constant value and further increase in the clay strength does not improve the bearing capacity. This limit is equal to the bearing capacity of the granular soil. Only when the clay is strong and the layer of sand overlying the clay is thin relative to the footing breadth can the bearing capacity increase beyond that expected for a homogeneous granular soil.

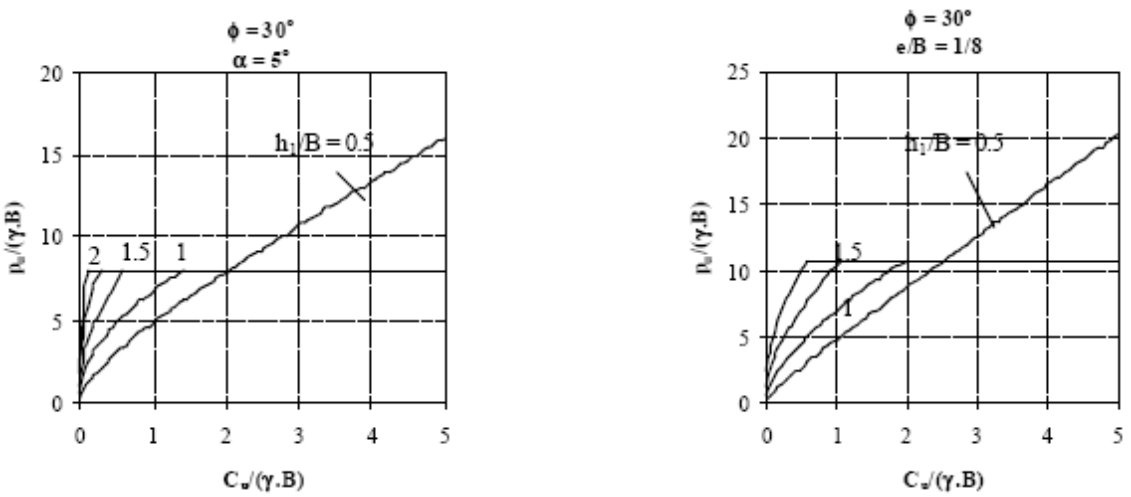

Figure 2.17, Design Charts for Bearing Pressure (Massih et al, 2005)

2.4 JUSTIFICATION OF PROBLEM

The critical review of literature suggests that the most of the work related to strip footings subjected to centrally applied inclined load and eccentrically applied inclined load has been carried out for estimating the bearing capacity of such footing either on sand or clay. However, not much work has been done in the area of pressure settlement characteristics of such footing using the constitutive laws. An attempt therefore been made in this thesis to estimate pressure settlement characteristics of strip footings on clays considering their elasto-plastic behavior.

CHAPTER - 3

THEORITICAL ANALYSIS

3.1 GENERAL

Although nonlinear elastic constitutive relations have been applied in finite element analysis and especially soil mechanics application (e.g. Duncan and Chang, 1970), the main physical feature of nonlinear material behavior is usually the phenomenon is to be found in the Theory of Plasticity (e.g. Hill, 1950). The simplest stress-strain law of this type that could be implemented in a finite element analysis involves elastic-perfectly plastic material behavior (Fig. 3.1, 3.2, 3.3). But it is more convenient in solid mechanics to introduce yield surface in principal stress space which separates stress states that give rise to elastic and to plastic (irrecoverable) strains.

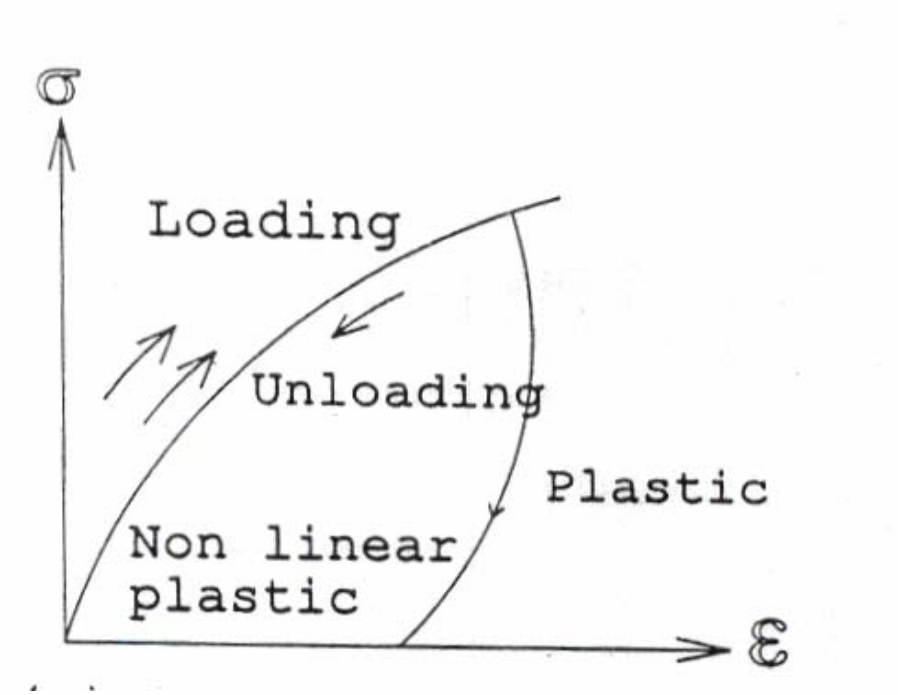

Figure 3.1, Non Linear Elastic & Plastic Behavior of Soil

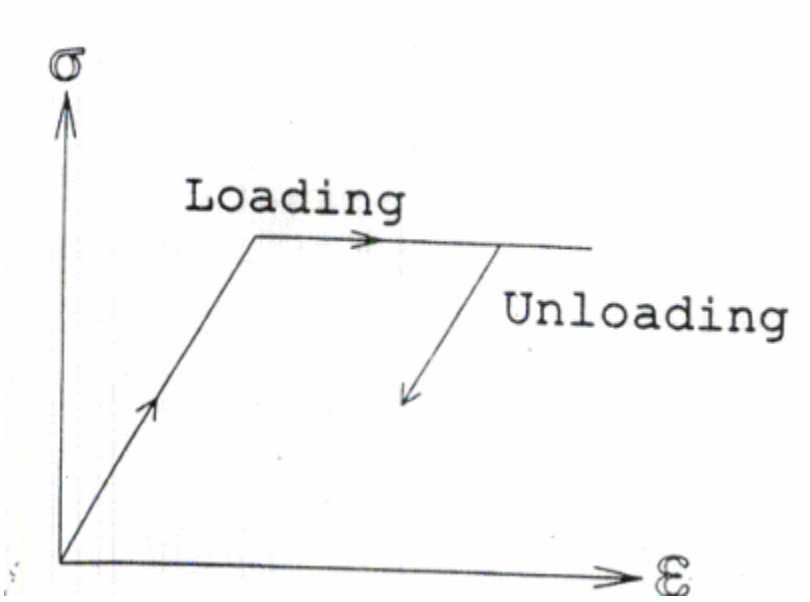

Figure 3.2, Ideal Plasticity Behavior of Soil

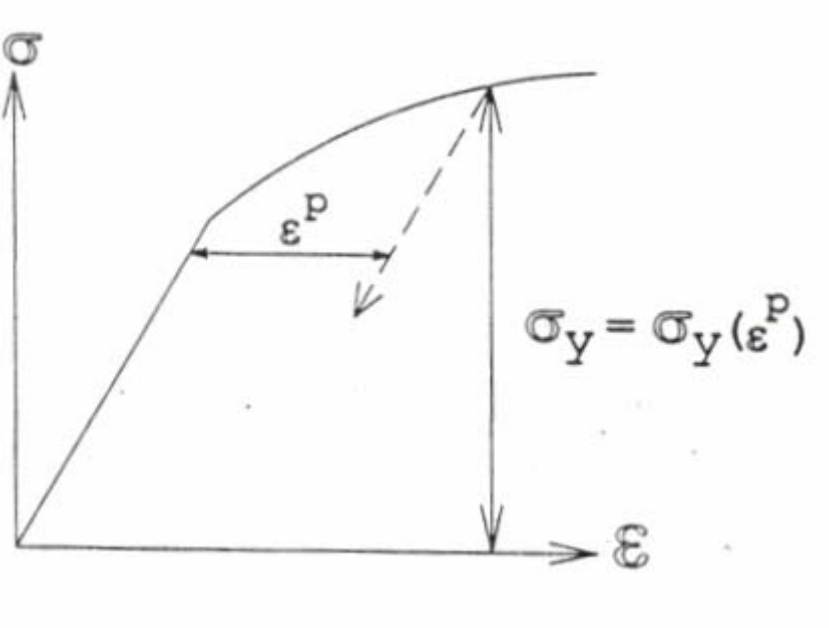

Figure 3.3, Strain Hardening Plasticity Behavior of Soil

3.2 ELASTO-PLASTIC ANALYSIS

The elasto-plastic behavior and its application to finite element analysis will be discussed herein.

3.2.1 Yield Criteria

Algebraically, the ultimate yield surfaces are expressed in terms of a yield or failure function F. This function, which has units of stress, depends on the material strength and invariant combinations of the stress components. The function is designed such that it is negative within the yield or failure surface and zero on the yield failure surface. Positive values of F imply stresses lying outside the yield or failure surface which are hypothetical and which must be redistributed via the iterative process sot that yield point always lies on the yield surface.

During plastic straining, the material may follow an associated flow theory involving normality principle and a plastic flow rule that is the vector of plastic strain increment will be normal to the yield surface. The material may as well follow with non-associated flow theory. Associated flow rule leads to various mathematically attractive simplifications and when applied to the Von Mises or Tresca failure criteria, correctly predicts zero plastic volume change during yield of undrained clays. For frictional materials, whose ultimate state is described by the Mohr-Coulomb criterion, associated flow rule leads to physically unrealistic volumetric expansion or dilation during yield. In such cases, non-associated flow rules must be preferred in which plastic straining is described by a plastic potential function, Q. This function friction angle Φ is replaced by dilation angle ψ. Before outlining the failure criteria and their representation in principal stress space, some useful stress-invariant expressions are briefly reviewed.

The Cartesian stress tensor defining the Stress conditions at a point within a loaded body is given by:

$$\{\sigma_x \quad \sigma_y \quad \sigma_z \quad \tau_{xy} \quad \tau_{yz} \quad \tau_{zx}\} \qquad \text{……..(3.1)}$$

where,

σ_x ,σ_y ,σ_z = normal stress acting along x, y, z-axes respectively.

τ_{xy} , τ_{xy} , τ_{xy} = shear stress acting on xy ,yz ,zx plane respectively.

which can be shown to be equivalent to three principal stresses acting on orthogonal planes

$$\{\sigma_1 \quad \sigma_2 \quad \sigma_3\} \qquad \text{…….(3.2)}$$

Principal stress space is obtained by treating the principal stresses as 3-D coordinates and such a plot represents a useful means of defining the stresses acting at a point. It may be noted that although principal stress space defines the magnitudes of the principal stresses, no indication is given of their orientation in physical space.

Instead of defining a point in principal stress space with coordinates $\{\sigma_1 \quad \sigma_2 \quad \sigma_3\}$, it is often more convenient to use invariants (s, t, θ) where

$$s = \frac{1}{\sqrt{3}}(\sigma_x + \sigma_y + \sigma_y) \qquad \text{…..…(3.3)}$$

$$t = \frac{1}{\sqrt{3}}[(\sigma_x - \sigma_y)^2 + (\sigma_y - \sigma_z)^2 + (\sigma_z - \sigma_x)^2 + 6\tau_{xy}^2 + 6\tau_{yz}^2 + 6\tau_{zx}^2] \qquad \text{….(3.4)}$$

$$\theta = 1/3 \arcsin(\frac{-3\sqrt{6J_3}}{t^3}) \qquad \text{….(3.5)}$$

where,

$$J_3 = S_x S_x S_x - S_x \tau_{yz}^2 - S_y \tau_{zx}^2 - S_z \tau_{zy}^2 + 2\tau_{xy}\tau_{yz}\tau_{zx} \quad \text{……..….(3.5a)}$$

is the third stress invariants, and

$$S_x = (2\sigma_x - \sigma_y - \sigma_z)/3 \text{ , etc} \qquad \text{……..(3.5b)}$$

As shown in Fig. 3.4 gives the distance from the origin to the π plane in which the stress point lies and *t* represents the perpendicular distance of the stress point from the space diagonal. The lode angle θ, is a measure of the angular position of the stress point within the π plane. It may be noted that in plane strain equations (3.3) are simplified because $\tau_{yx} = \tau_{zx} = 0$.

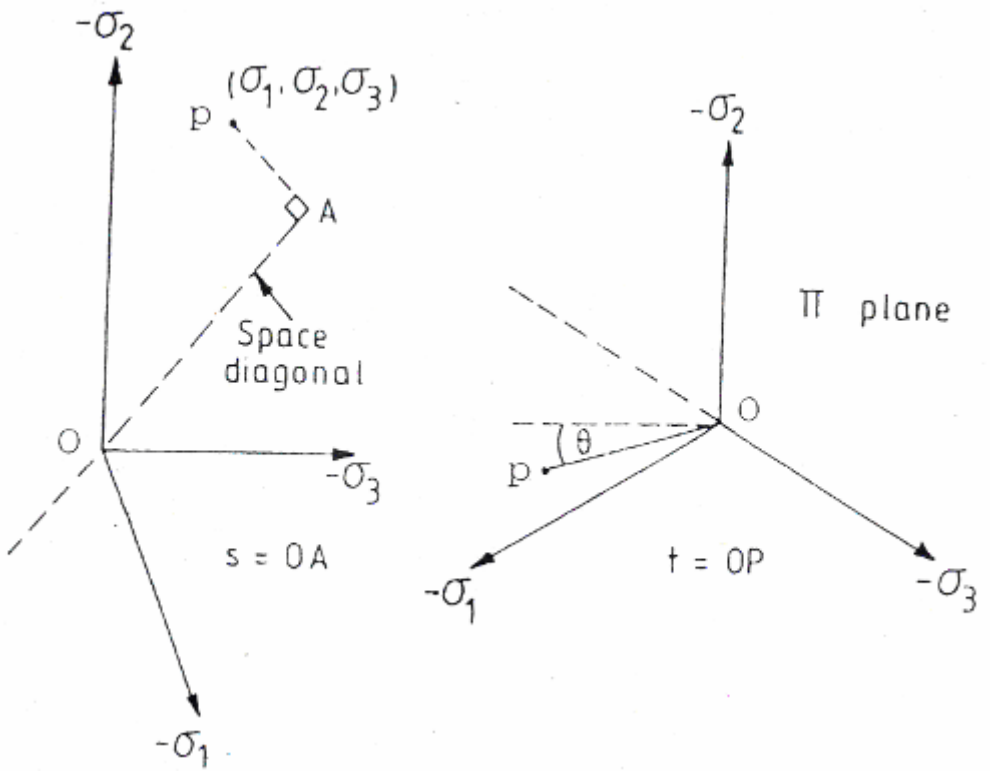

Figure 3.4, Principal Stress Space

Several failure criteria have been proposed as suitable for representing the strength of soils as engineering material. For soils possessing both frictional and cohesive components of shear strength, the best known criterion is undoubtedly that due to Mohr-Coulomb and takes the form of an irregular hexagonal cone in principal stress space.

For undrained clays which behave in a frictionless (Φ_u=0) manner, cylindrical failure criteria are appropriate. These are the simplest criteria, which do not depend on the first stress invariant, s (or σ_m). The Tresca criterion, in fact, does not require separate treatment mathematically because

it is a special case of the Mohr-Coulomb criterion. Alternatively, the Von Mises criterion may be used. The difference in strengths predicted by the two criteria does not exceed by about 15%.

As shown in Fig. 3.3, Von Mises criterion takes the form of a right circular cylinder lying along the space diagonal. Only one of the three invariants, namely t (or σ), is of any significance when determining whether a stress state has reached the limit of elastic behavior. The onset of yield in a Von Mises material is not dependent upon invariants, s or θ.

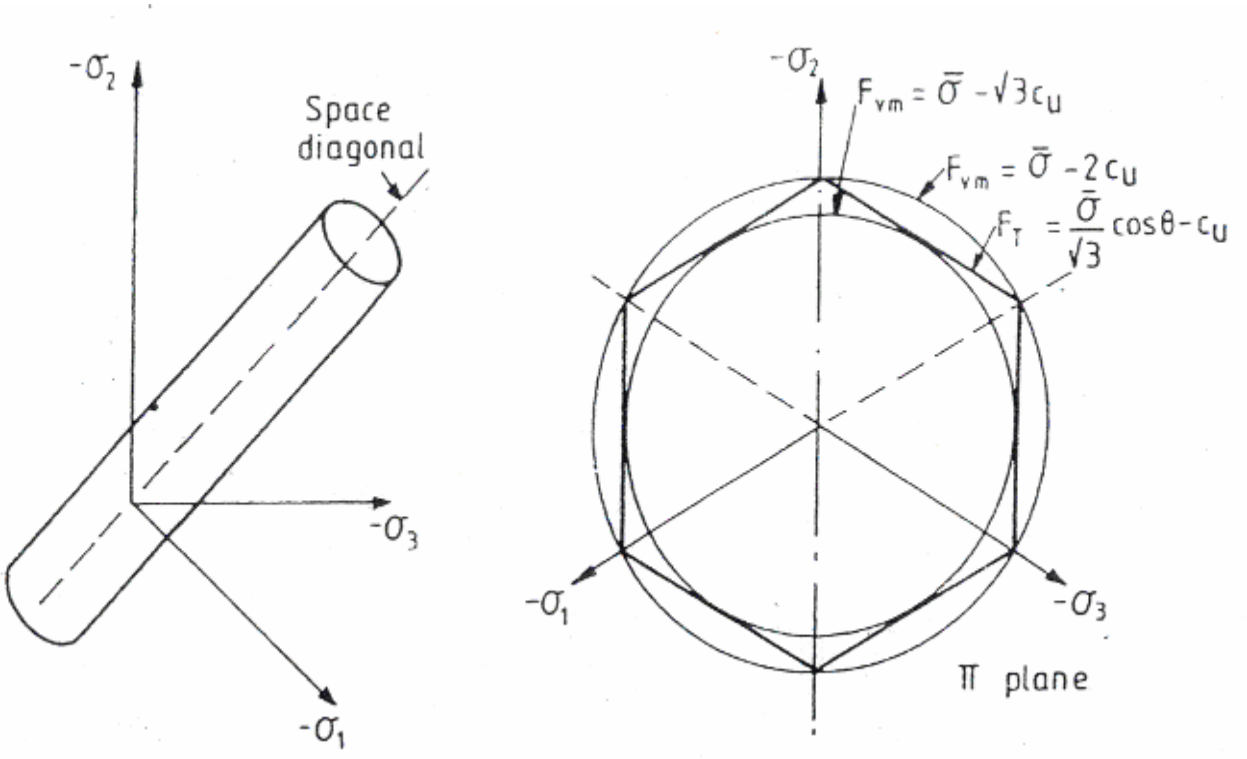

Figure 3.5 Mises and Tresca Failure Criteria

The symmetry of the Von Mises criterion when viewed in the π plane indicates why it is not ideally suited to correlations with traditional soil mechanics concepts of strength. The criterion gives equal weight to all three principal stresses, so if it is to be used to model undrained clay behavior, consideration must be given to the value of the intermediate principal stress, σ_2 at failure.

For plane strain application, it can be shown that at failure

$$\sigma_2 = \frac{\sigma_1 + \sigma_3}{2} \quad \text{.....(3.6)}$$

Hence, the failure criterion is given by

$$F = \bar{\sigma} - \sqrt{3}c_u \quad \text{.....(3.7)}$$

Where c_u = undrained cohesion of the soil.

Under triaxial conditions, where at all times

$$\sigma_2 = \sigma_3 \quad \text{.....(3.8)}$$

The criterion is given by :

$$F = \sigma - 2c_u \quad \text{.....(3.9)}$$

Both of these expressions ensure that at failure

$$c_u = \frac{\sigma_1 - \sigma_3}{2} \quad \text{.....(3.10)}$$

3.3 NON-LINEAR SOLUTION STRATEGY

In practical finite element analysis, mainly two procedures can adopted to model material non-linearity. The first approach involves constant stiffness iterations in which nonlinearity is introduced by iteratively modifying the right-hand side "load" vectors. The (usually elastic) global stiffness matrix in such an analysis is formed only once. Each iteration thus represents an elastic analysis. Convergence is said to occur when stresses generated by the loads satisfy some stress-strain law or yield or failure criterion within prescribed tolerances. The load vectors at each iteration consist of externally applied loads and self-equilibrating body loads. The body-loads have the effect of redistributing stresses within the system, but as they are self-equilibrating, they do not alter the net loading on the system. The constant stiffness method is shown diagrammatically in fig 3.4. For load-controlled problems, more iteration may be required for convergence as failure is approached because the elastic (constant) global stiffness matrix

starts to seriously overestimate the actual material stiffness. The numbers in parentheses in the Fig. 3.6 indicate the number of iterations which might typically be required to reach convergence.

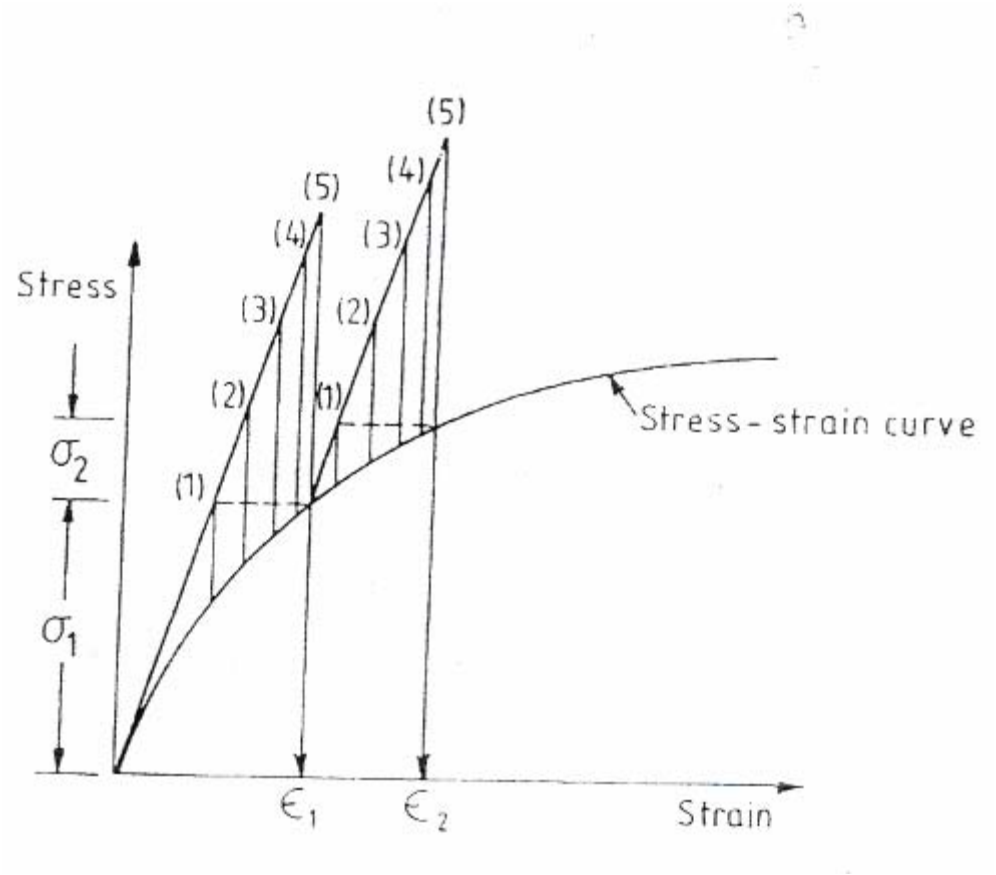

Figure 3.6, Constant Stiffness Method

Less iterations per load step are required if the second approach, namely the variable or tangent stiffness method, is adopted. This method, shown in Fig. 3.5, takes account of the reduction in stiffness of the material as failure is approached. If small enough load steps are taken, the method can become equivalent to a simple Euler Explicit method. In practice, the global stiffness matrix may be updated periodically and body-loads iterations employed to achieve convergence. In contrasting the two methods, the extra effort of reforming and factorizing the global stiffness matrix in the variable stiffness method is offset by reduced numbers of iterations, especially as failure is approached. A further possibility is the implicit integration of the rate equations which

rather reduce the explicit methods just described. This helps to further reduce the number of iterations for convergence.

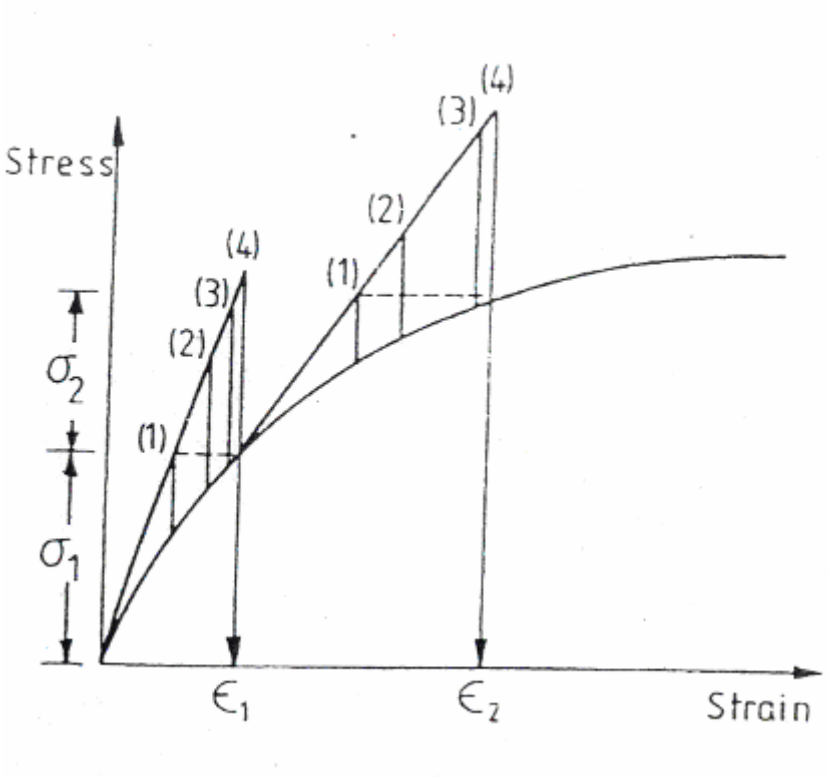

Figure 3.7, Variable Stiffness Method

Constant stiffness methods of the type described in this analysis use repeated elastic solutions to achieve convergence by iteratively varying the loads on the system. Within each load increment, the system of equations

$$K\,\delta^i = p^i \qquad \ldots.(3.11)$$

must be solved for the displacement increments δ^i, where i represents the iteration number , K the global stiffness and p^i the external loads.

The element displacement increments, u^i are extracted from δ^i , and these lead to total strain increments via the element strain-displacement relationships:

$$\Delta\varepsilon^i = Bu^i \qquad \ldots.(3.12)$$

Assuming the material is yielding, the strains will contain both elastic and (visco) plastic components; thus

$$\Delta\varepsilon^i = (\Delta\varepsilon^e + \Delta\varepsilon^p)^i \quad \ldots.(3.13)$$

It is only the elastic strain increments $\Delta\varepsilon^e$ that generate stresses through the elastic stress-strain matrix; hence

$$\Delta\sigma^i = D(\Delta\varepsilon^e)^i \quad \ldots.(3.14)$$

These stress increments are added to stresses already existing from the previous load step and the updated stresses substituted into the failure criterion.

If stress redistribution; is necessary, this is done by altering the load increment vector p^i in equation (3.11). In general, this vector holds two types of load, as given by:

$$p^i = p_a + p^i_b \quad \ldots.(3.15)$$

Where p_a is the actual applied load increment that is required and p_b^i is the body-loads vector that varies from one iteration to the next. The p_b^i vector must be self-equilibrating so that the net loading on the system is not affected by it.

CHAPTER -4

RESULTS & DISCUSSION

4.1 GENERAL

In this chapter, an attempt has been made to analyze and study the behavior of a strip footing resting on the surface of uniform clay soil in an undrained state. The strip footing-soil system is subjected to centrally applied inclined load. The problem has been idealized as a plane strain problem (Figure 4.1, 4.2). An elasto-plastic finite element analysis has been carried out using incremental theory of plasticity. The clay soil in an undrained state has been assumed to yield according to Von Mises criterion.

The elasto-plastic analysis of soil-strip footing system has been carried out to predict;

- Pressure-settlement characteristics for eccentric loading of the footing
- Ultimate bearing capacity of strip footing, and
- the value of bearing capacity factor, N_c

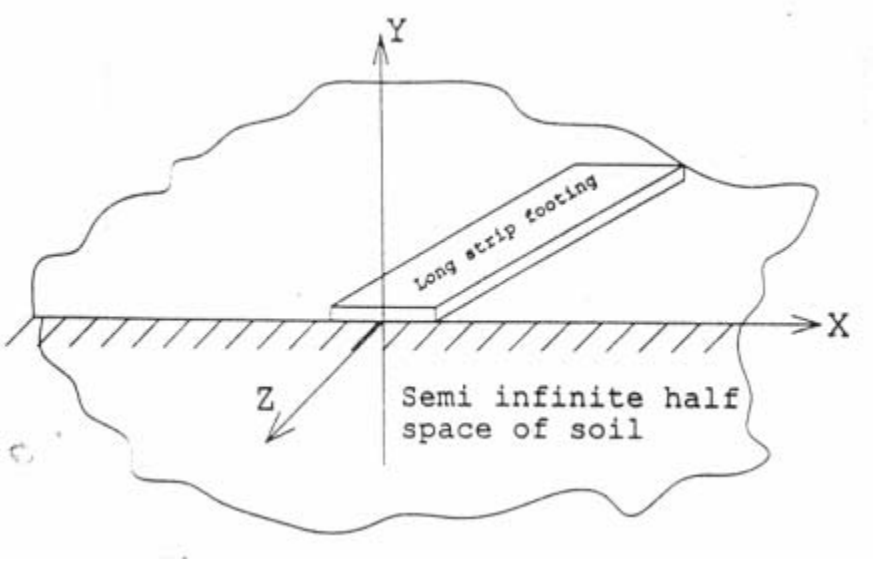

Figure 4.1, Strip Footing as a Plain Strip Footing

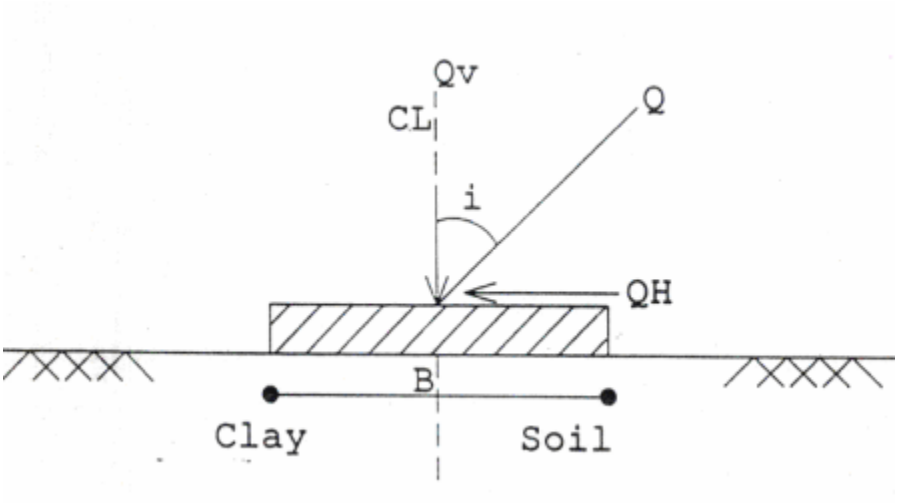

Figure 4.2, Surface Footing with Inclined Loading Strip

4.2 PARAMETER CONSIDERED IN ANALYSIS

The type of soil which will be analyzed is clay soil with $\Phi = 0$ as it is in an undrained state. All the six states of consistency have been considered. The elasto-plastic state has been described by three parameters, namely the elastic properties, E_s, ν, and the undrained cohesion c_u. Table 4.1 displays numerical values of these properties corresponding to different states of consistency. The values of inclination of load considered for analysis of soil-footing system are $i = 0^0$, 10^0, 20^0, 30^0. The width of footing considered is 2.0 m. The values has been taken from 'Behavior of Eccentrically Loaded Footing in Clay' by C. Prakash, University of Roorkee, (1975)

4.3 FINITE ELEMENT MESH

For finite element analysis using 2-D plane strain state, the eight-noded isoparametric parabolic elements have been used. A 2 x 2 Gaussian quadrature scheme has been used for numerical integration. The footing supports a uniform stress, q, which is increased incrementally to failure. Fig. 4.3 shows the finite element mesh used in the analysis. It has:

Number of elements: 64 elements

Number of nodal points : 233 nodal points

Number of restrained nodes: 49 nodes.

For this elasto-plastic analysis, the load was increased proportionally using the load increments. It is usual in the problem of this type to make load increments smaller as the failure load is

Table 4.1 Parameters of Clay Used in the Analysis.

Type of Clay (Consistency)	**Undrained Cohesion, c_u, (kN/m^2)**	**Initial Tangent Modulus, E_s (kN/m^2)**	**Poisson Ratio (v)**
Hard	200	100000	0.1
Very Stiff	150	80000	0.15
Stiff	75	60000	0.2
Medium	37.5	40000	0.2
Soft	18.75	15000	0.25
Very Soft	10	10000	0.3

approached. At load levels well before failure, convergence should occur in relatively few iterations. In the data provided in this analysis, the limit of iterations is set to 250 iterations in each load increment. This value will become the maximum number of iterations allowed within one load increment. The tolerance provided for convergence in this is 0.001.

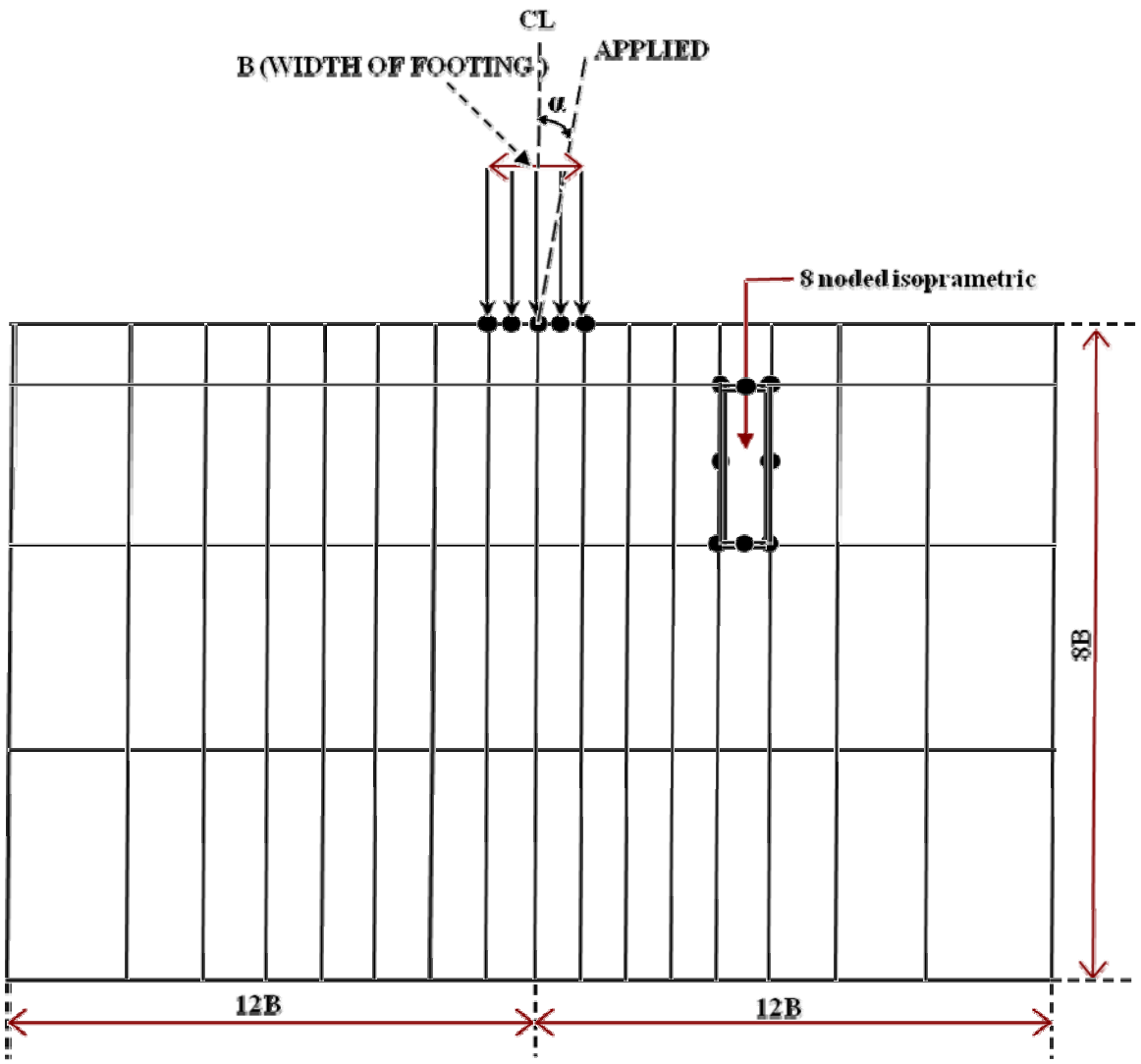

Figure 4.3, Typical Mesh for Idealization of Soil Mass & Eight Noded Isoparametric Element

4.4 DISCUSSION OF RESULTS

4.4.1 Pressure Vs Elasto-Plastic Vertical Settlement Characteristics

Pressure versus vertical settlement curves for a strip footing (B = 2.0 m), resting on various type of clays (Table 4.1) have been obtained of values of load inclination i = 0^0, 10^0, 20^0, 30^0. Fig. 4.4 to Fig. 4.9 show pressure-settlement characteristics of a centrally loaded strip footing for load inclination i = 0^0, i.e. for the case of centrally vertical loading.

The curves have been plotted for footing resting on hard clay, stiff clay and soft clay respectively. The values of ultimate bearing capacity of strip footing obtained by double tangent method are respectively 1025 kN/m^2, 385 kN/m^2, and 94 kN/m^2.

Similarly plots have been presented for pressure-settlement behavior of strip footing resting on clay stratum having six states of consistency for load inclination i = 10^o, 20^o, 30^o (Fig. 4.10 to Fig. 4.27)

All the pressure-settlement characteristics display an initial linear elastic behavior followed by inelastic behavior till failure during which large settlement occurs for every successive pressure increment.

The number of iterations needed to achieve convergence in each load increment also varies for successive load increments. For example, for case of medium clay and i = 30^0, it is seen that the convergence was achieved for the 9^{th} load increment, when q = 154 kN/m^2 in 59 iterations. For the 9^{th} load increment when q = 162 kN/m^2, the number of iterations needed to achieve convergence jumped up to 203 iterations, but the convergence could not be achieved within the upper limit of 250 iterations when the load was incremented to 168 kN/m^2. This significant change of number of iterations needed to achieve convergence indicates that the soil failure has approached, and the corresponding displacement increments at this stage were also very high. These conditions have been observed typically for all cases of soil and loading.

It has been found that the values of ultimate bearing capacity decrease with the decrease of consistency of clay from hard to very soft. As the inclination of load increases, the values of ultimate bearing capacity and failure load decrease. This reduction of ultimate bearing capacity is significant in the high consistency range of clay.

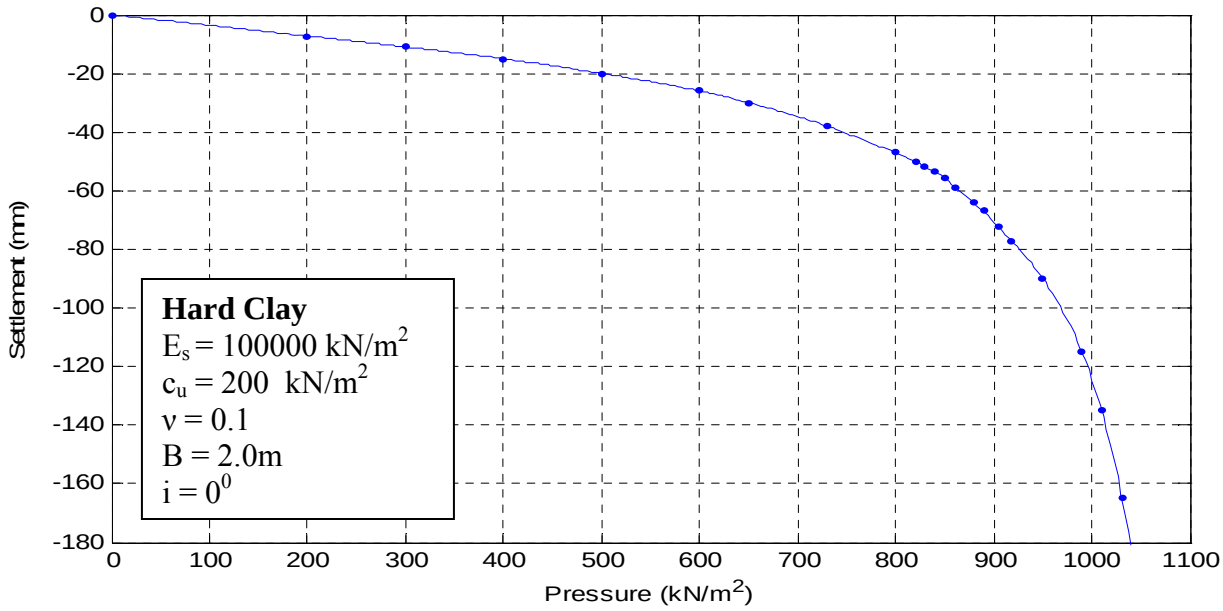

Figure 4.4, Pressure Vs Elasto-plastic Settlement Curve of Strip Footing under Centrally Vertical Load

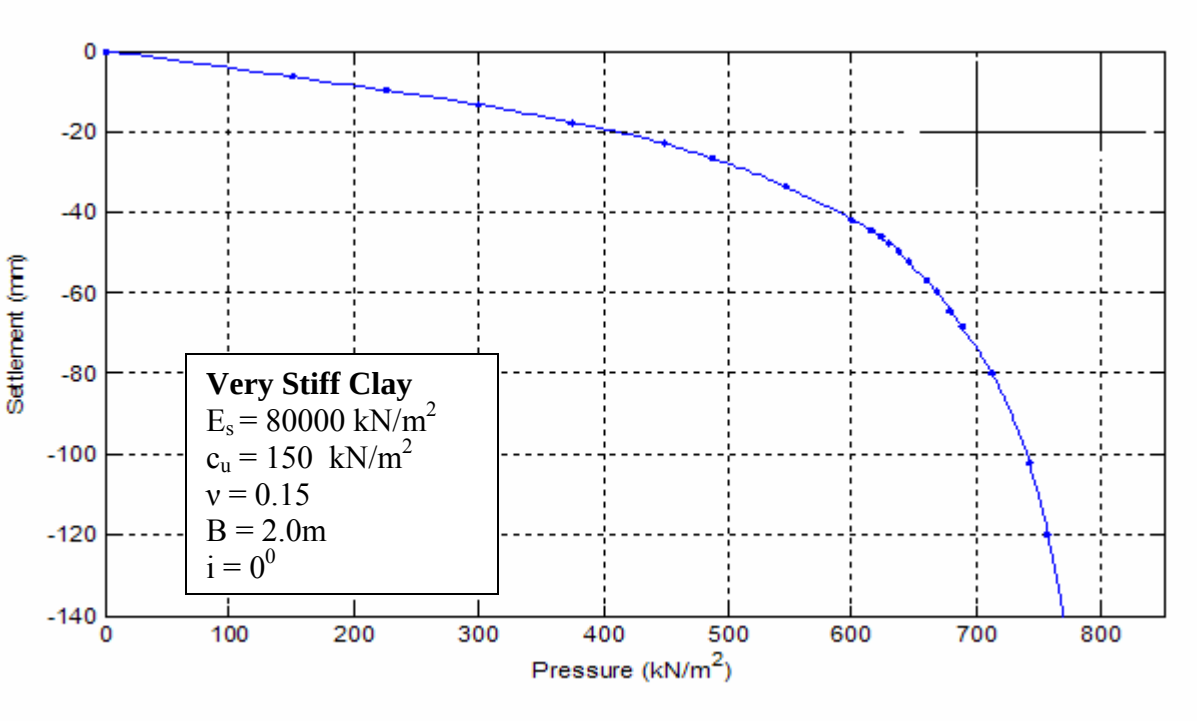

Figure 4.5, Pressure Vs Elasto-plastic Settlement Curve of Strip Footing under Centrally Vertical Load

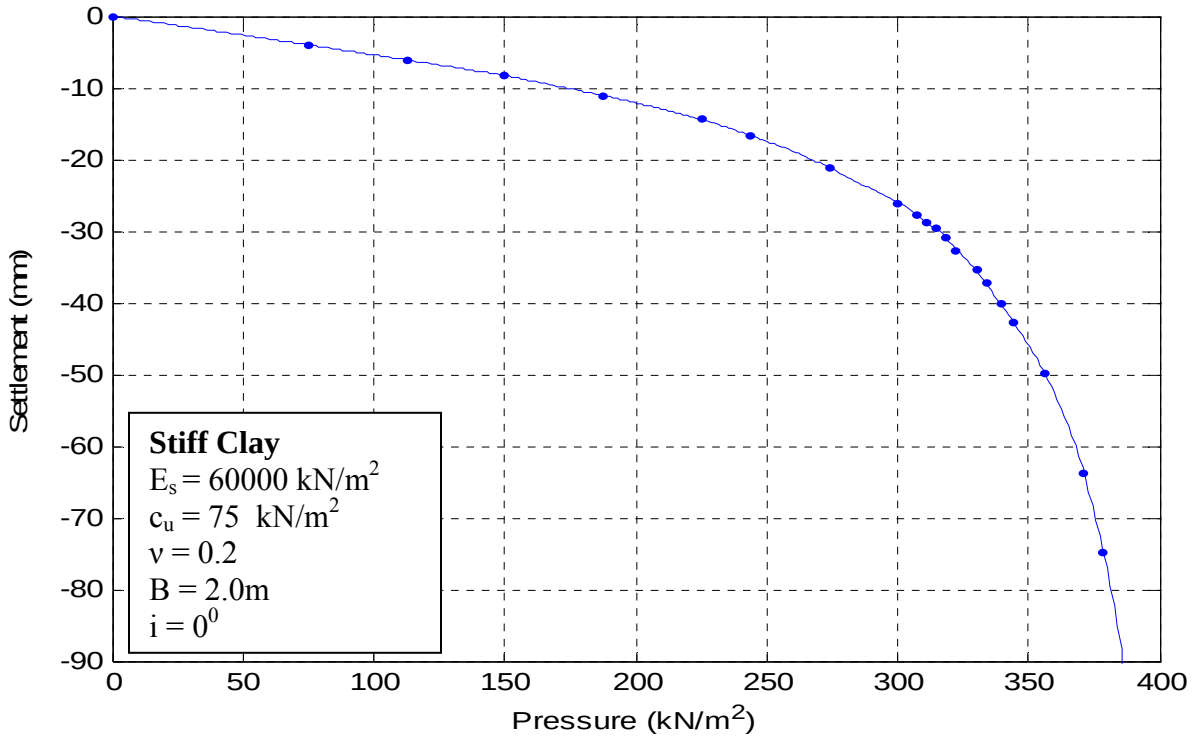

Figure 4.6, Pressure Vs Elasto-plastic Settlement Curve of Strip Footing under Centrally Vertical Load

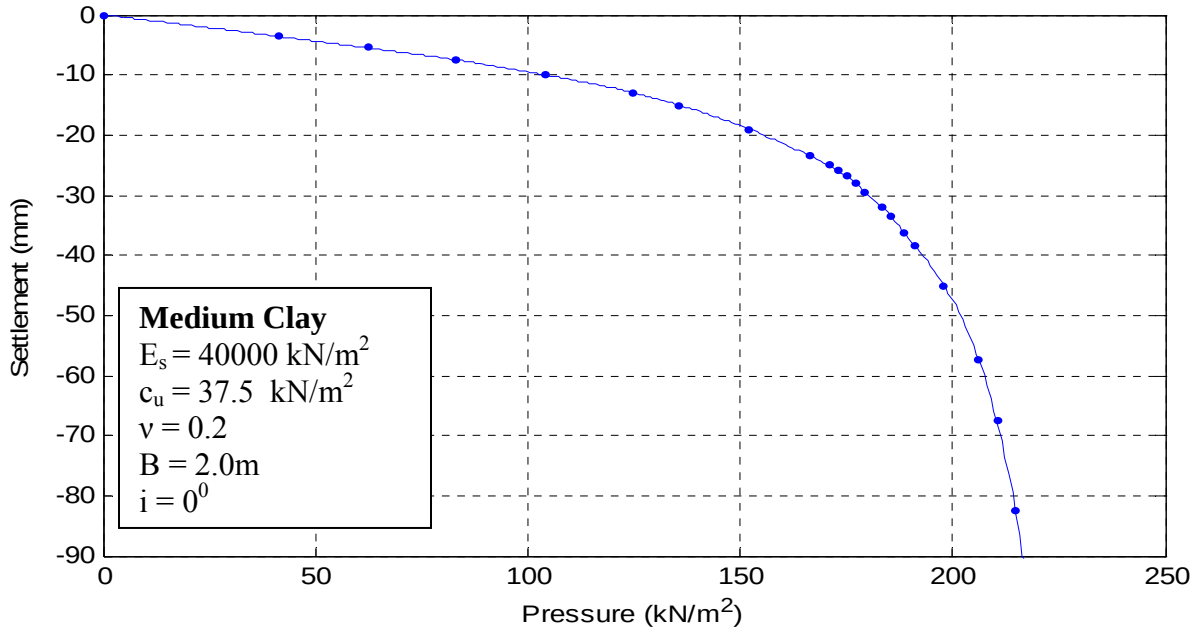

Figure 4.7, Pressure Vs Elasto-plastic Settlement Curve of Strip Footing under Centrally Vertical Load

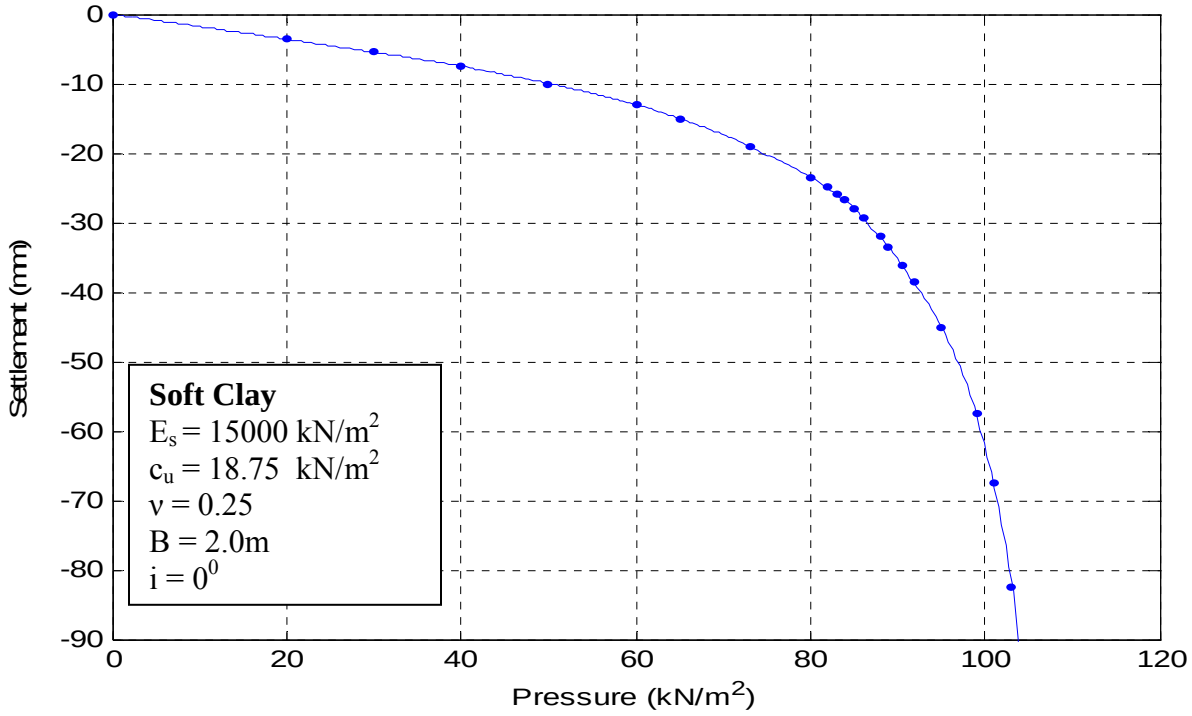

Figure 4.8, Pressure Vs Elasto-plastic Settlement Curve of Strip Footing under Centrally Vertical Load

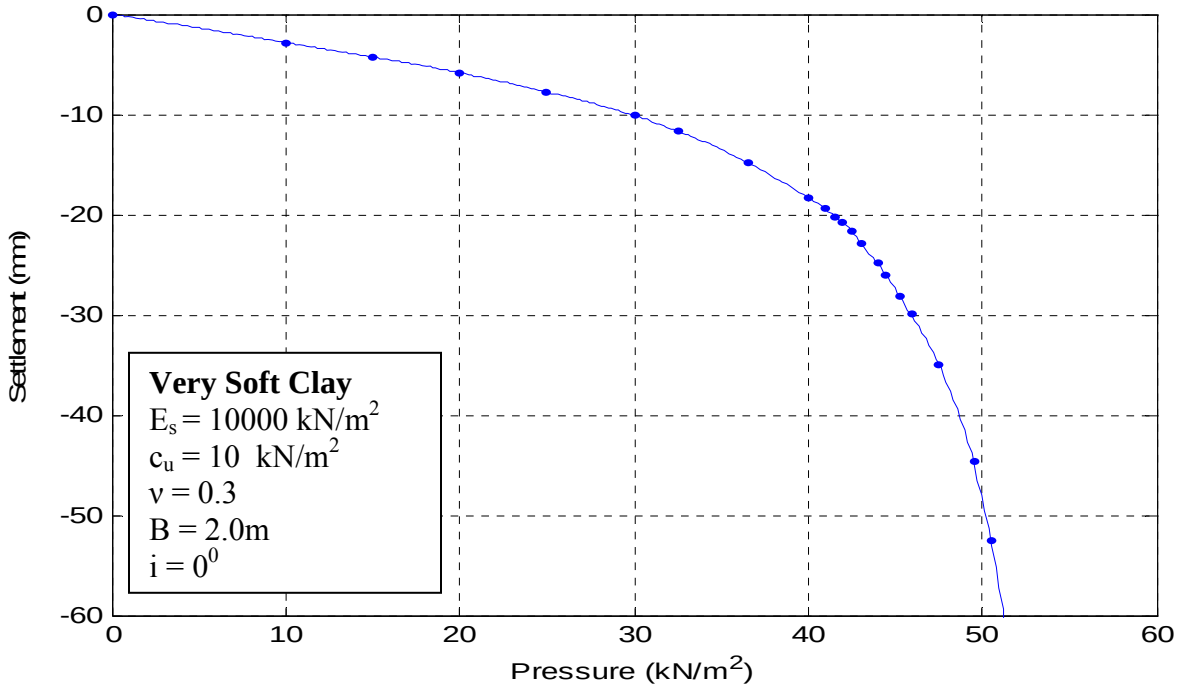

Figure 4.9, Pressure Vs Elasto-plastic Settlement Curve of Strip Footing under Centrally Vertical Load

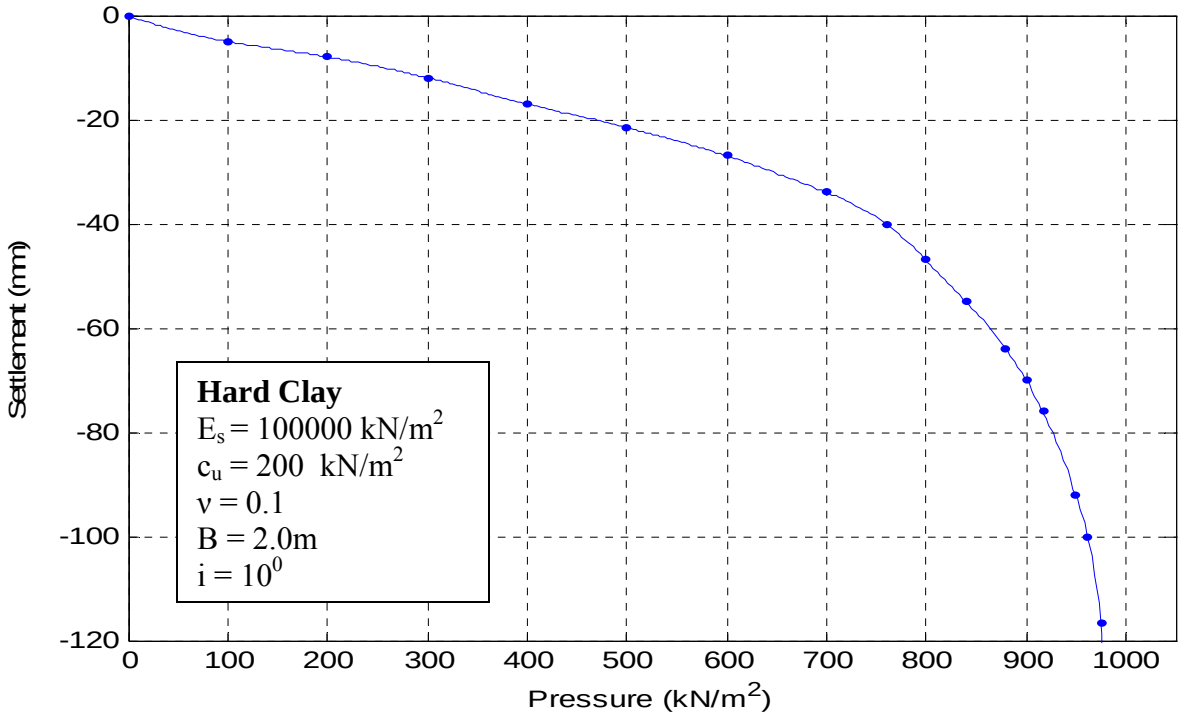

Figure 4.10, Pressure Vs Elasto-plastic Settlement Curve of Strip Footing under Centrally Vertical Load

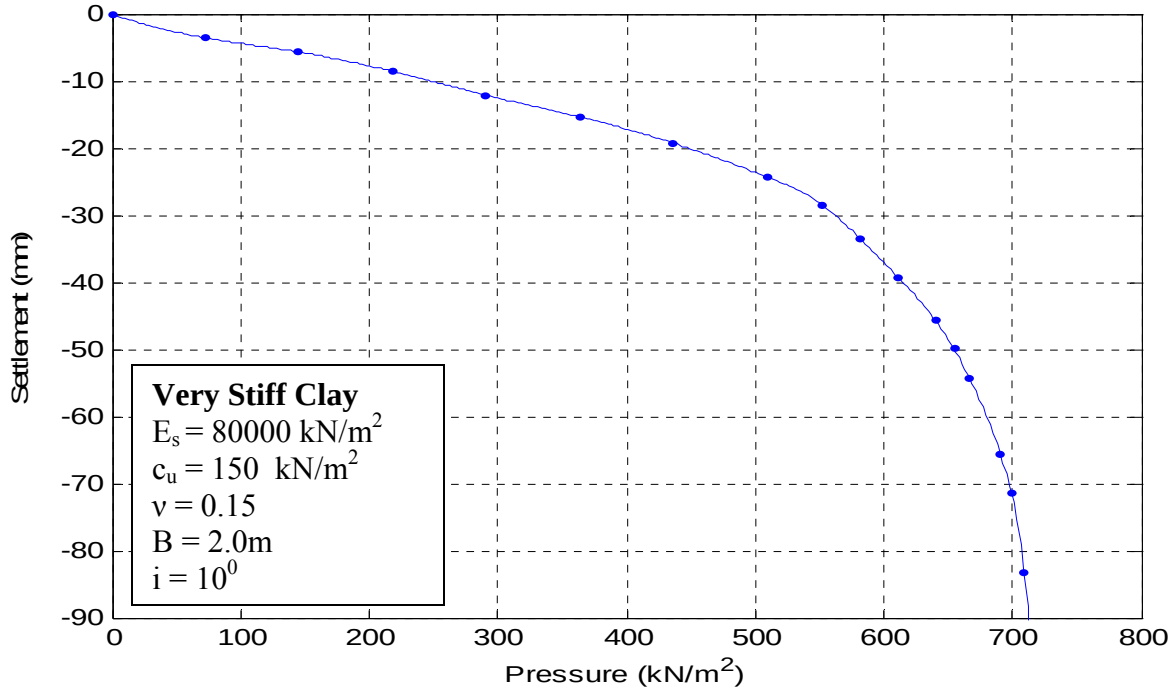

Figure 4.11, Pressure Vs Elasto-plastic Settlement Curve of Strip Footing under Centrally Inclined Load

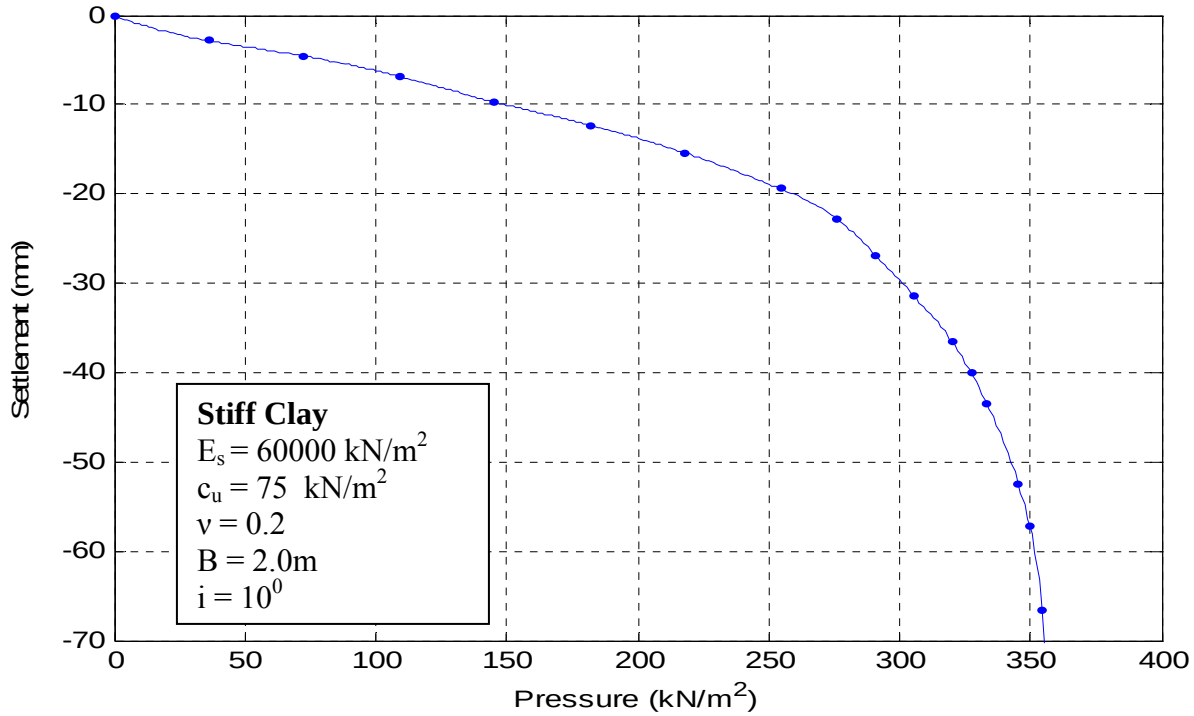

Figure 4.12, Pressure Vs Elasto-plastic Settlement Curve of Strip Footing under Centrally Inclined Load

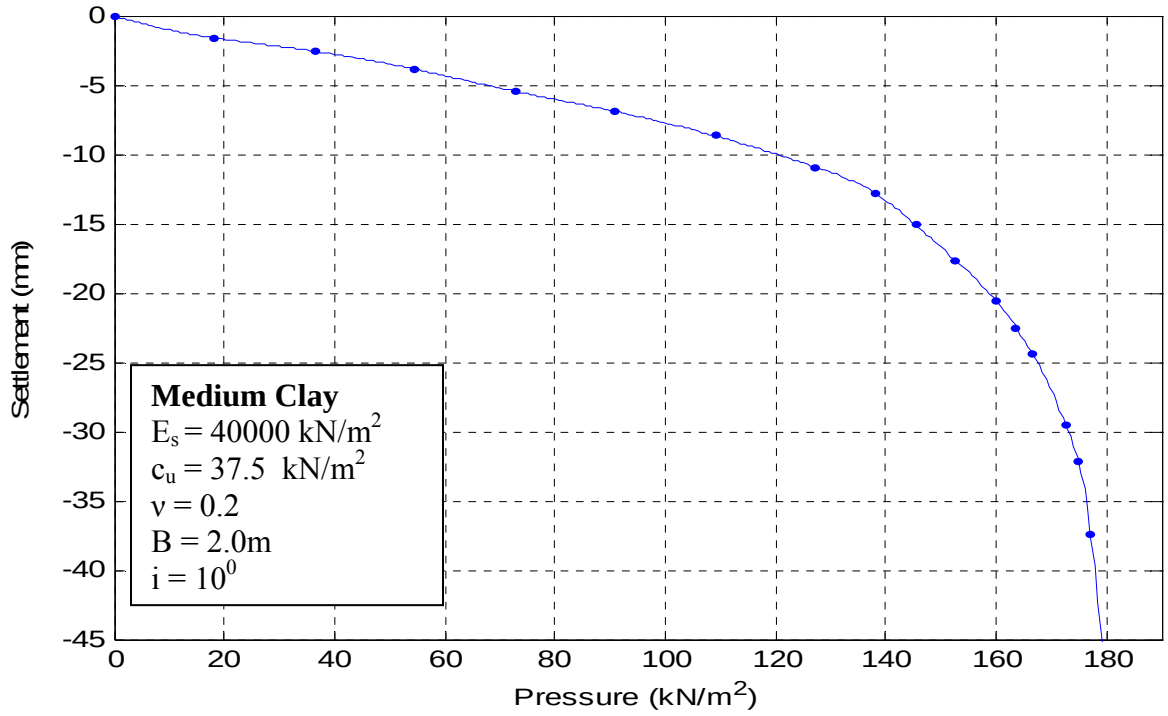

Figure 4.13, Pressure Vs Elasto-plastic Settlement Curve of Strip Footing under Centrally Inclined Load

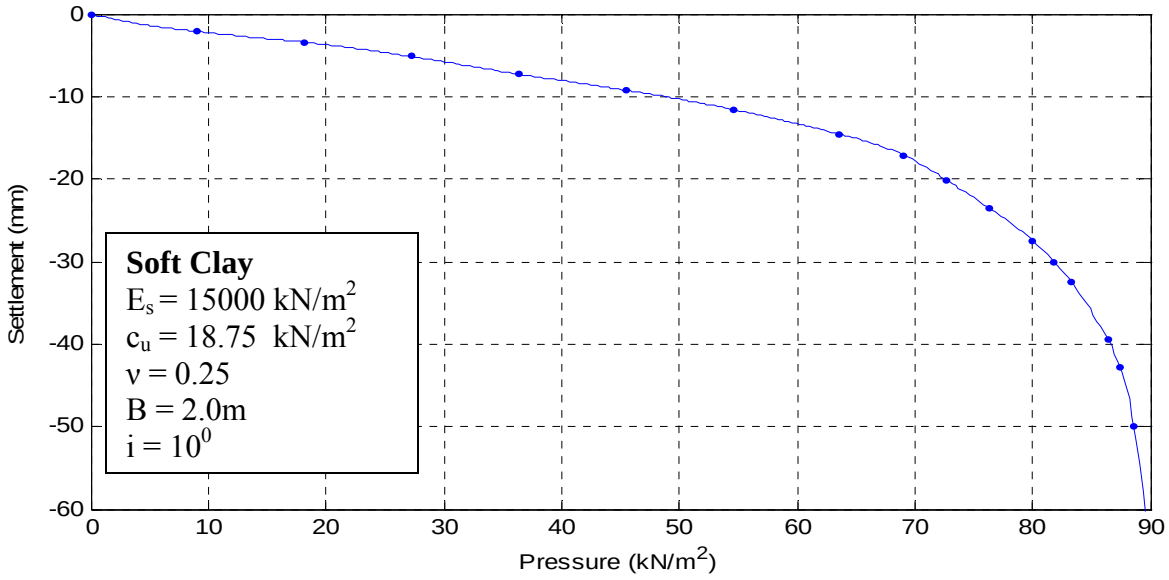

Figure 4.14, Pressure Vs Elasto-plastic Settlement Curve of Strip Footing under Centrally Inclined Load

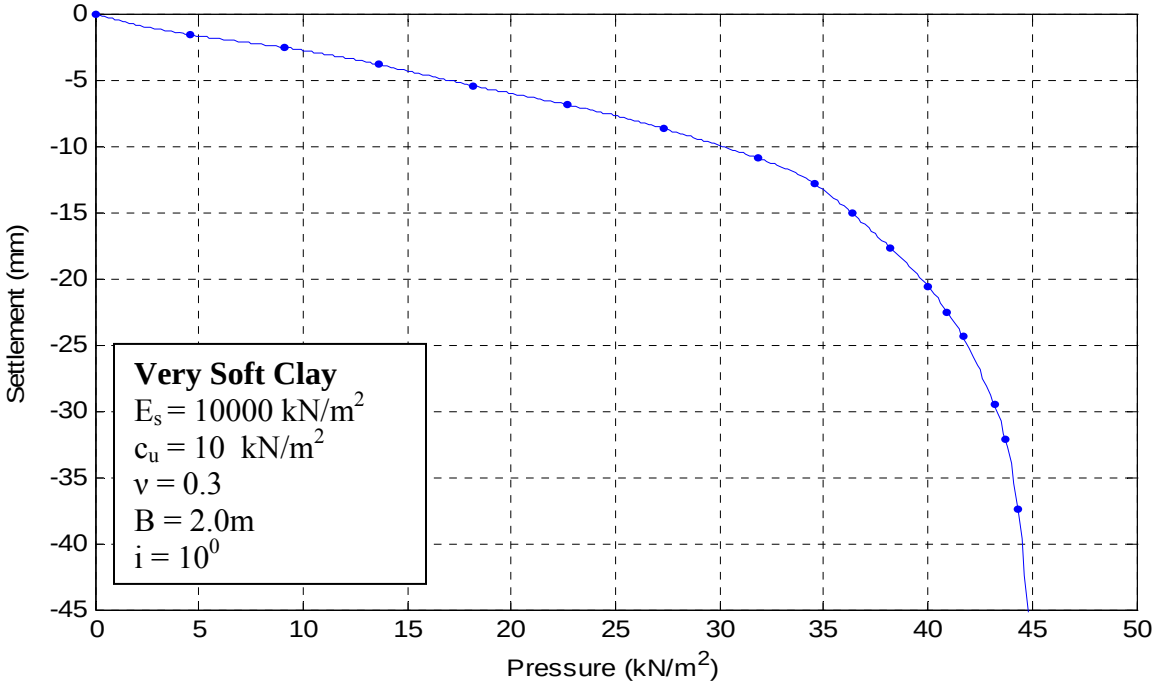

Figure 4.15, Pressure Vs Elasto-plastic Settlement Curve of Strip Footing under Centrally Inclined Load

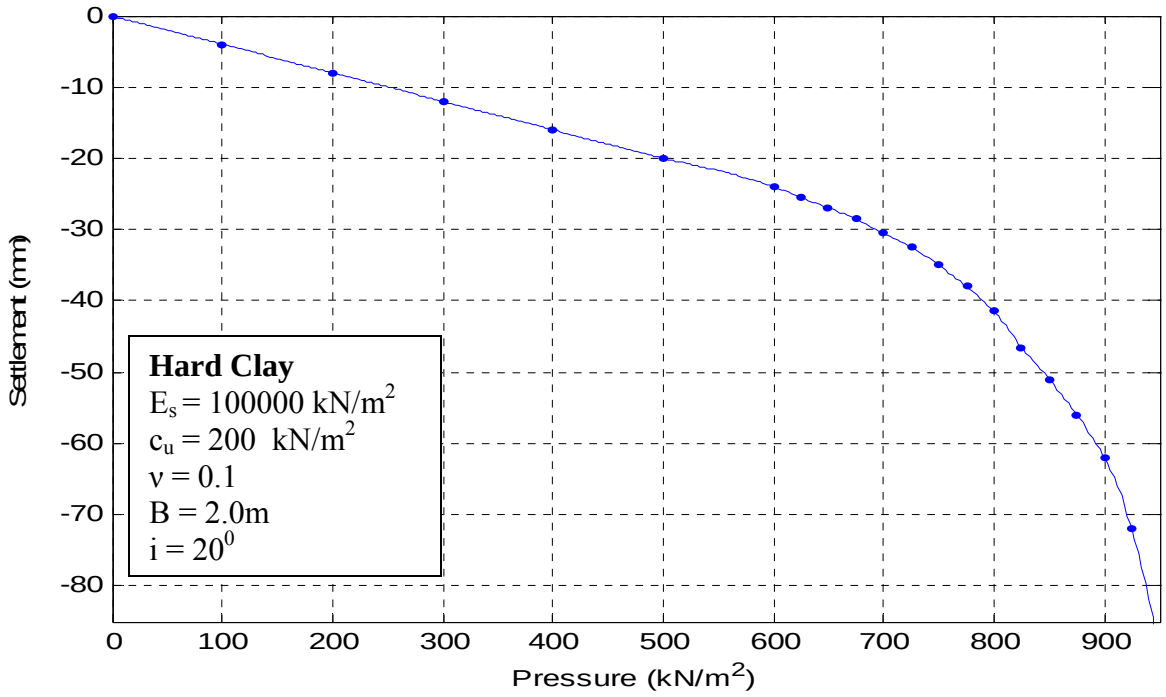

Figure 4.16, Pressure Vs Elasto-plastic Settlement Curve of Strip Footing under Centrally Inclined Load

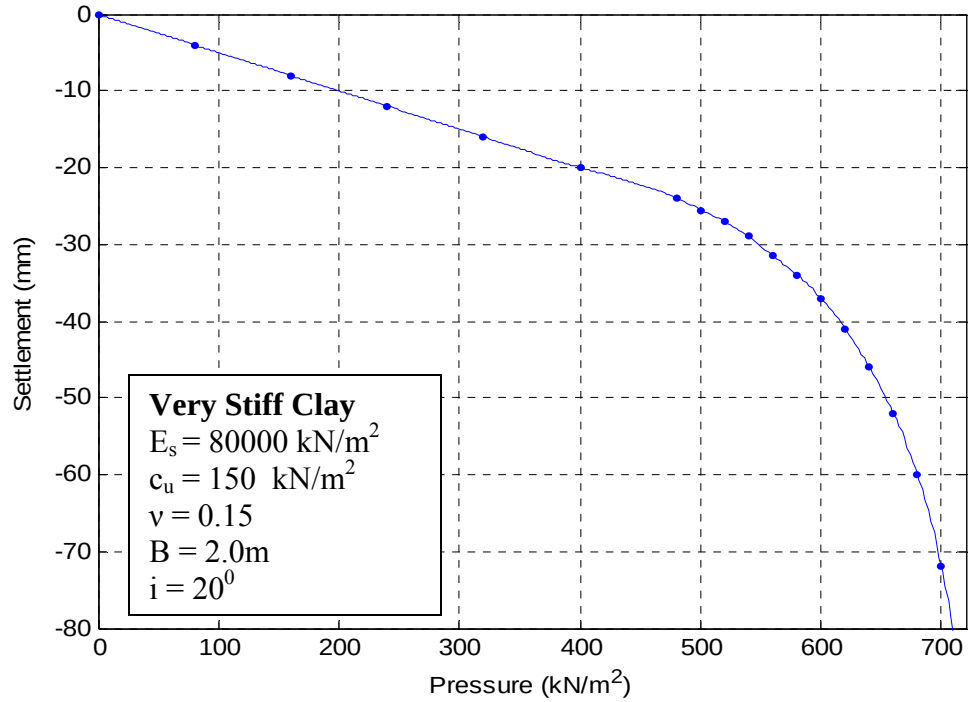

Figure 4.17, Pressure Vs Elasto-plastic Settlement Curve of Strip Footing under Centrally Inclined Load

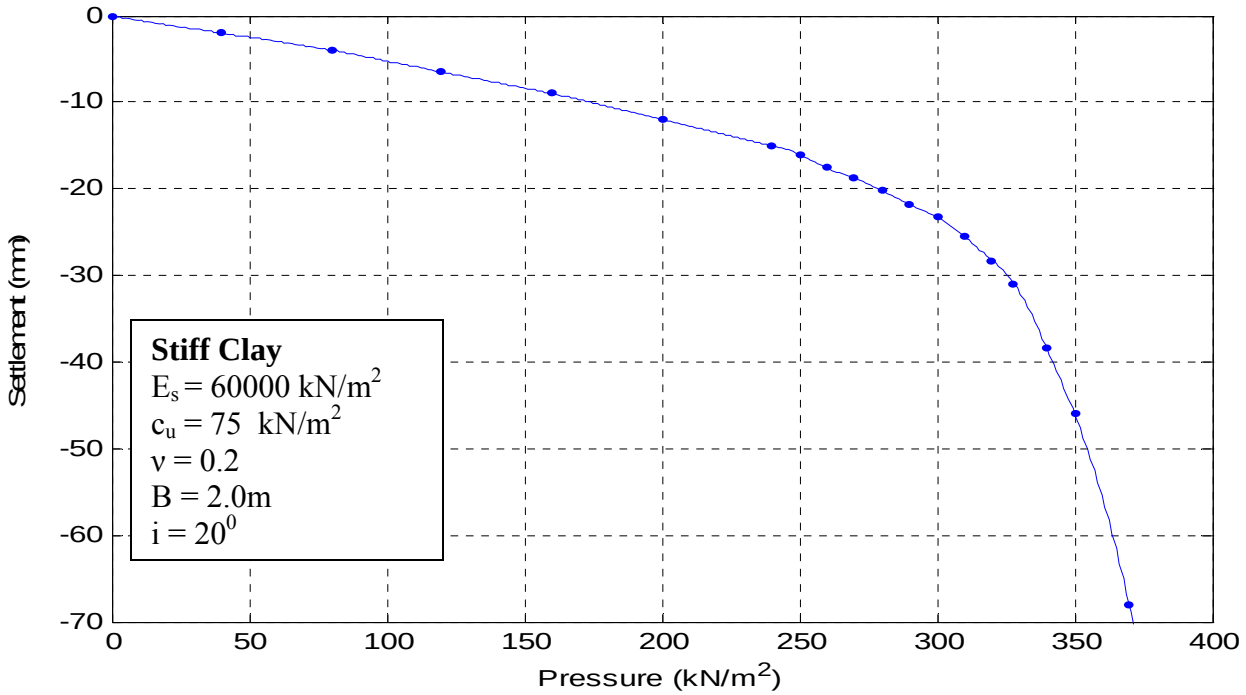

Figure 4.18, Pressure Vs Elasto-plastic Settlement Curve of Strip Footing under Centrally Inclined Load

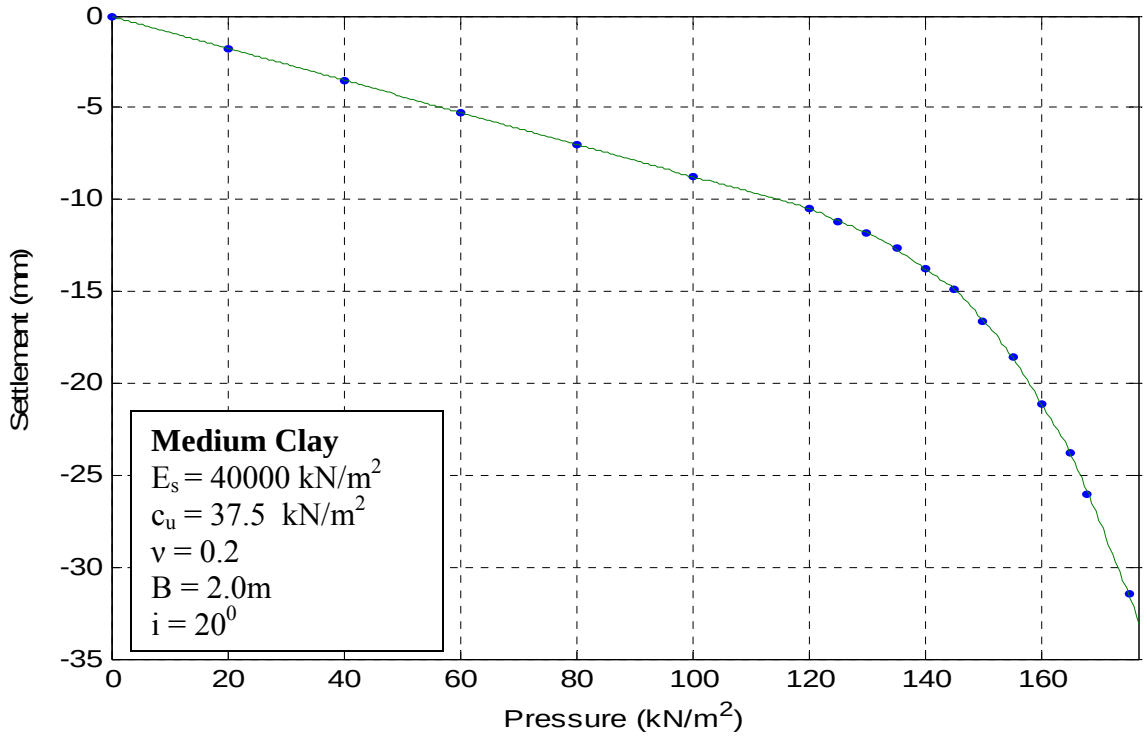

Figure 4.19, Pressure Vs Elasto-plastic Settlement Curve of Strip Footing under Centrally Inclined Load

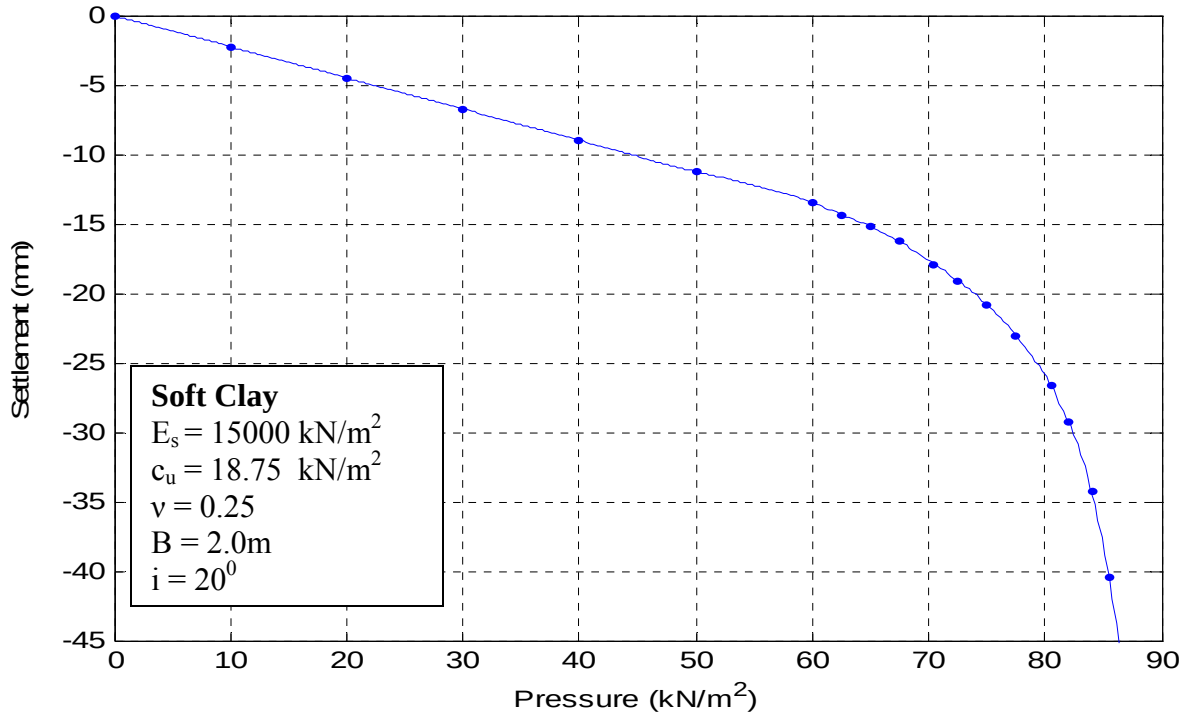

Figure 4.20, Pressure Vs Elasto-plastic Settlement Curve of Strip Footing under Centrally Inclined Load

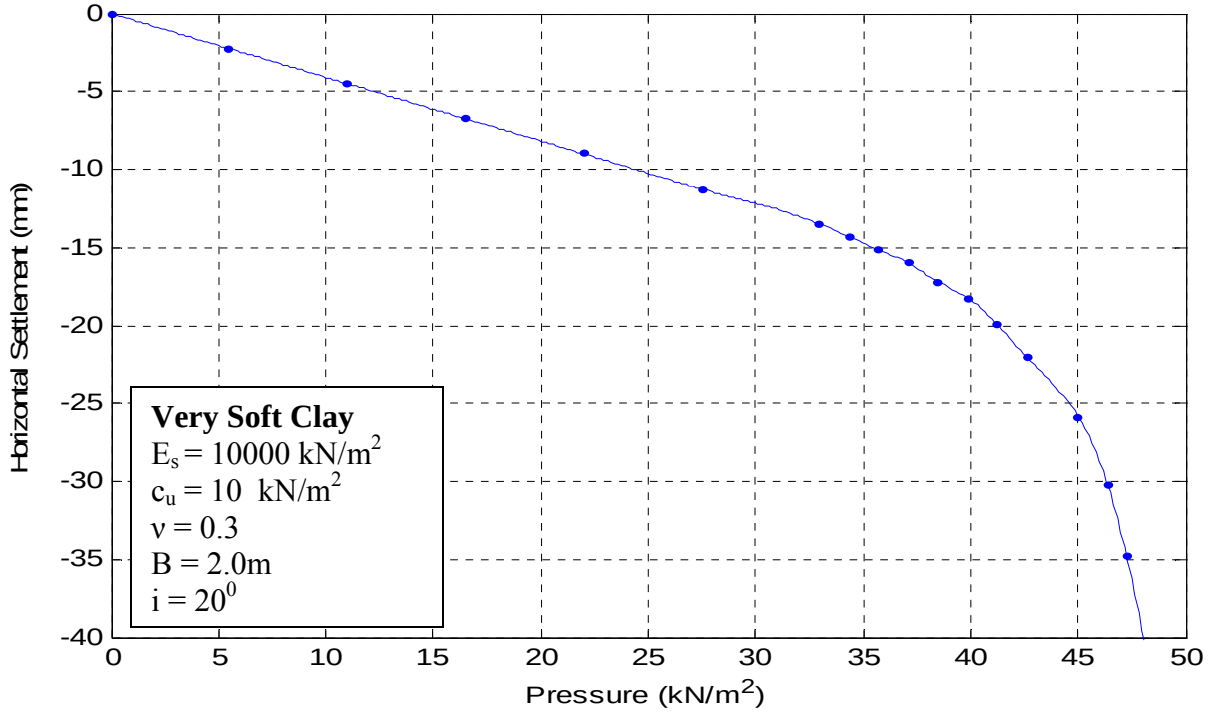

Figure 4.21, Pressure Vs Elasto-plastic Settlement Curve of Strip Footing under Centrally Inclined Load

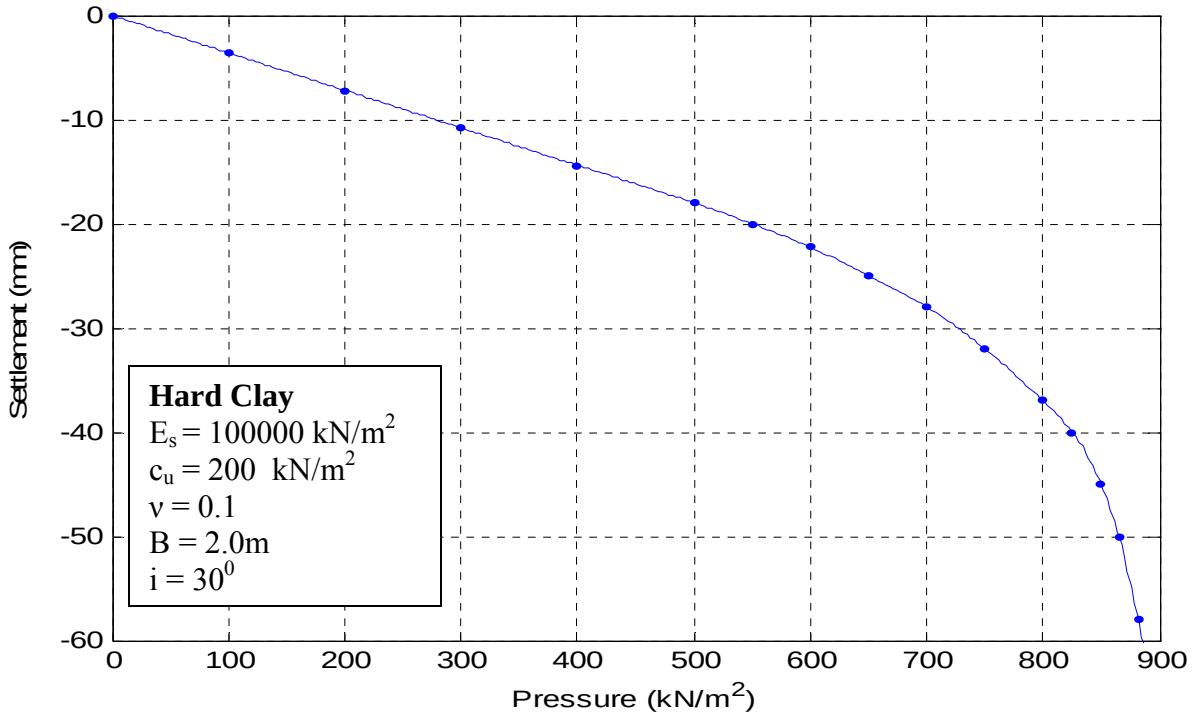

Figure 4.22, Pressure Vs Elasto-plastic Settlement Curve of Strip Footing under Centrally Inclined Load

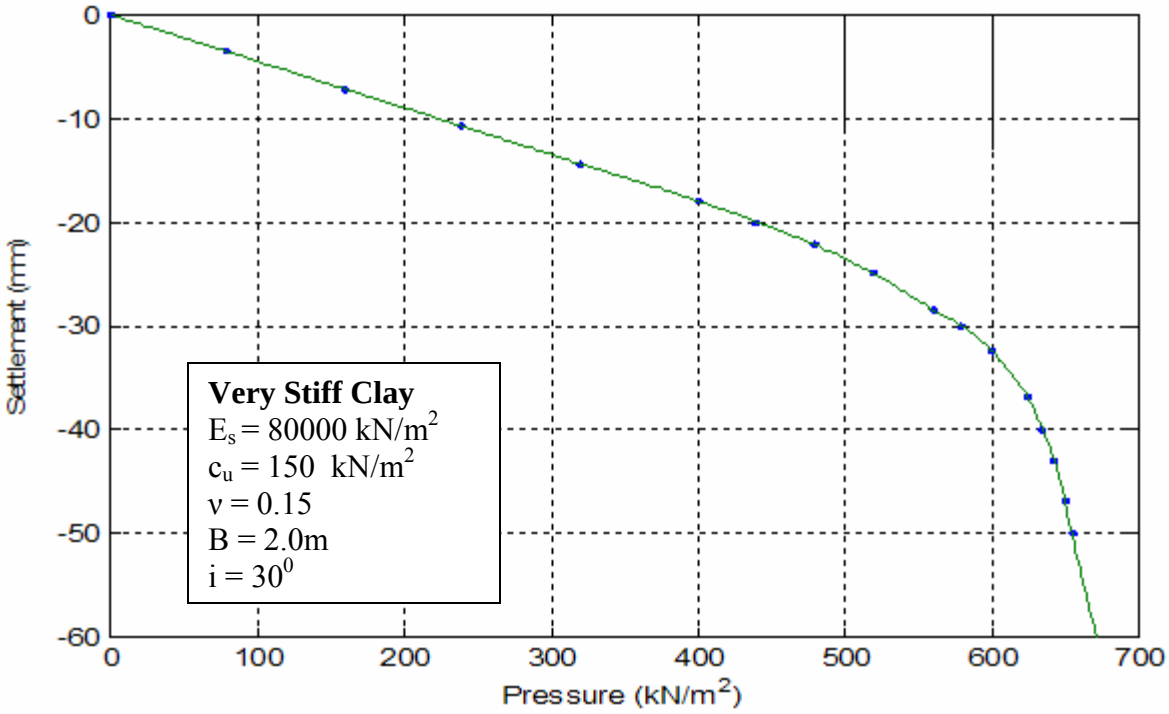

Figure 4.23, Pressure Vs Elasto-plastic Settlement Curve of Strip Footing under Centrally Inclined Load

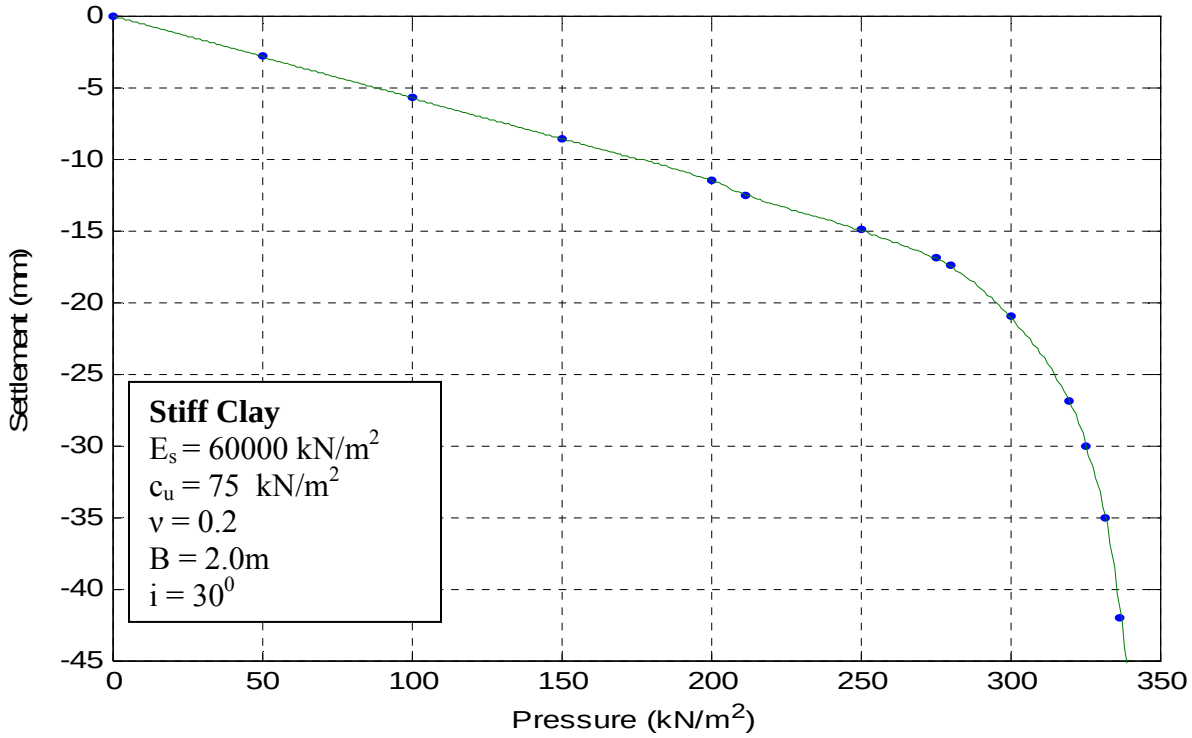

Figure 4.24, Pressure Vs Elasto-plastic Settlement Curve of Strip Footing under Centrally Inclined Load

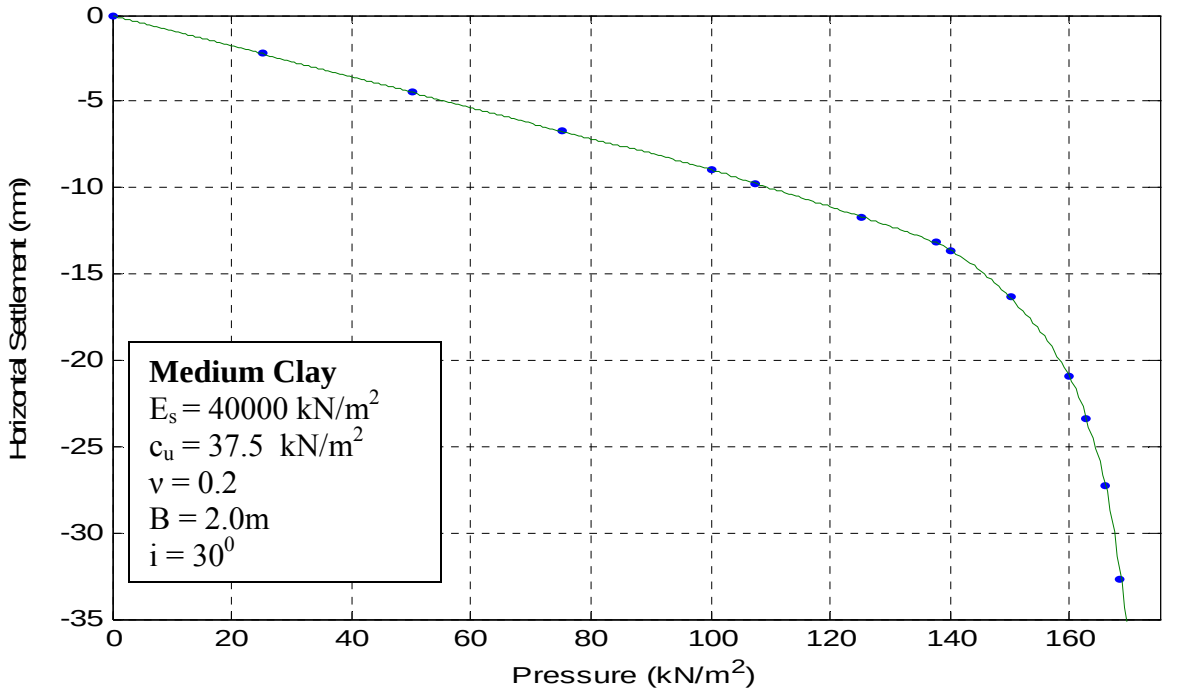

Figure 4.25, Pressure Vs Elasto-plastic Settlement Curve of Strip Footing under Centrally Inclined Load

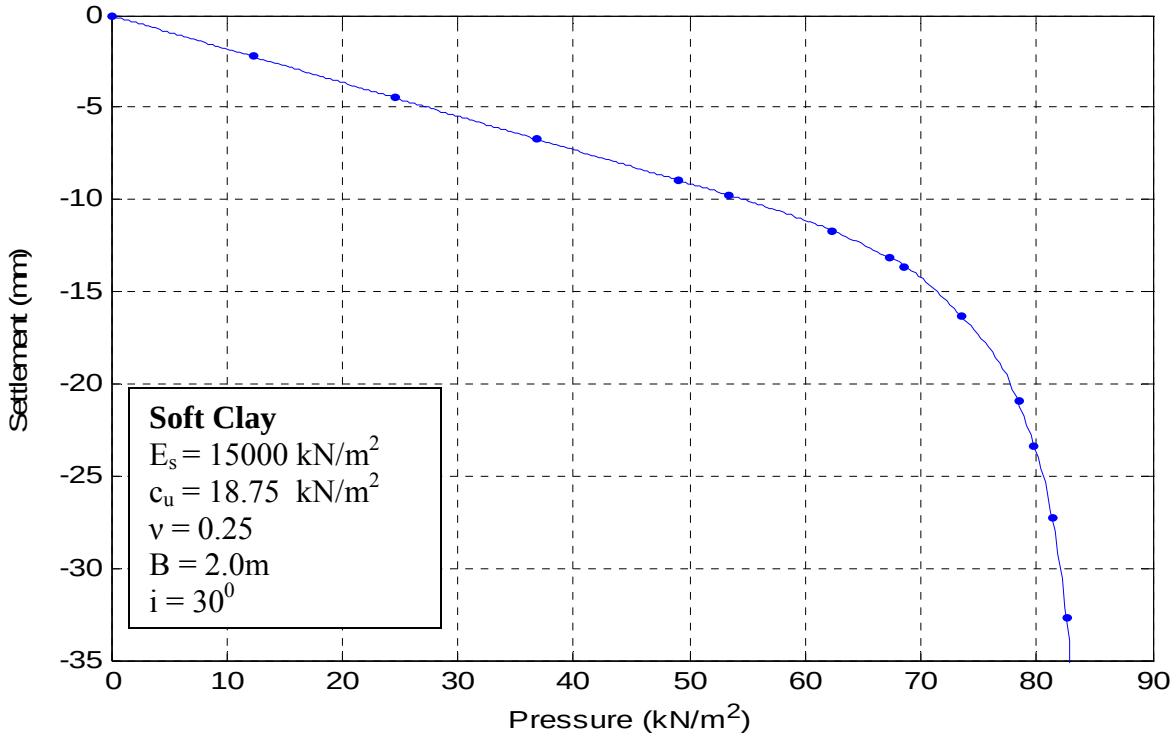

Figure 4.26, Pressure Vs Elasto-plastic Settlement Curve of Strip Footing under Centrally Inclined Load

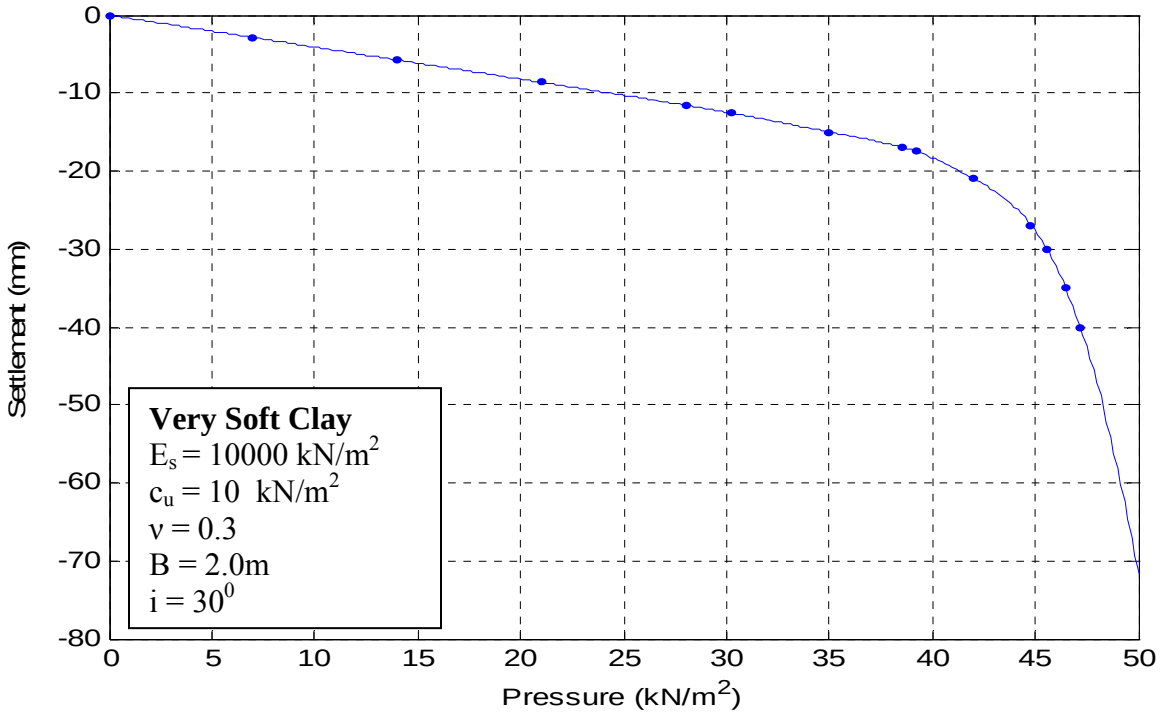

Figure 4.27, Pressure Vs Elasto-plastic Settlement Curve of Strip Footing under Centrally Inclined Load

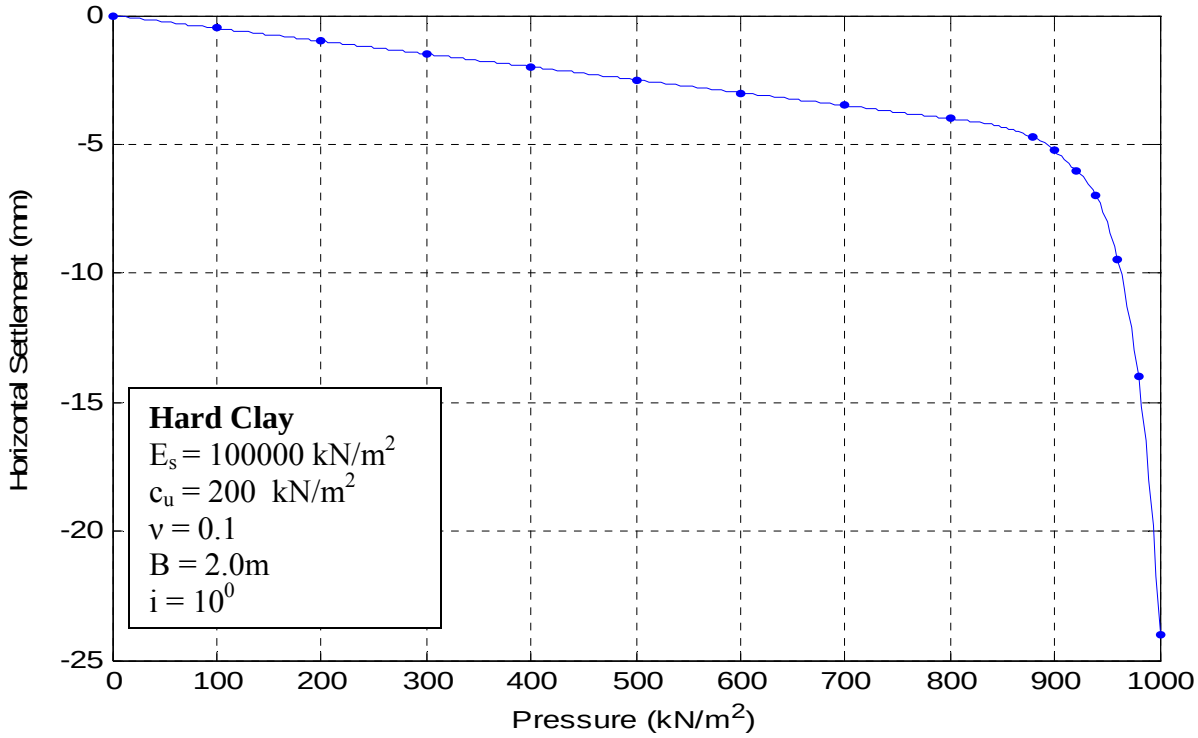

Figure 4.28, Pressure Vs Elasto-plastic Horizontal Settlement Curve of Strip Footing under Centrally Inclined Load

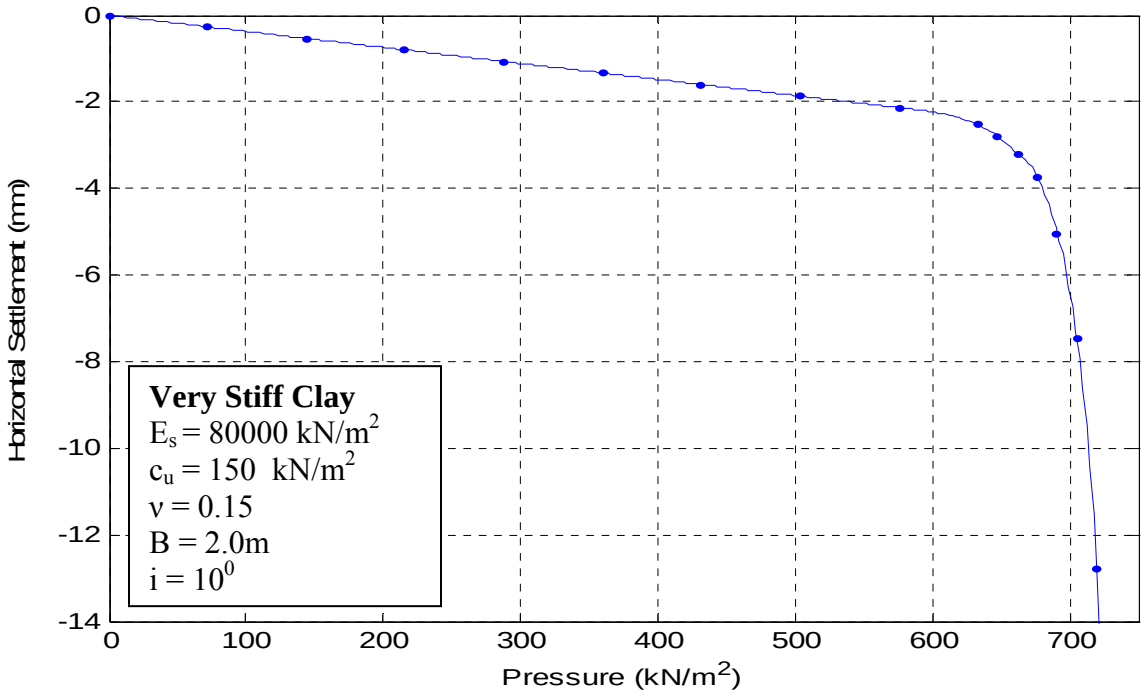

Figure 4.29, Pressure Vs Elasto-plastic Horizontal Settlement Curve of Strip Footing under Centrally Inclined Load

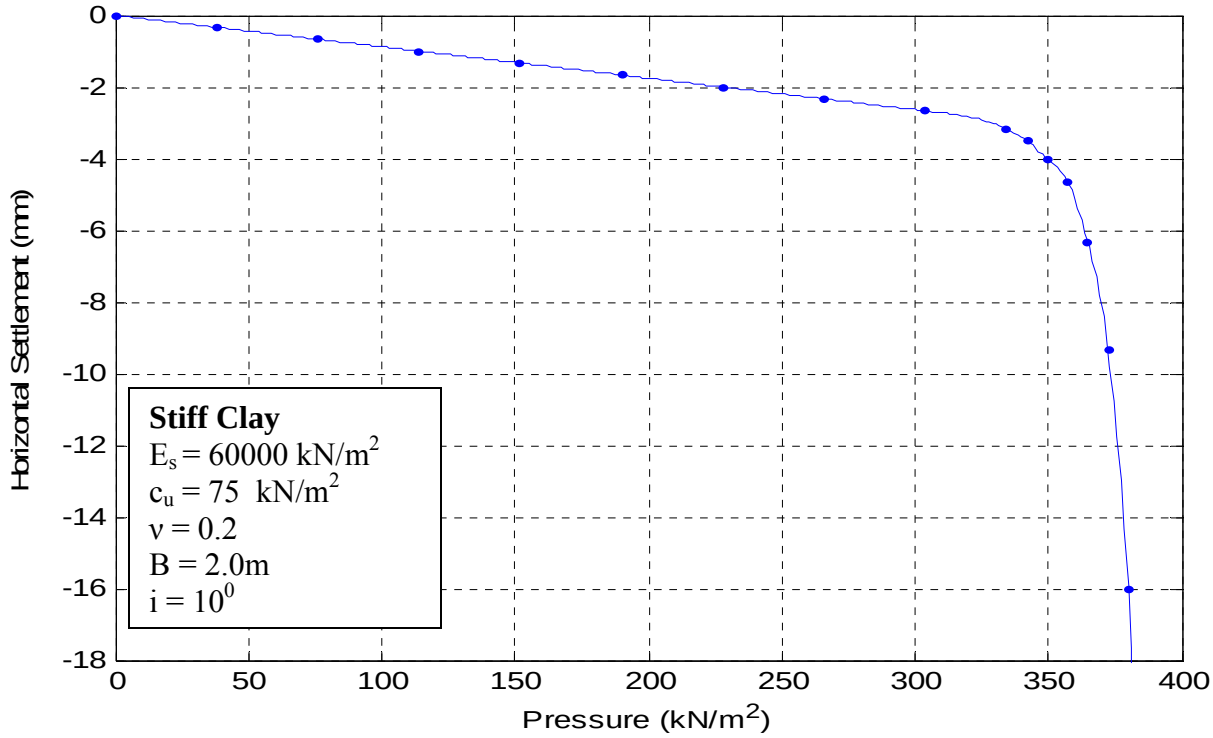

Figure 4.30, Pressure Vs Elasto-plastic Horizontal Settlement Curve of Strip Footing under Centrally Inclined Load

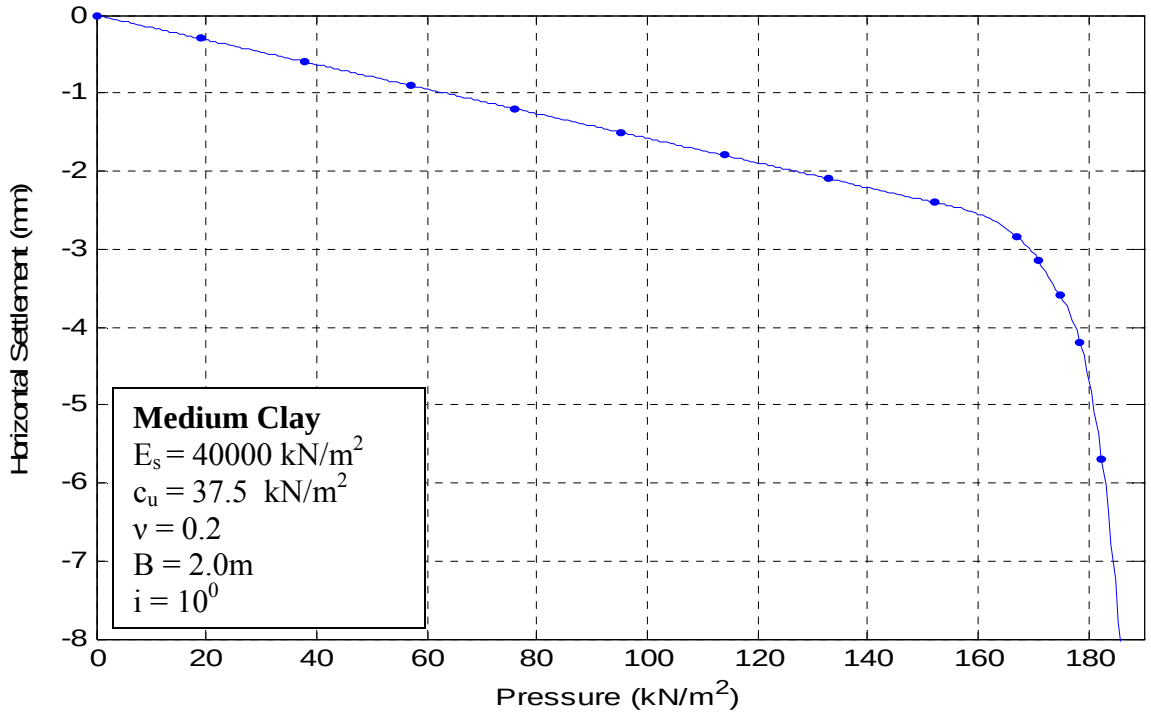

Figure 4.31, Pressure Vs Elasto-plastic Horizontal Settlement Curve of Strip Footing under Centrally Inclined Load

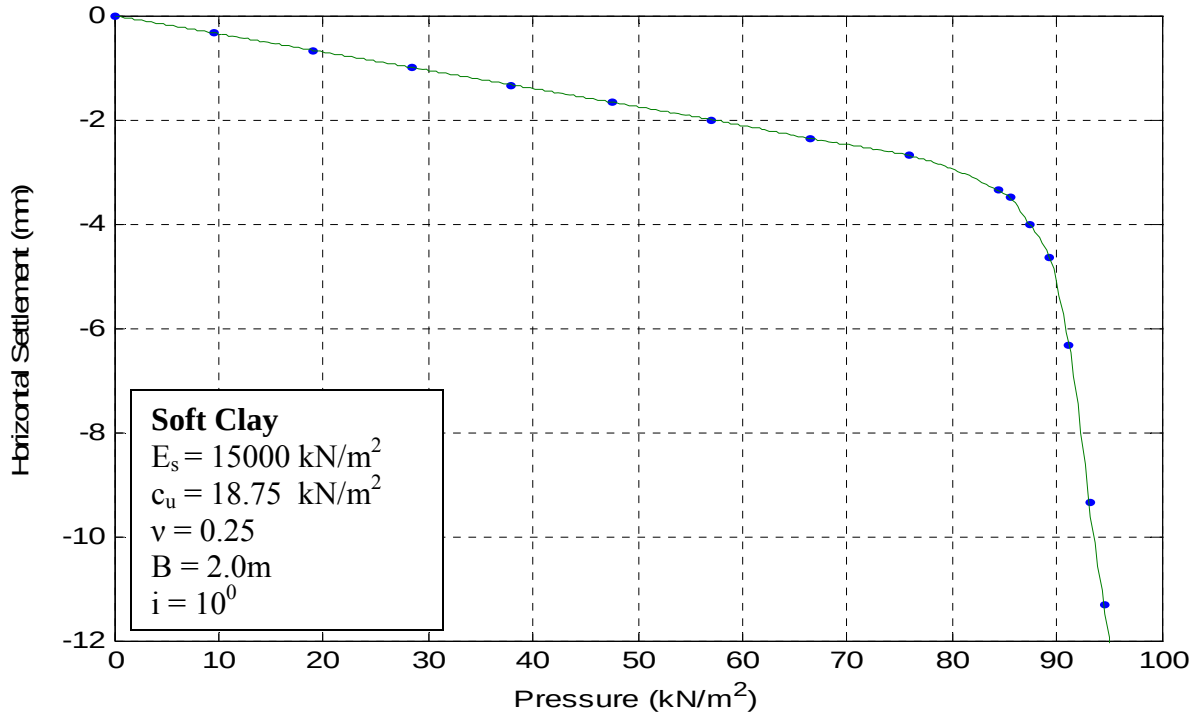

Figure 4.32, Pressure Vs Elasto-plastic Horizontal Settlement Curve of Strip Footing under Centrally Inclined Load

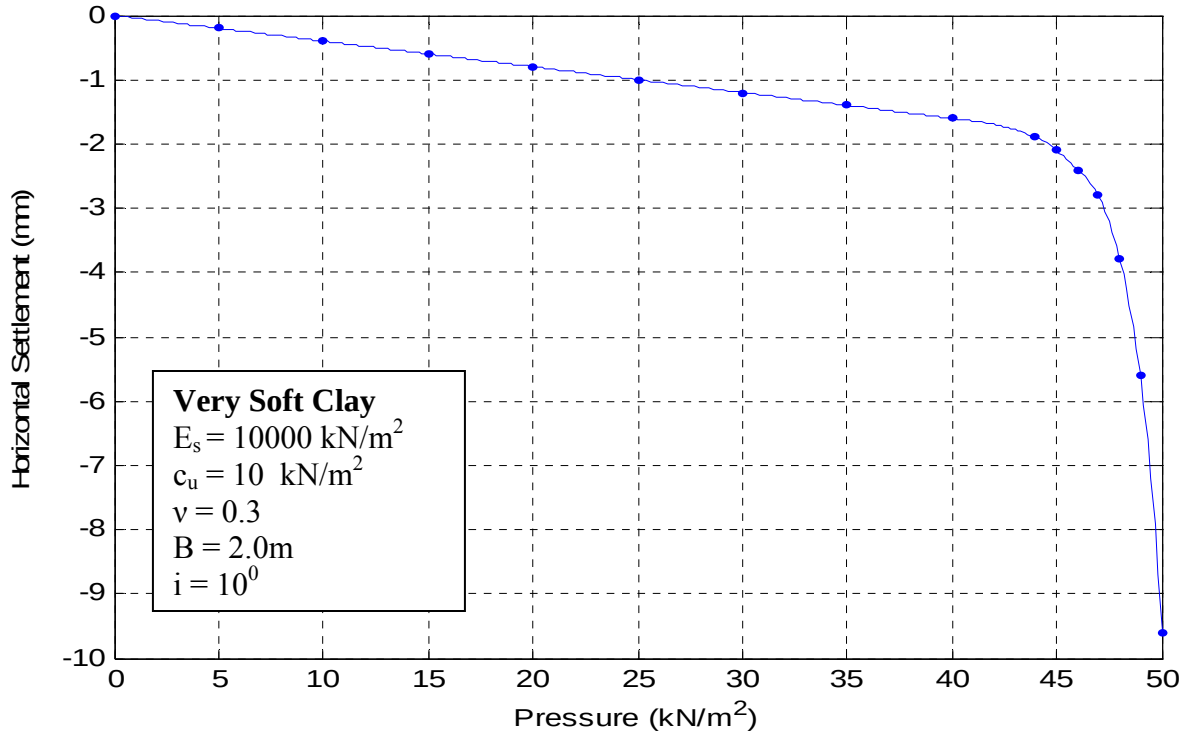

Figure 4.33, Pressure Vs Elasto-plastic Horizontal Settlement Curve of Strip Footing under Centrally Inclined Load

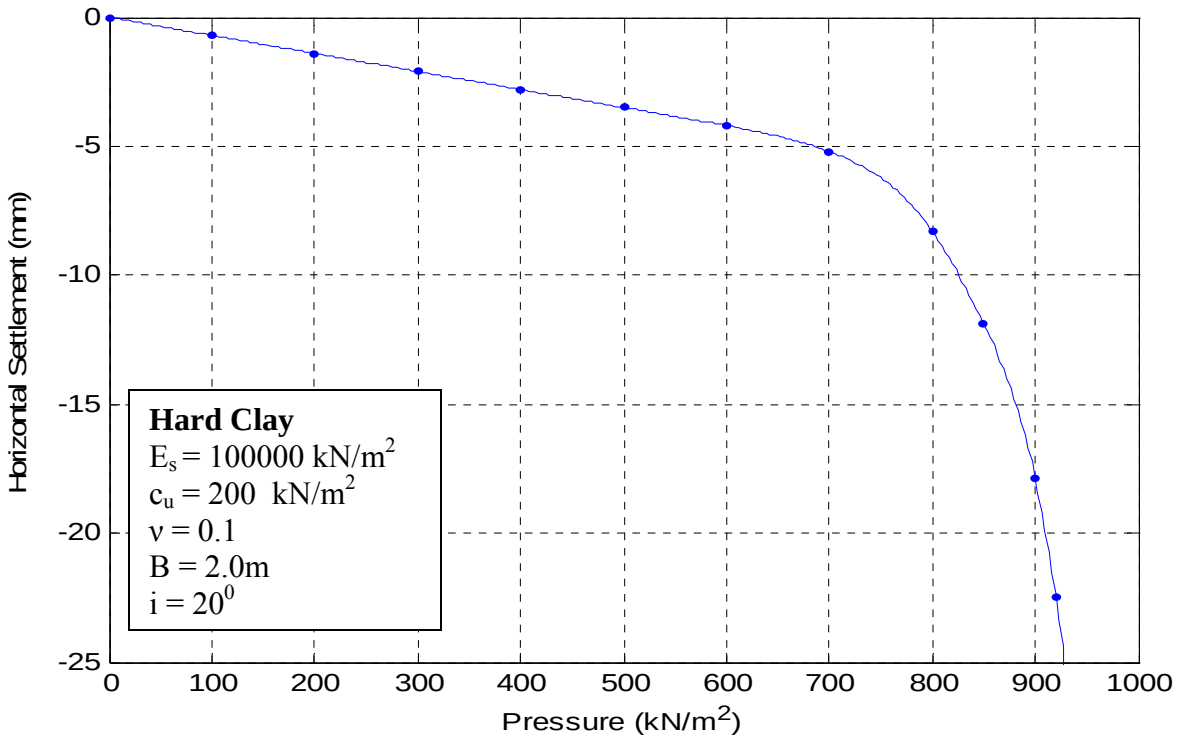

Figure 4.34, Pressure Vs Elasto-plastic Horizontal Settlement Curve of Strip Footing under Centrally Inclined Load

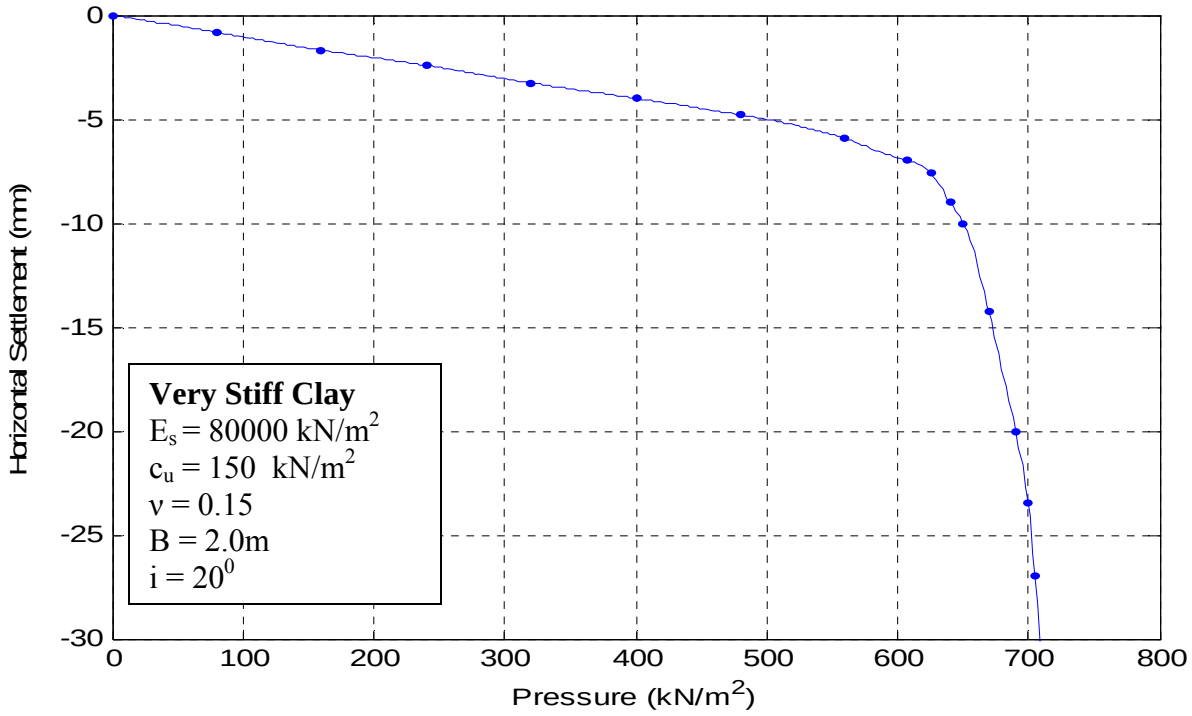

Figure 4.35, Pressure Vs Elasto-plastic Horizontal Settlement Curve of Strip Footing under Centrally Inclined Load

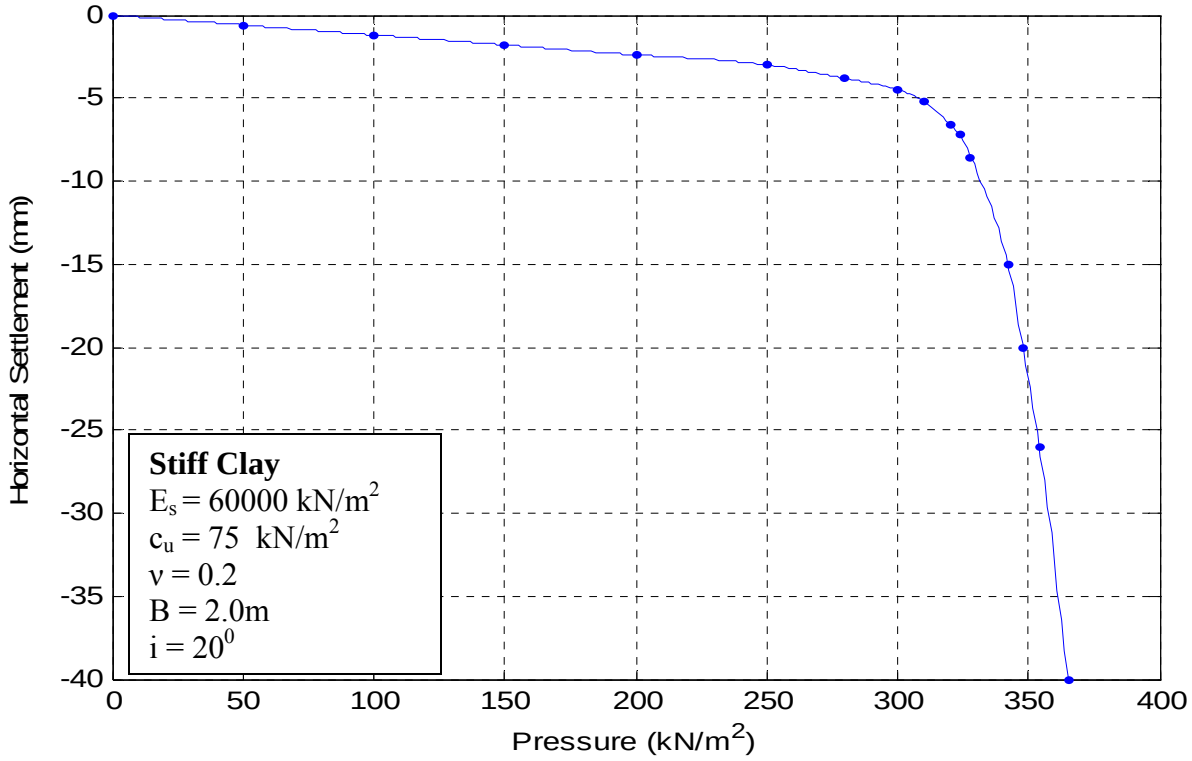

Figure 4.36, Pressure Vs Elasto-plastic Horizontal Settlement Curve of Strip Footing under Centrally Inclined Load

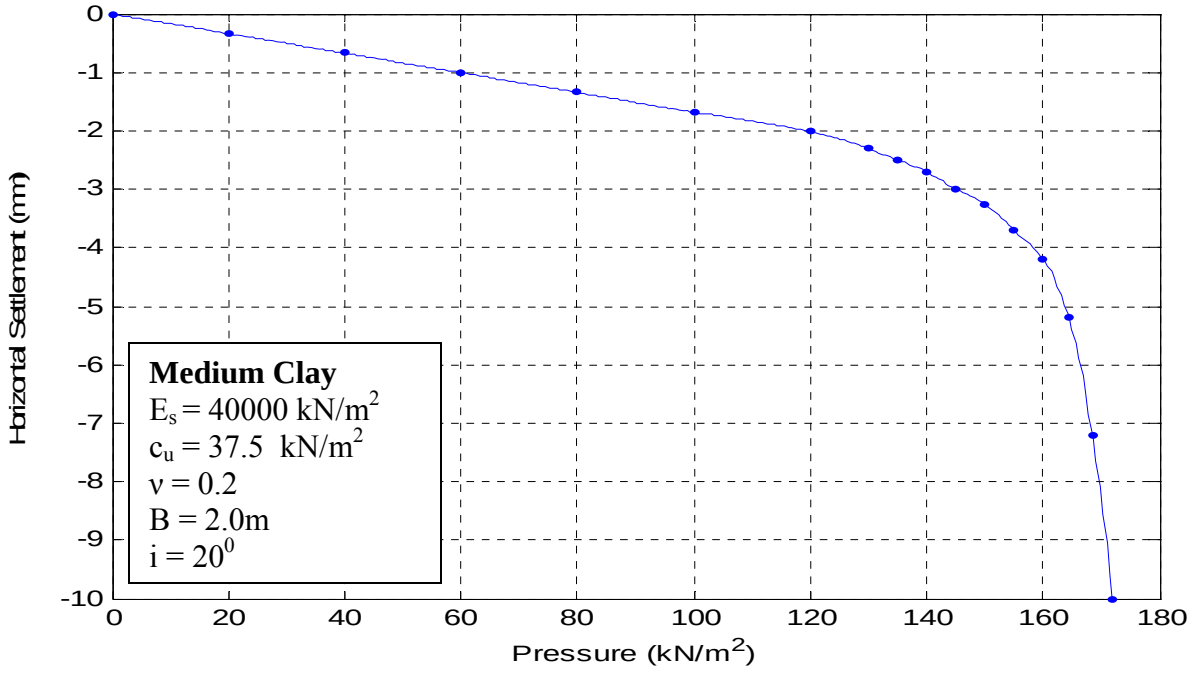

Figure 4.37, Pressure Vs Elasto-plastic Horizontal Settlement Curve of Strip Footing under Centrally Inclined Load

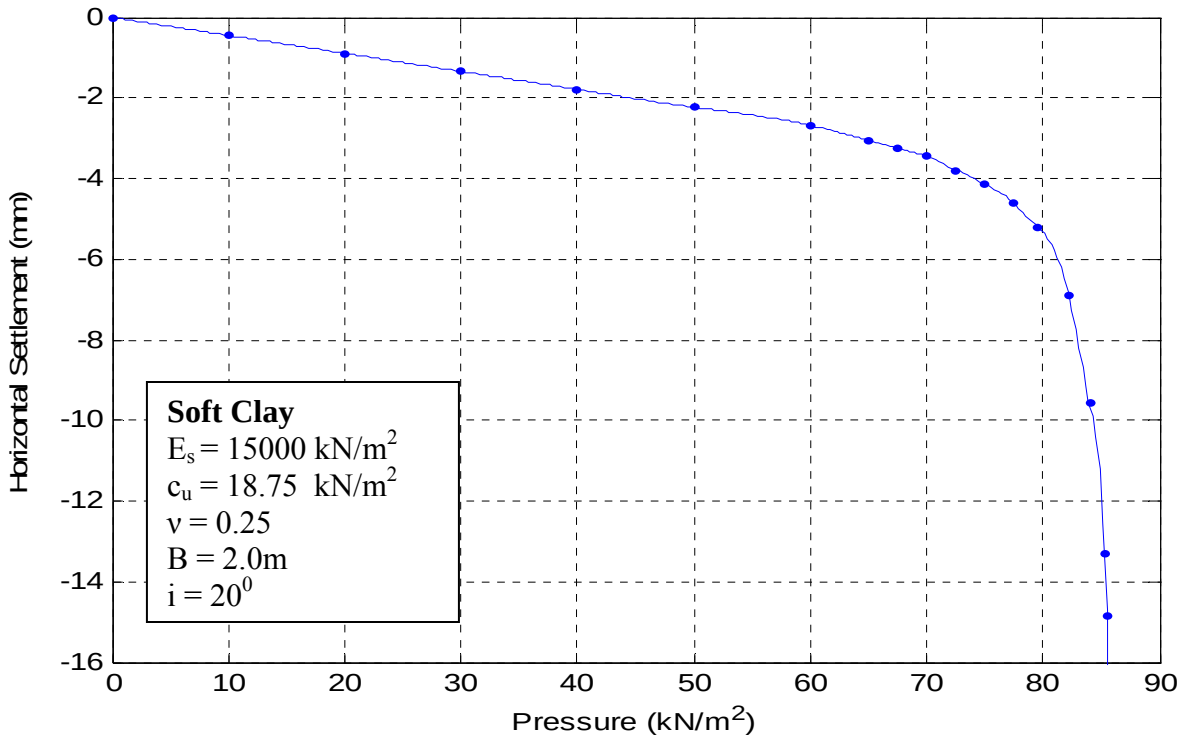

Figure 4.38, Pressure Vs Elasto-plastic Horizontal Settlement Curve of Strip Footing under Centrally Inclined Load

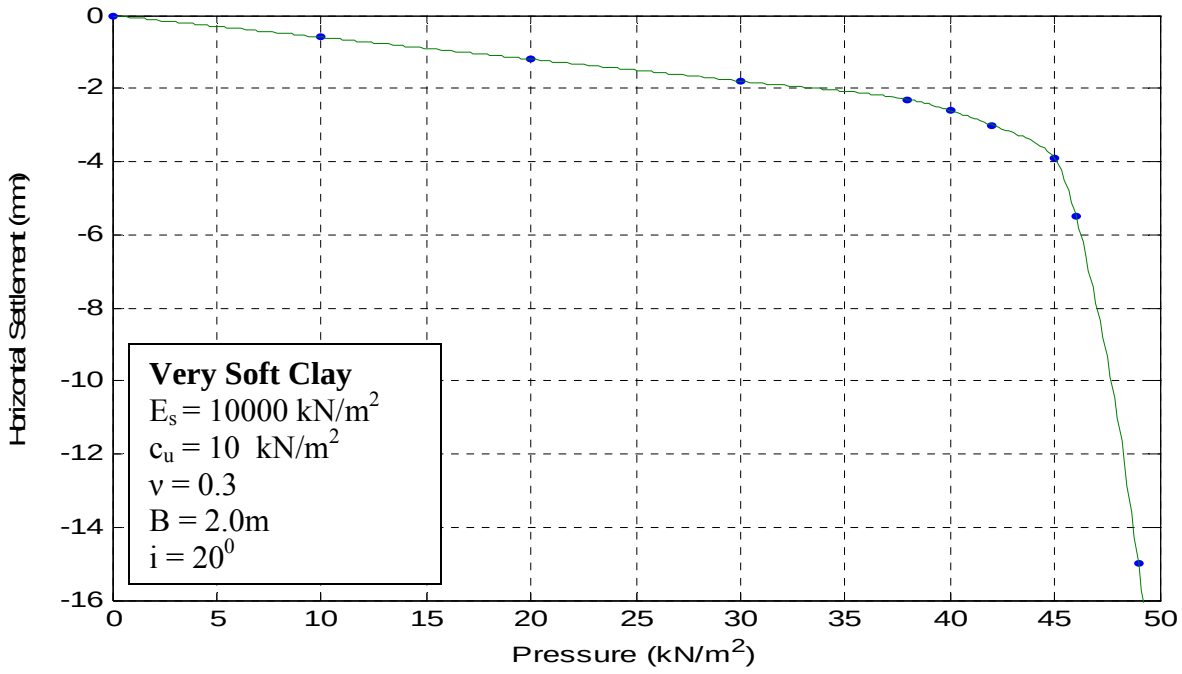

Figure 4.39, Pressure Vs Elasto-plastic Horizontal Settlement Curve of Strip Footing under Centrally Inclined Load

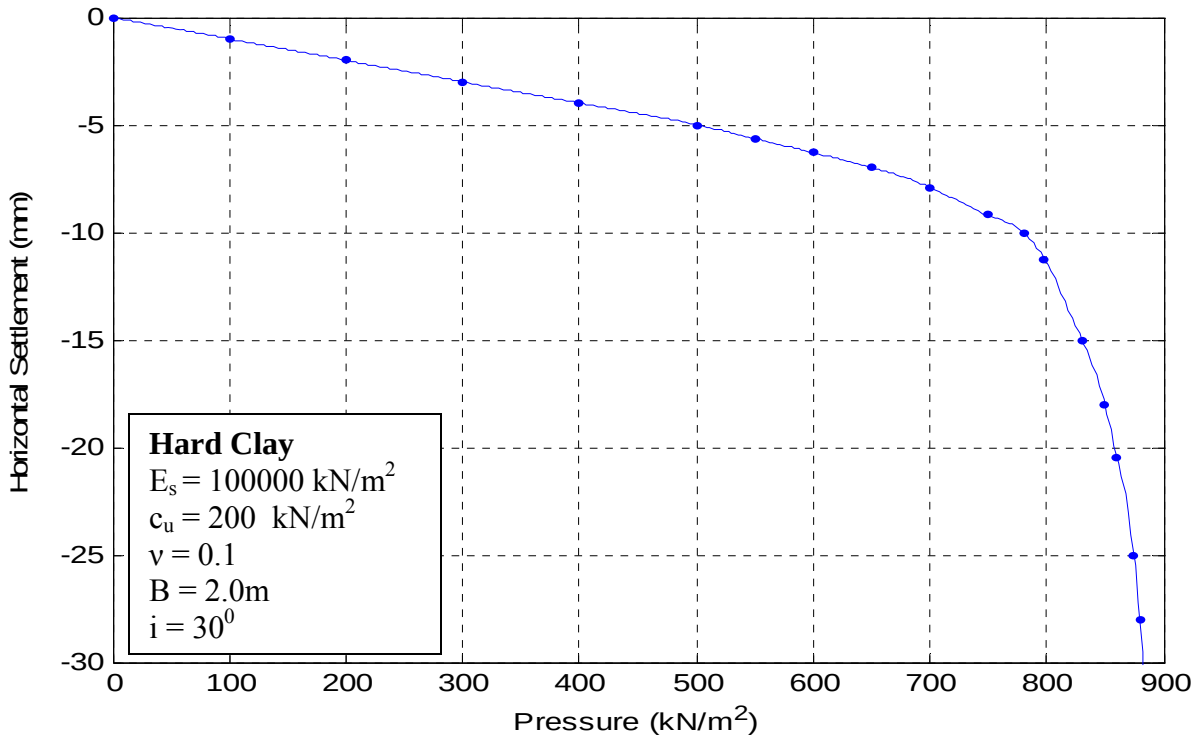

Figure 4.40, Pressure Vs Elasto-plastic Horizontal Settlement Curve of Strip Footing under Centrally Inclined Load

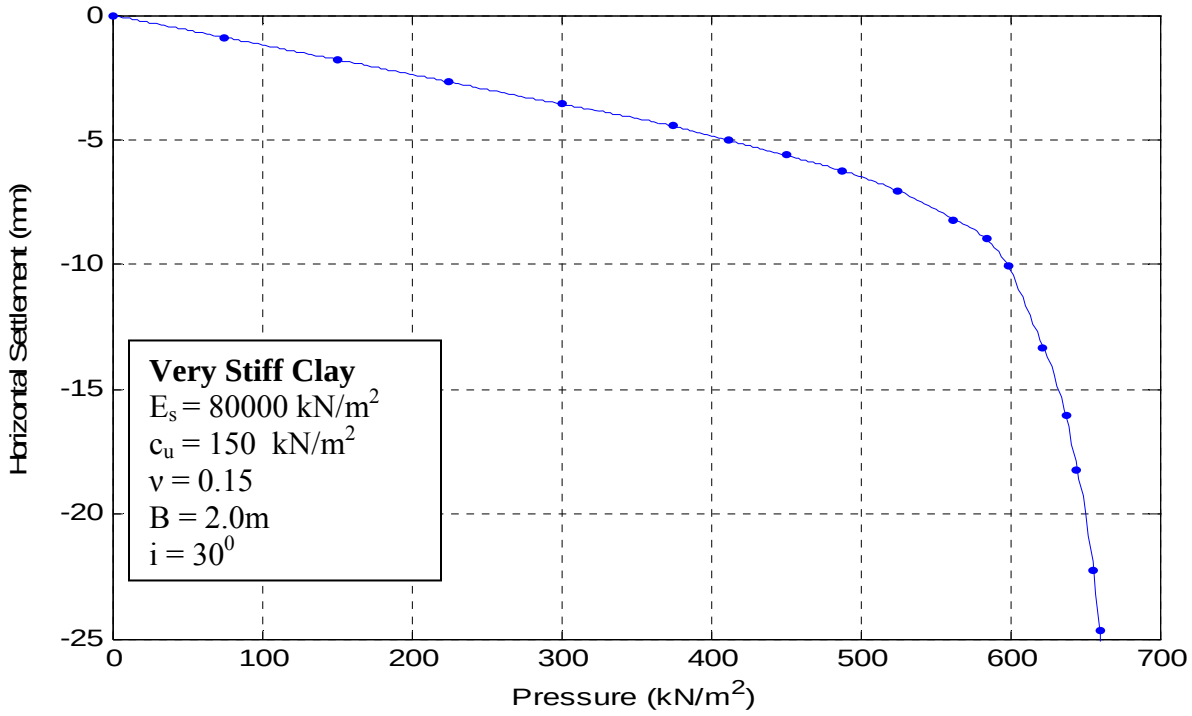

Figure 4.41, Pressure Vs Elasto-plastic Horizontal Settlement Curve of Strip Footing under Centrally Inclined Load

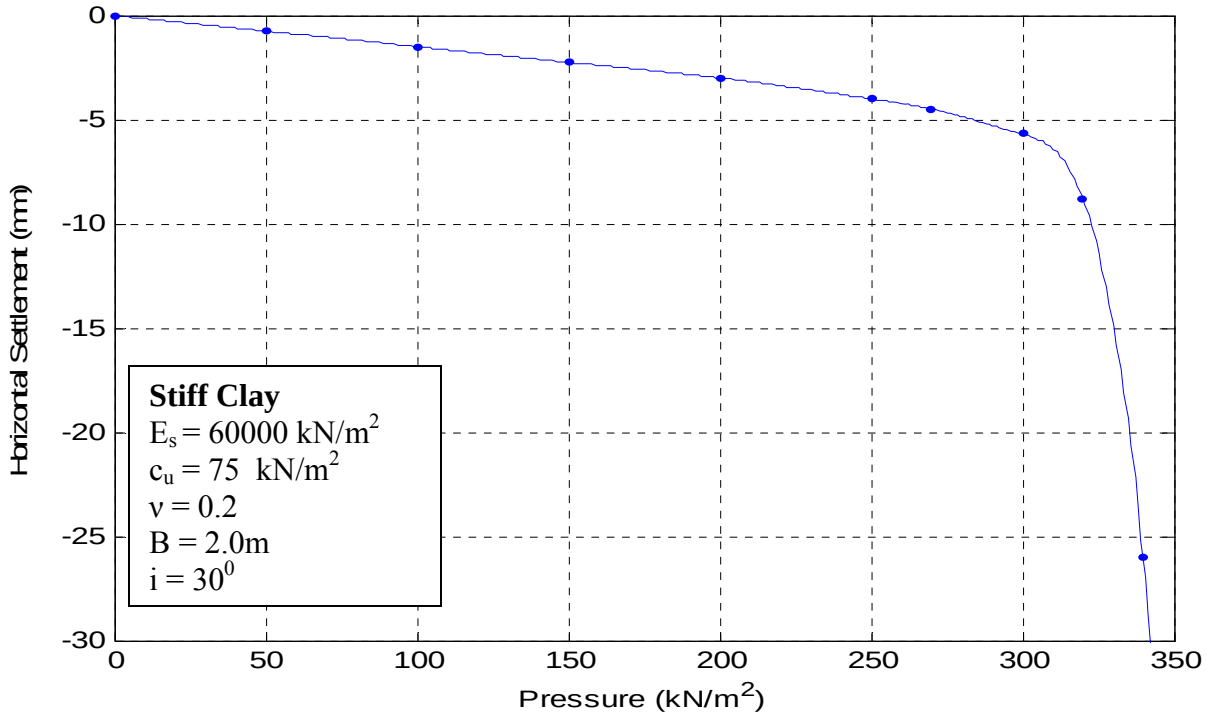

Figure 4.42, Pressure Vs Elasto-plastic Horizontal Settlement Curve of Strip Footing under Centrally Inclined Load

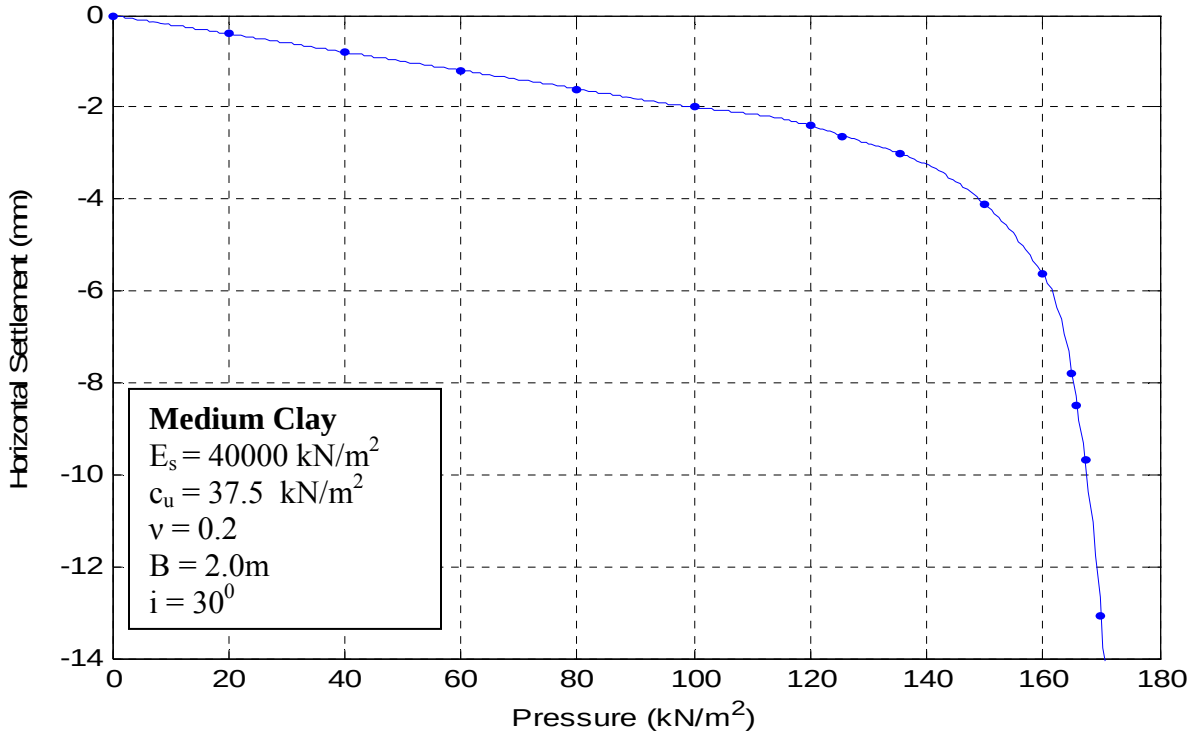

Figure 4.43, Pressure Vs Elasto-plastic Horizontal Settlement Curve of Strip Footing under Centrally Inclined Load

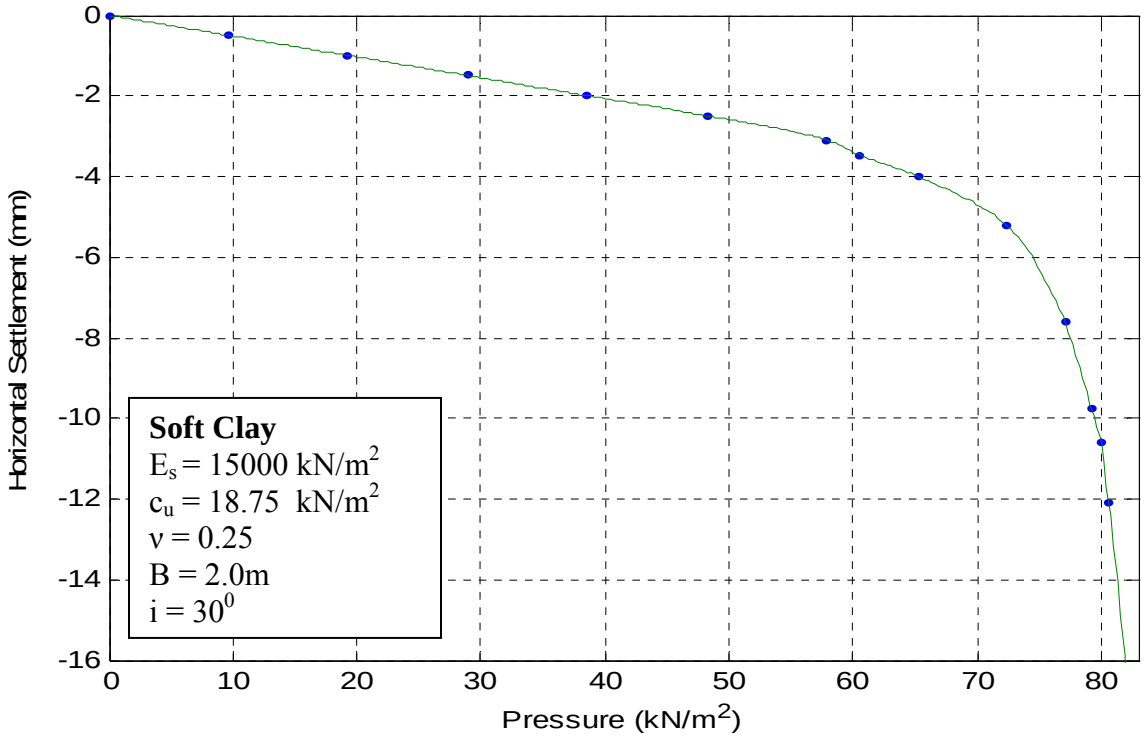

Figure 4.44, Pressure Vs Elasto-plastic Horizontal Settlement Curve of Strip Footing under Centrally Inclined Load

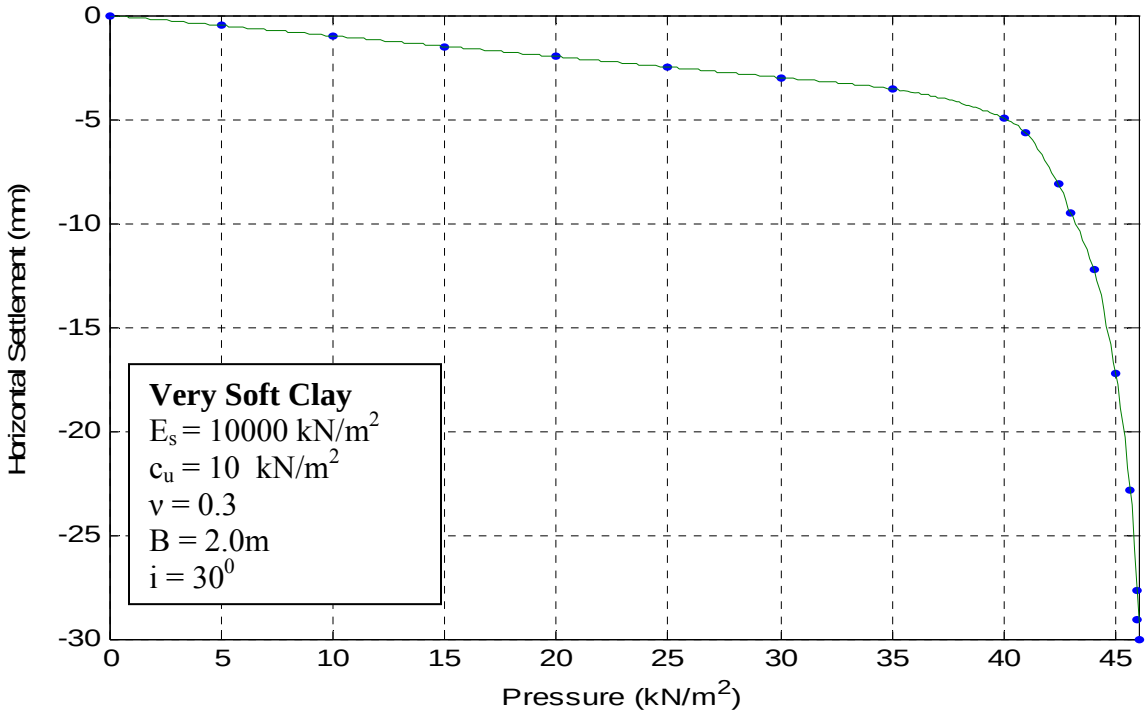

Figure 4.45, Pressure Vs Elasto-plastic Horizontal Settlement Curve of Strip Footing under Centrally Inclined Load

4.4.2 Pressure vs Elasto-Plastic Horizontal Settlement Characteristics

Pressure versus horizontal displacement plots for the strip footing for six different states of consistency of clay corresponding to load inclination i = 10^0, 20^0, 30^0.

Similarly to the pressure-vertical settlement characteristics, the change of average horizontal displacement is less at the low pressure but at he pressure increases and approaches the failure, the horizontal displacements increase rapidly. This is indicated by the quite smooth graph at low-pressure, and curves suddenly drop down as the failure is approached.

From these graph, it can also be seen that as the inclination of load increases, the horizontal displacements at the failure also increase. This is obvious because by increasing the inclination of loading towards horizontal, the component of horizontal load which is acting on the soil mass also increases. For the same inclination of load, the values of the horizontal displacement decrease as the soil consistency changes from hard to very soft. The horizontal displacements, at the same level of pressure for the same load inclination of loading, increase as the consistency of clay decreases.

4.4.3 Settlement Profiles of Footing

The nodal points which represent the loaded nodes are 5 nodal points. The direction of loading in the modal is given towards the right side of footing from the center line.

In order to understand whether the strip footing behaves as a rigid footing or as a flexible footing, the vertical settlement profiles of the footings have been plotted. Fig 4.46 a to 4.46 *l* show the vertical settlement profiles for the case of strip footing on hard clay carrying central vertical load (i = 0^0) corresponding to various load increments. It can be seen from these plots that:

(i) Settlement profile of the footing is symmetric non-uniform

(ii) The profile is parabolic in shape for the first few load increments, and

(iii)The parabolic profile changes to trapezoidal profile at higher pressure intensities.

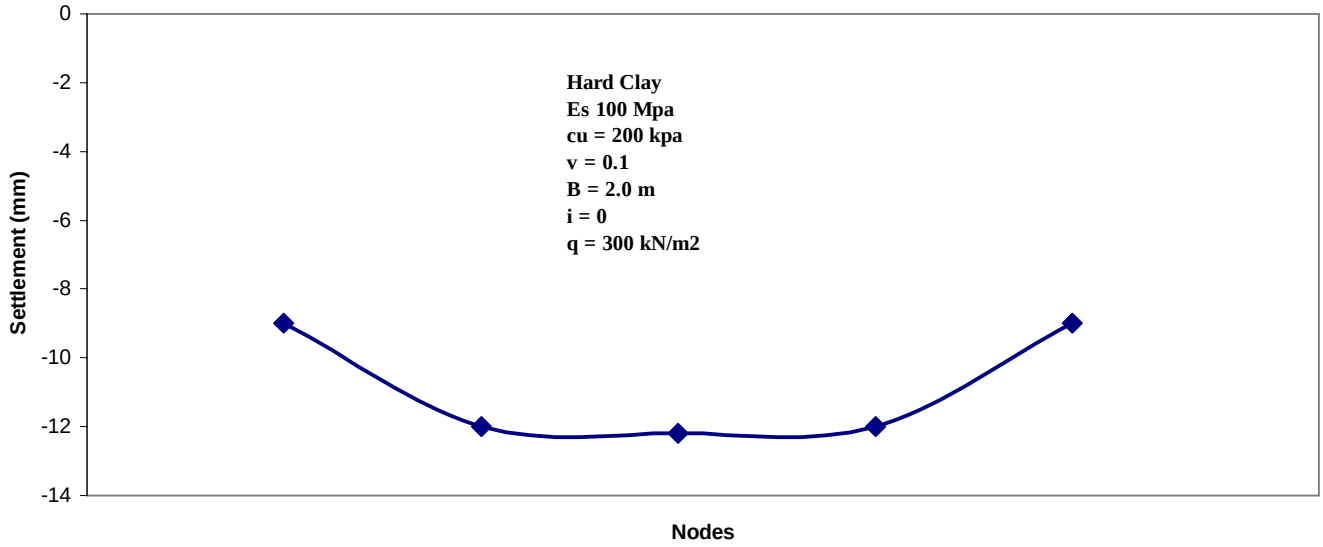

Figure 4.46, Settlement Profile of Footing under Centrally Vertical Loading

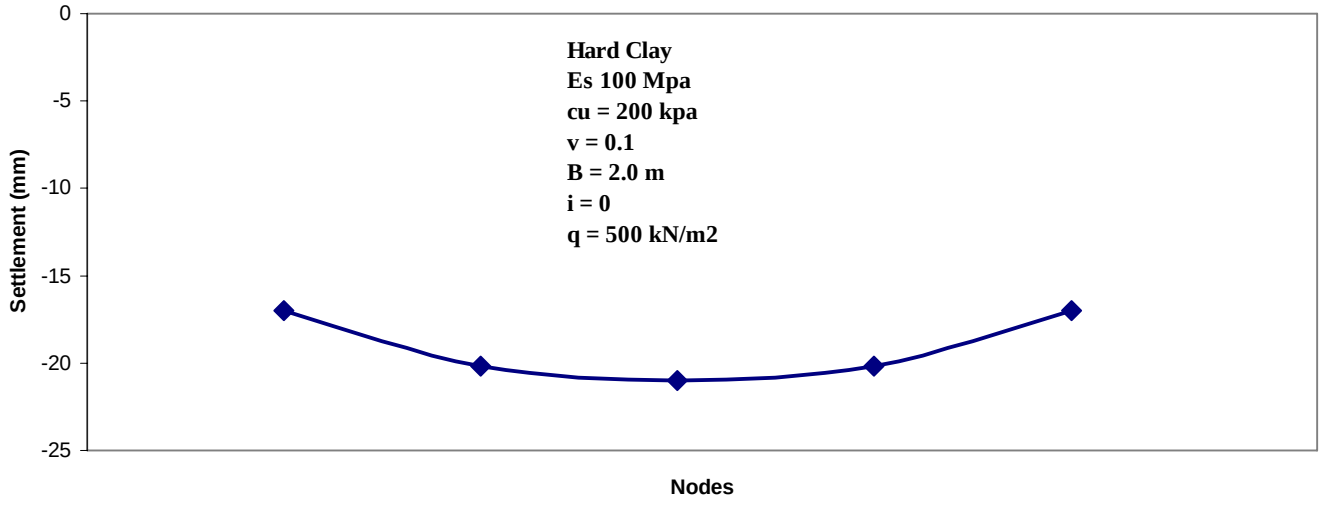

Figure 4.47, Settlement Profile of Footing under Centrally Vertical Loading

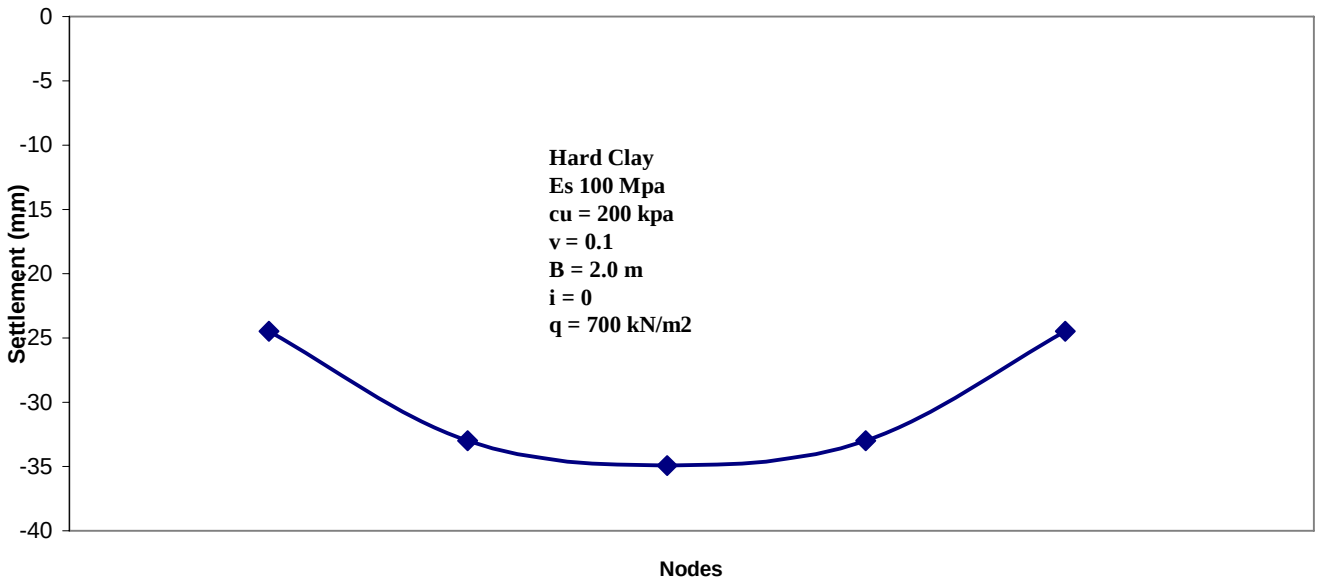

Figure 4.48, Settlement Profile of Footing under Centrally Vertical Loading

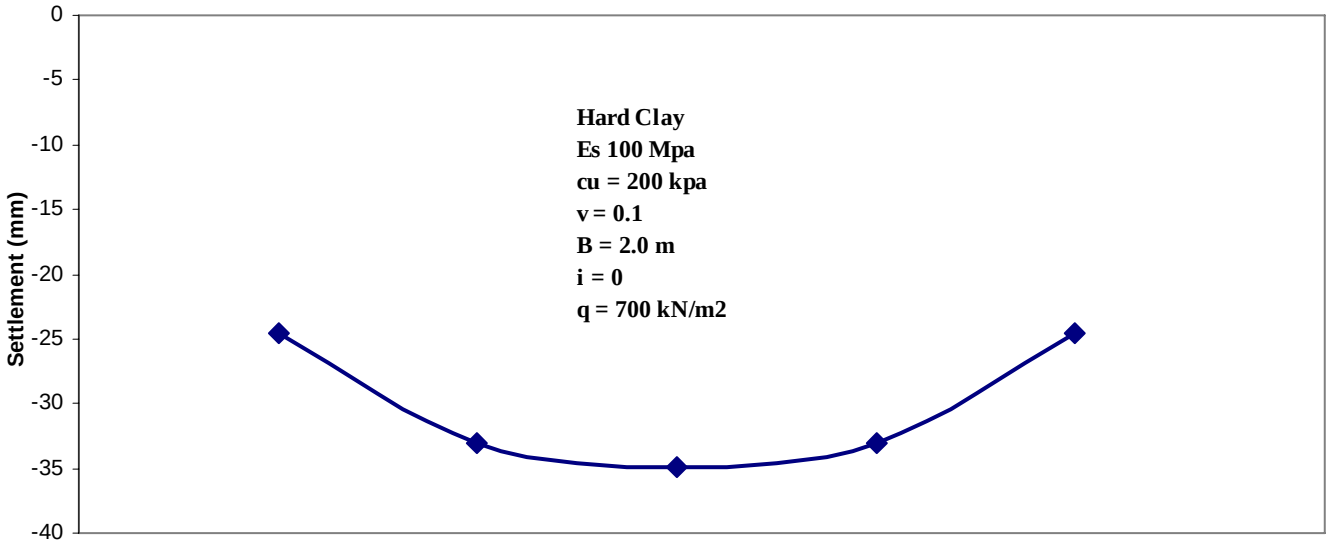

Figure 4.49, Settlement Profile of Footing under Centrally Vertical Loading

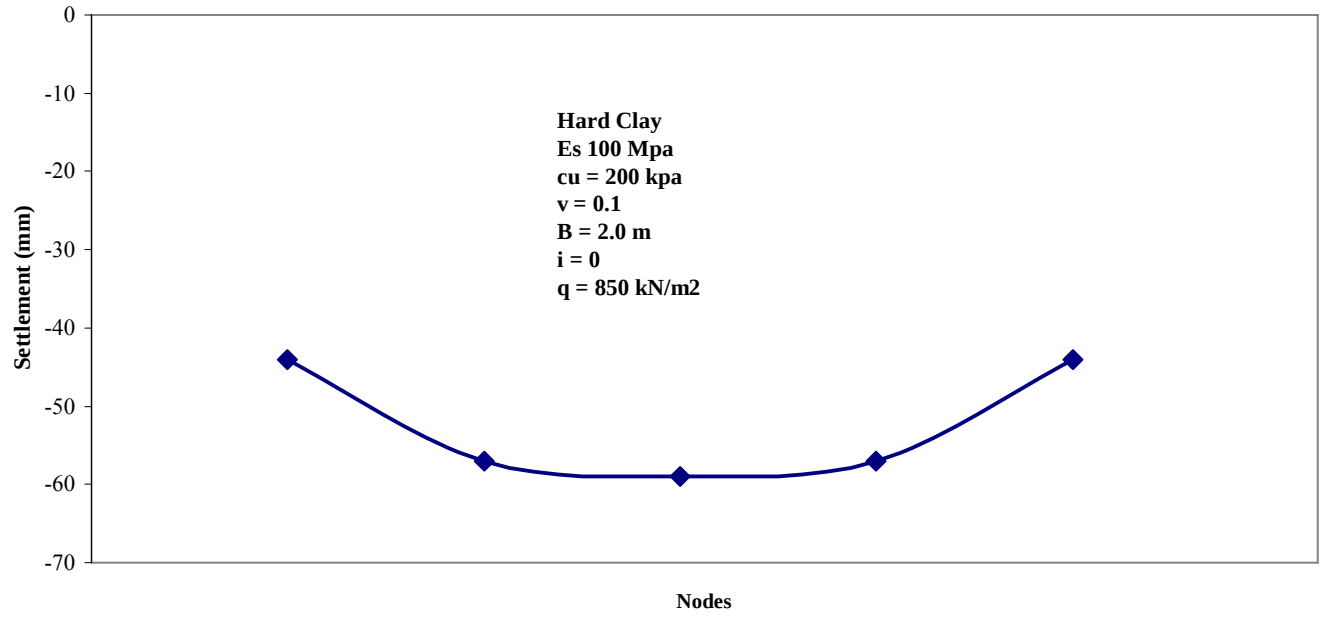

Figure 4.50, Settlement Profile of Footing under Centrally Vertical Loading

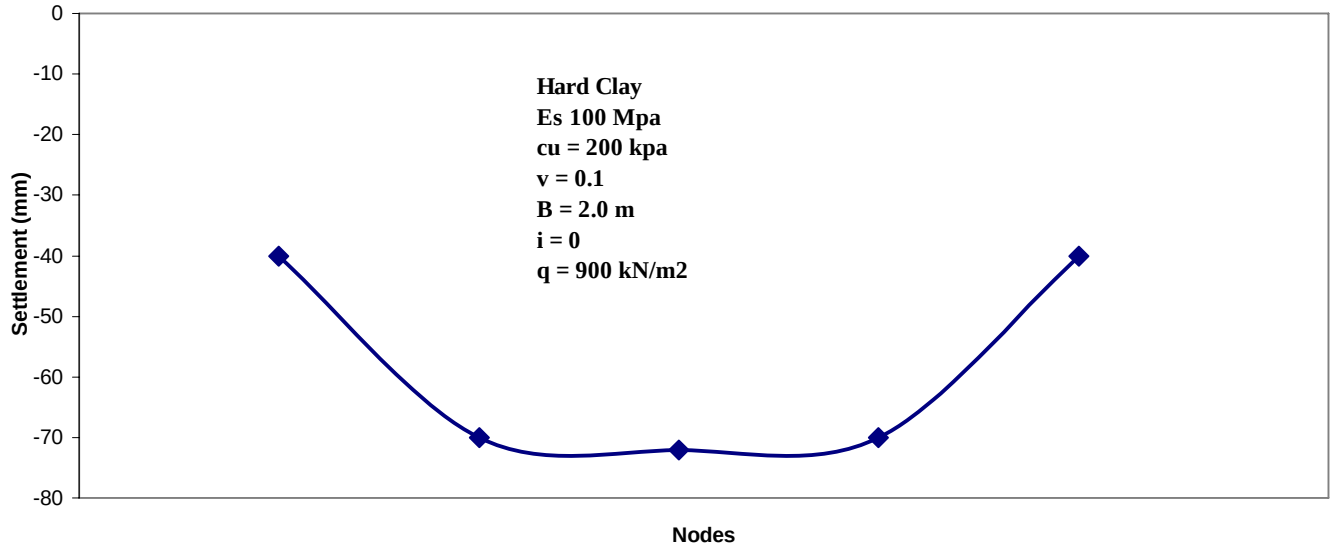

Figure 4.51, Settlement Profile of Footing under Centrally Vertical Loading

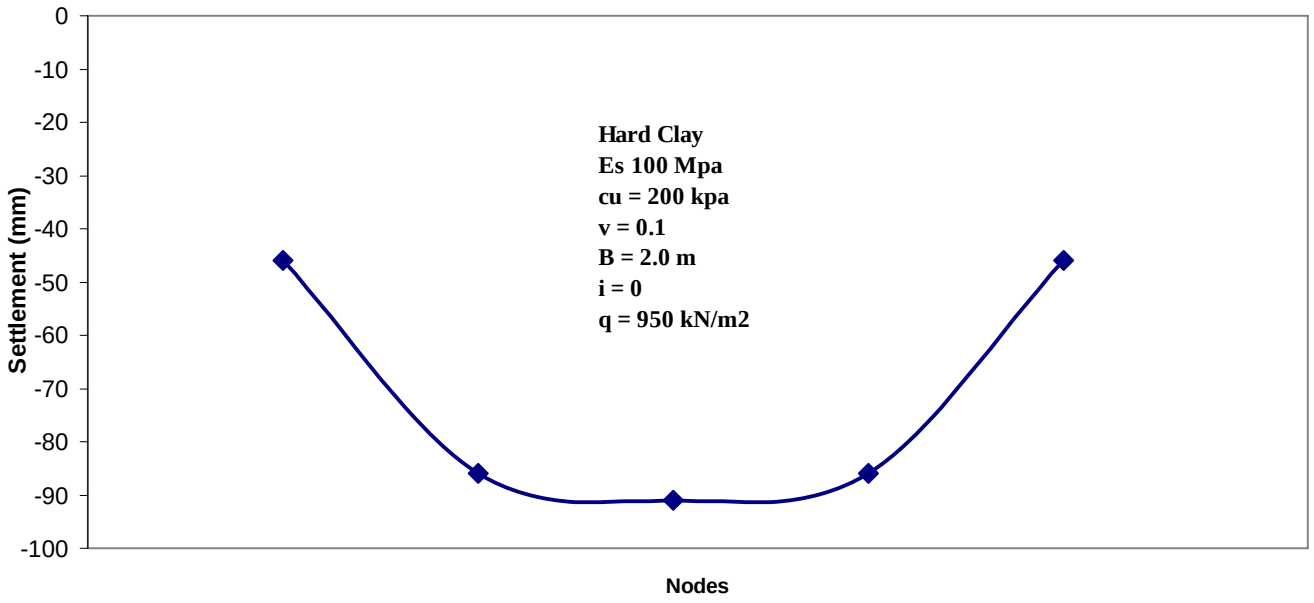

Figure 4.52, Settlement Profile of Footing under Centrally Vertical Loading

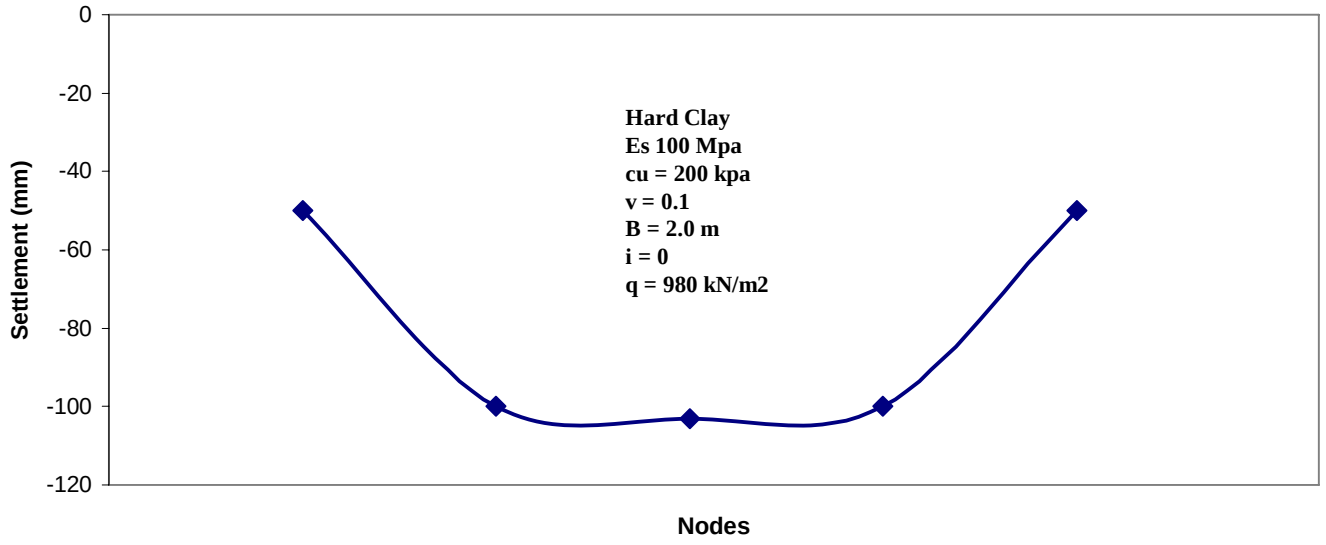

Figure 4.53, Settlement Profile of Footing under Centrally Vertical Loading

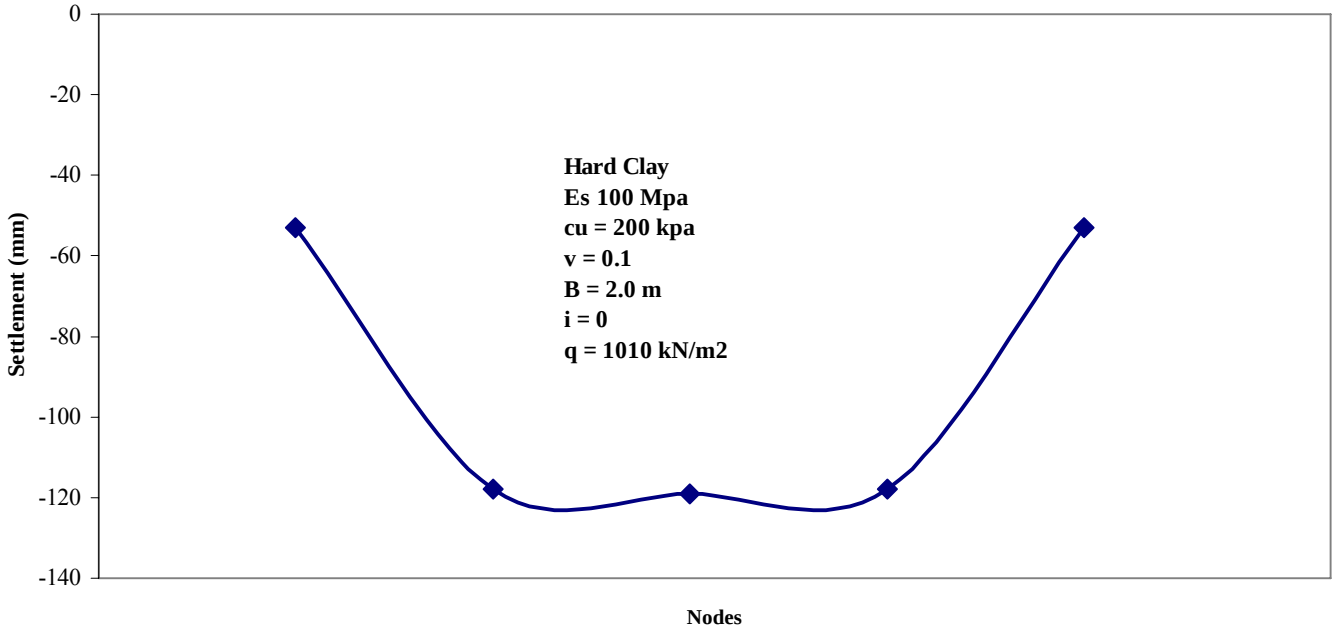

Figure 4.54, Settlement Profile of Footing under Centrally Vertical Loading

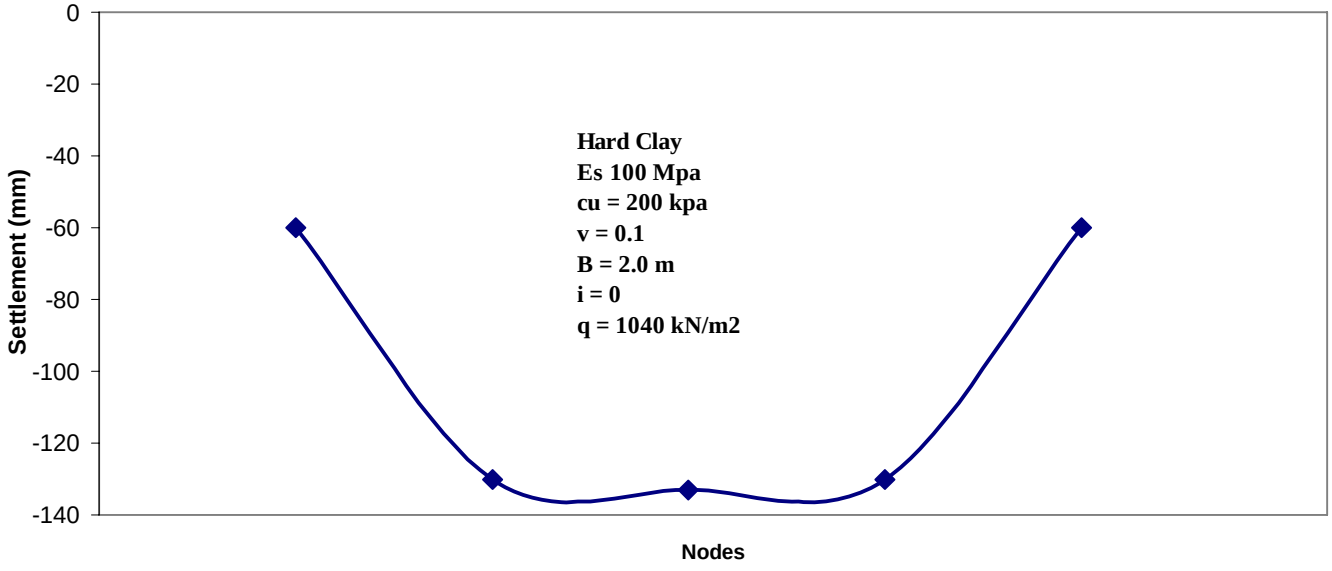

Figure 4.55, Settlement Profile of Footing under Centrally Vertical Loading

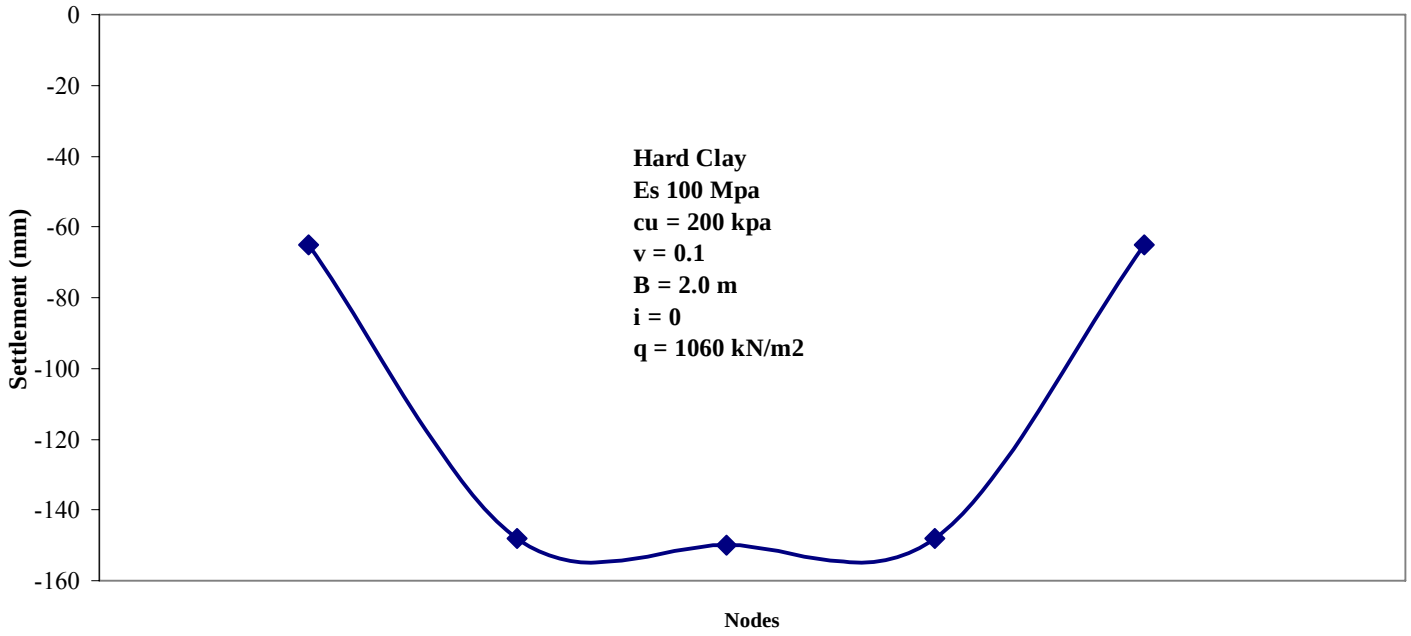

Figure 4.56, Settlement Profile of Footing under Centrally Vertical Loading

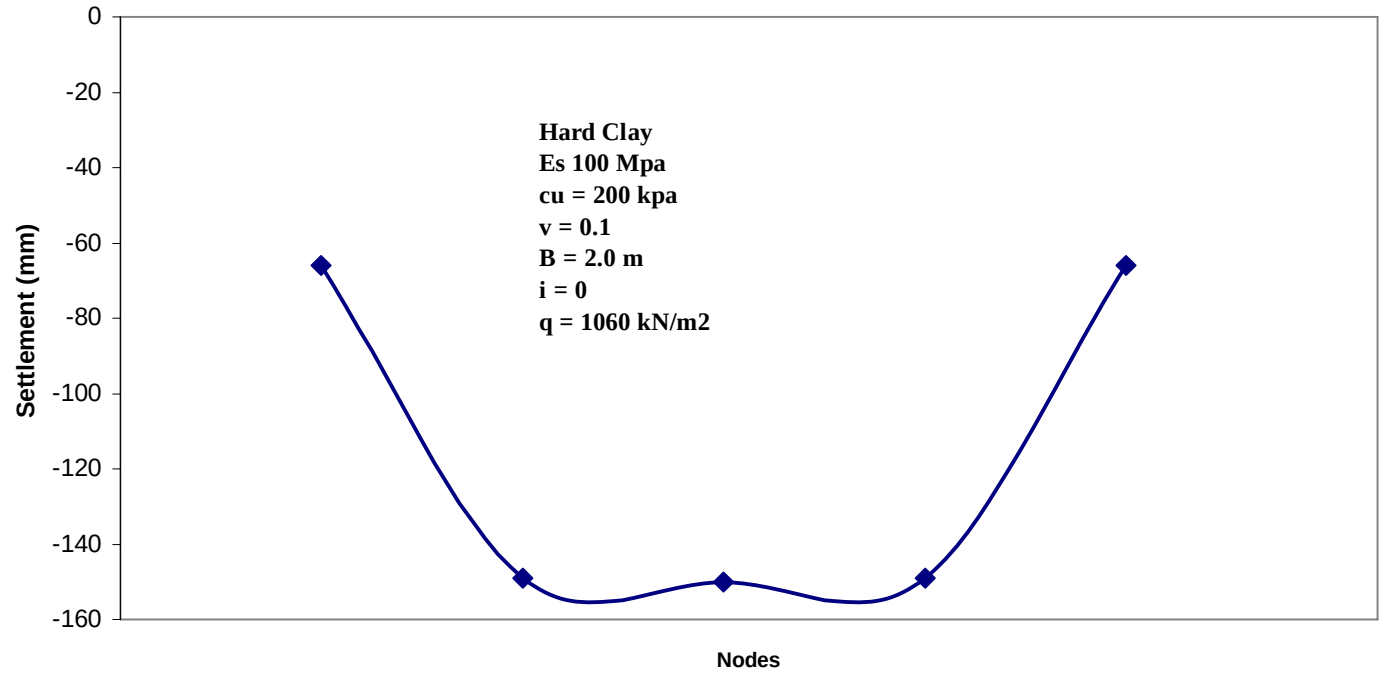

Figure 4.57, Settlement Profile of Footing under Centrally Vertical Loading

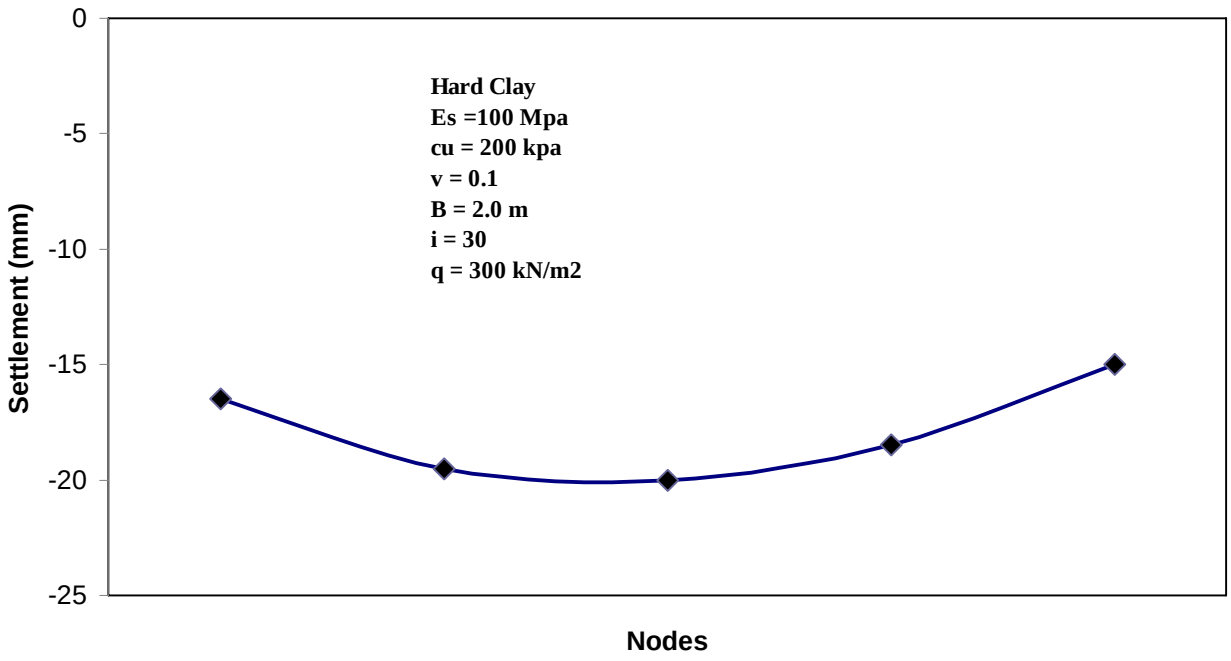

Figure 4.58, Settlement Prifile of Strip Footing under Centrally Applied Inclined Loading

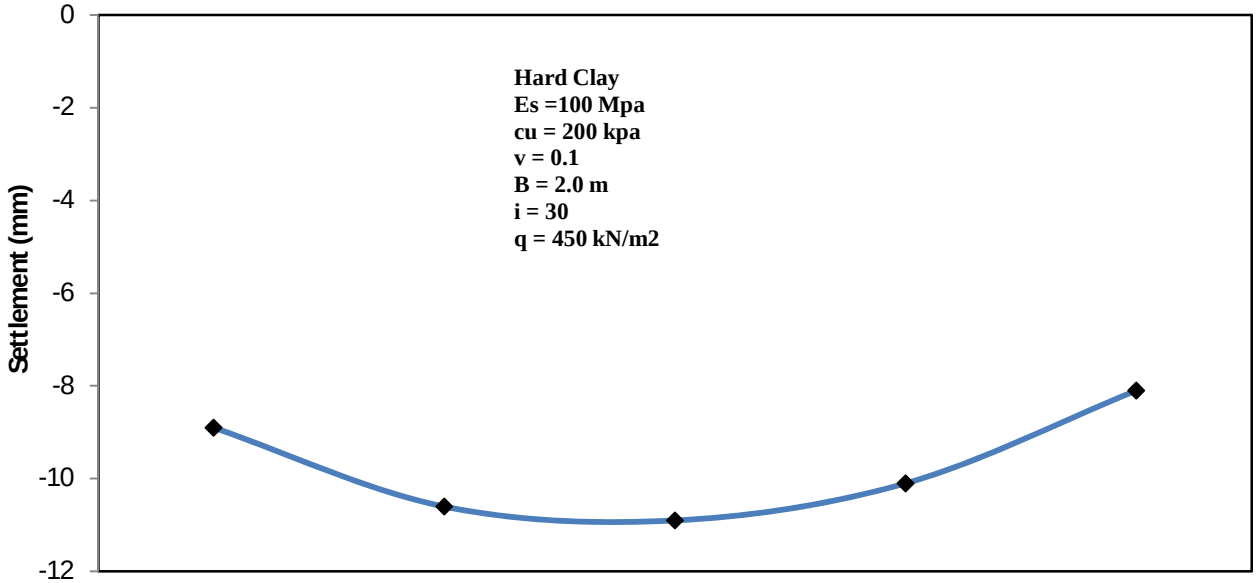

Figure 4.59, Settlement Prifile of Strip Footing under Centrally Applied Inclined Loading

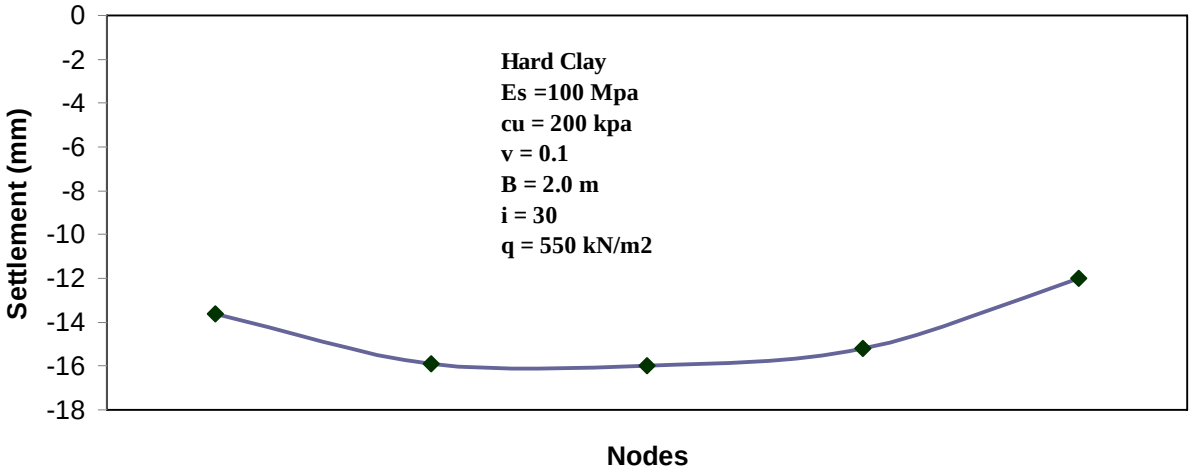

Figure 4.60, Settlement Prifile of Strip Footing under Centrally Applied Inclined Loading

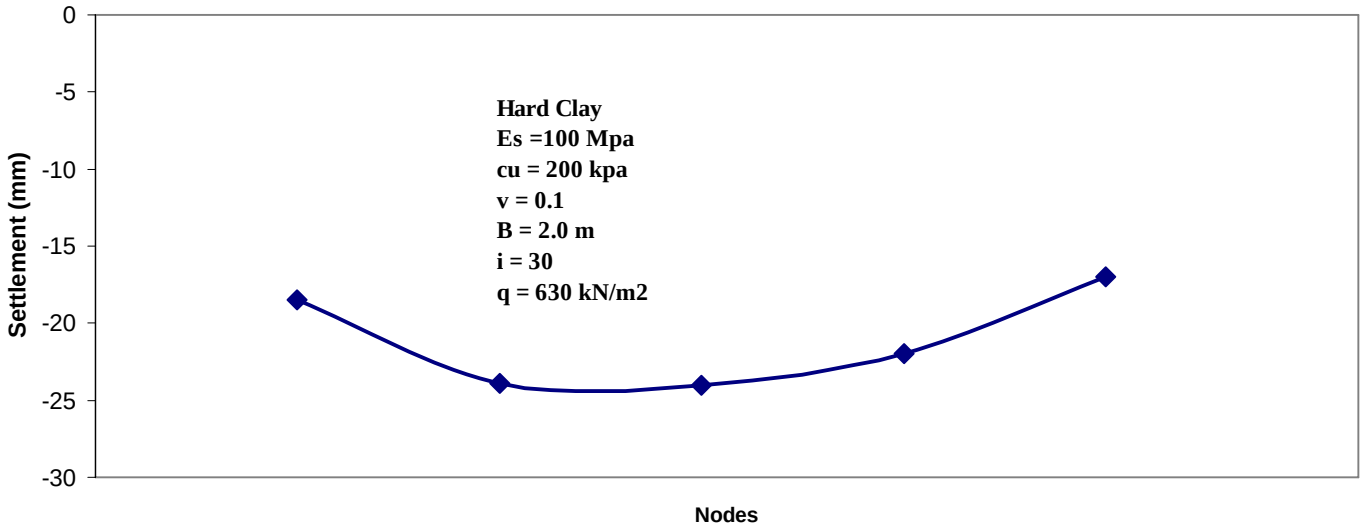

Figure 4.61, Settlement Prifile of Strip Footing under Centrally Applied Inclined Loading

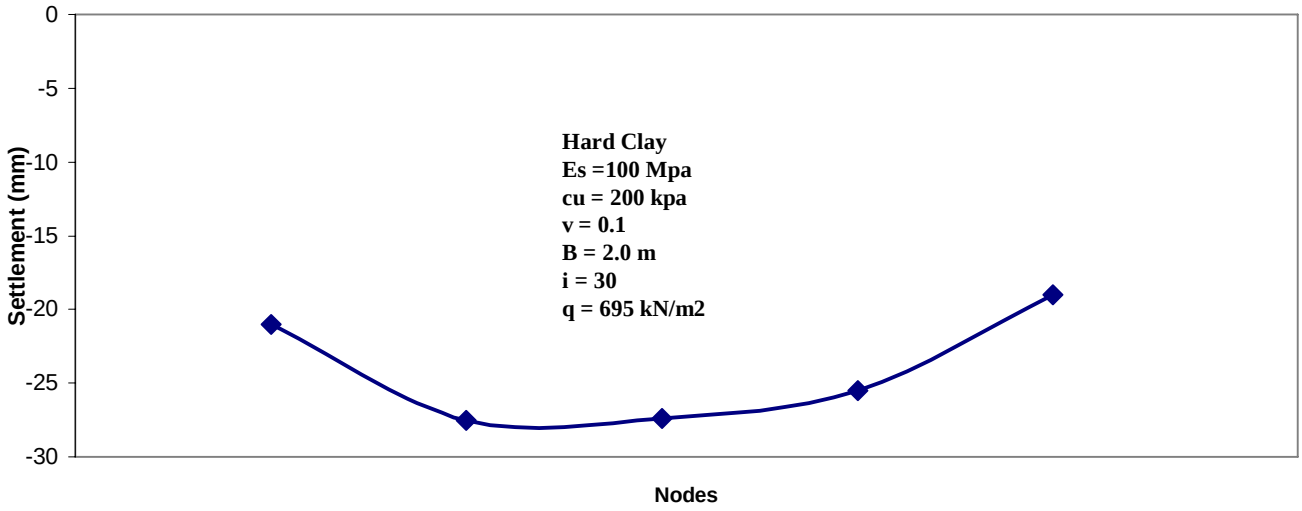

Figure 4.62, Settlement Prifile of Strip Footing under Centrally Applied Inclined Loading

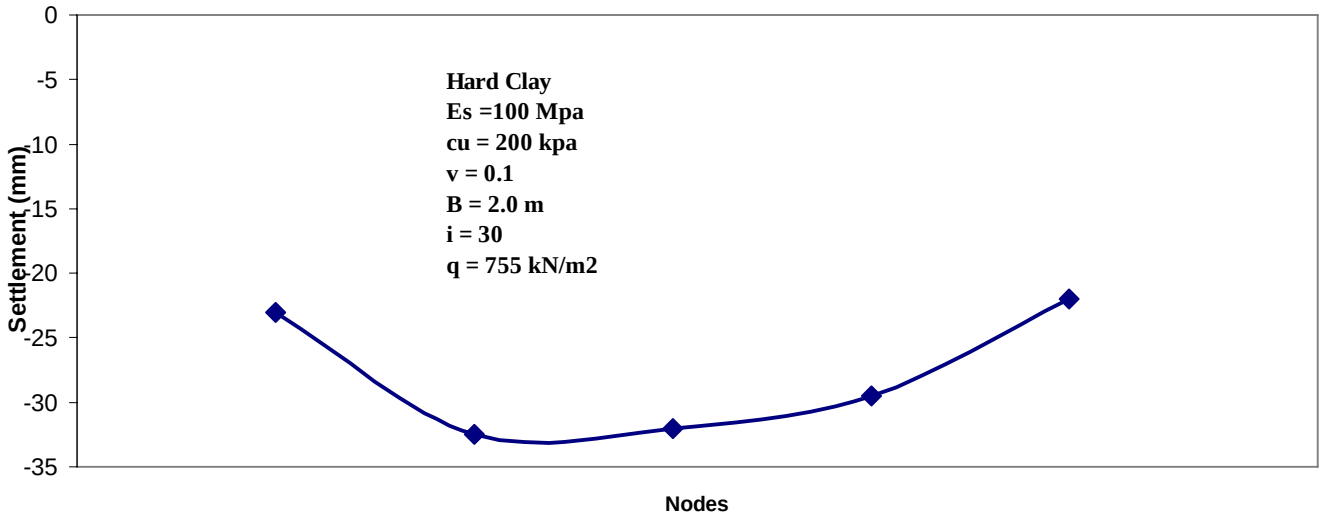

Figure 4.63, Settlement Prifile of Strip Footing under Centrally Applied Inclined Loading

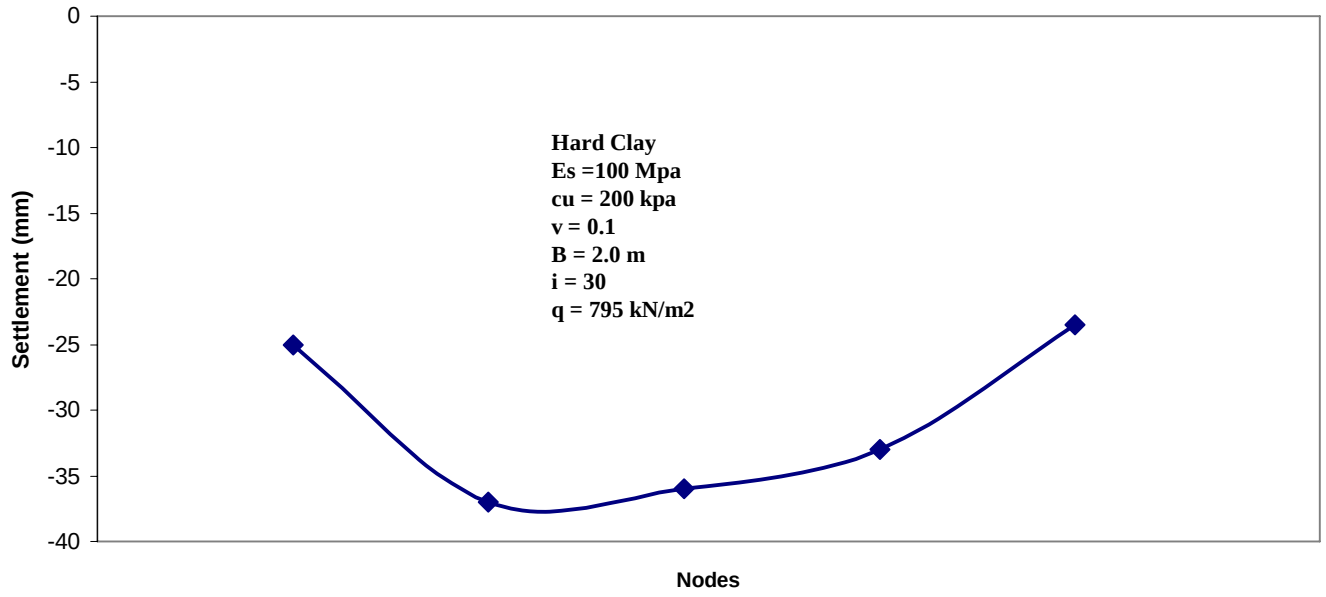

Figure 4.64, Settlement Prifile of Strip Footing under Centrally Applied Inclined Loading

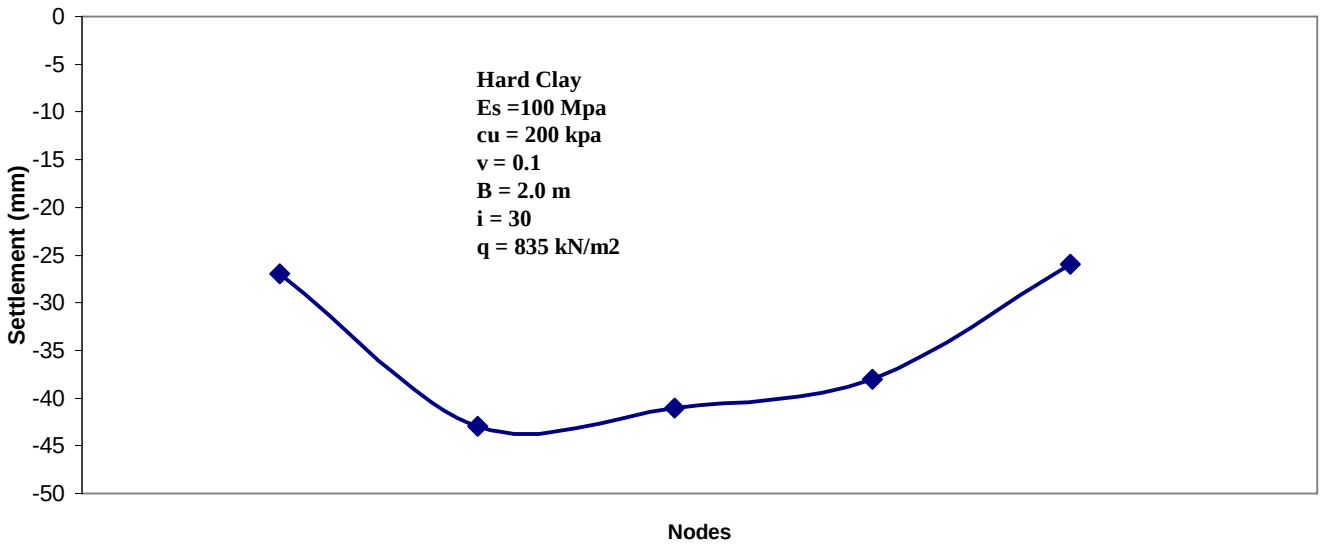

Figure 4.65 Settlement Prifile of Strip Footing under Centrally Applied Inclined Loading

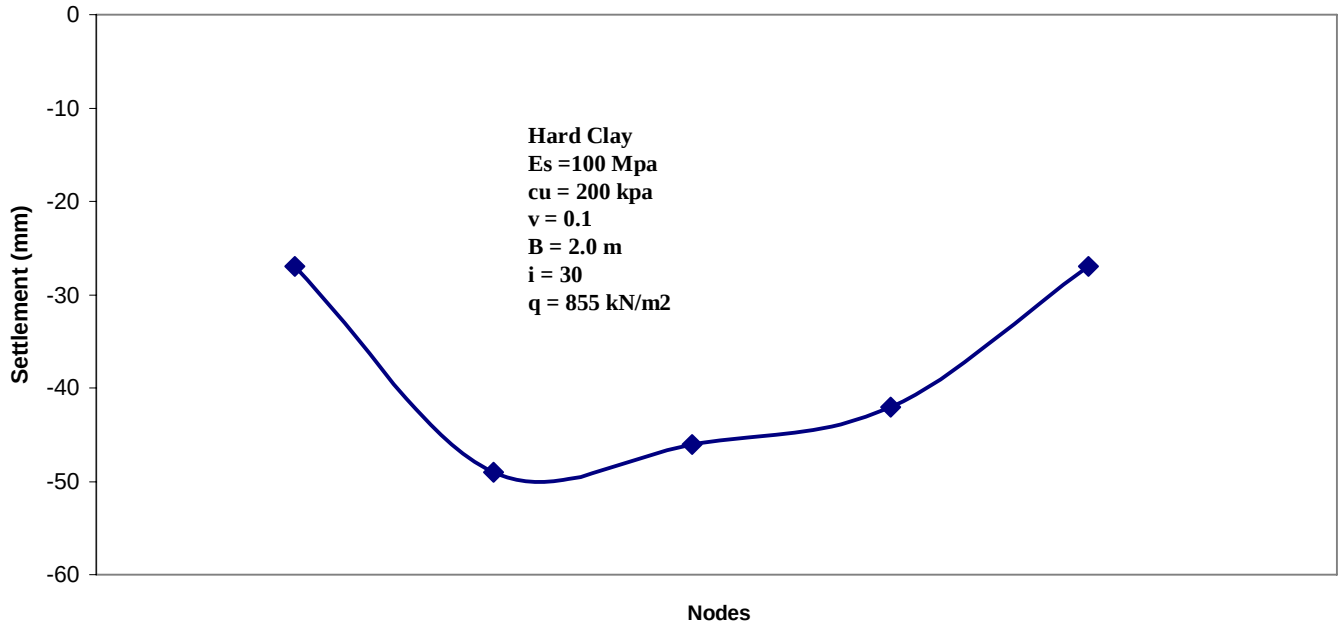

Figure 4.66 Settlement Prifile of Strip Footing under Centrally Applied Inclined Loading

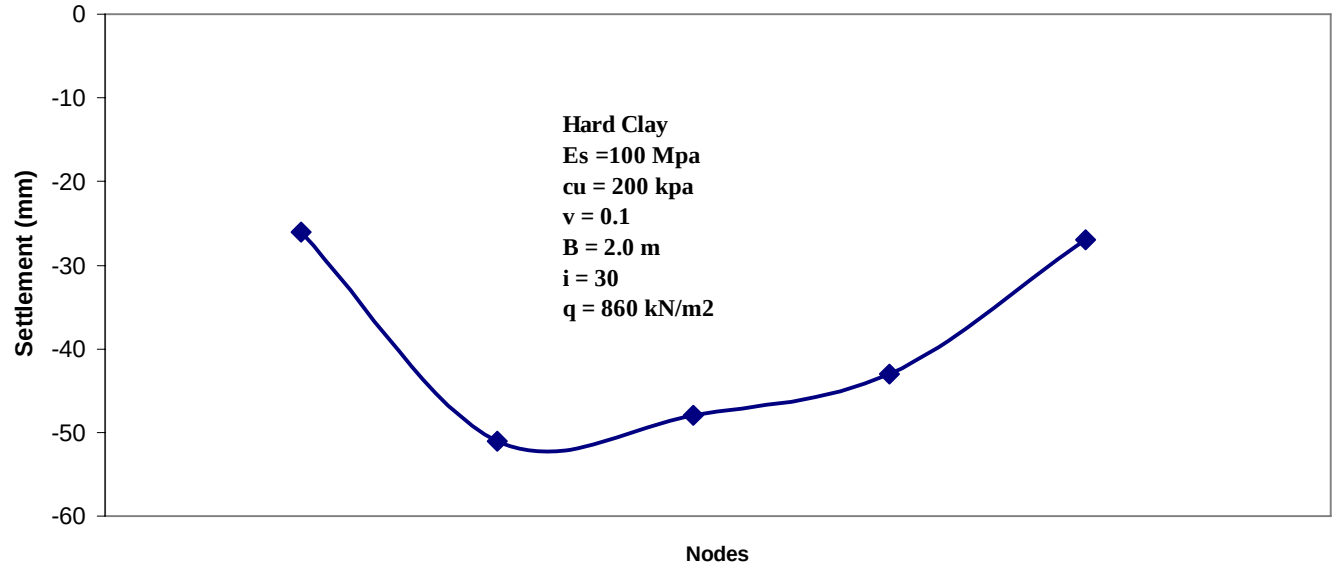

Figure 4.67 Settlement Prifile of Strip Footing under Centrally Applied Inclined Loading

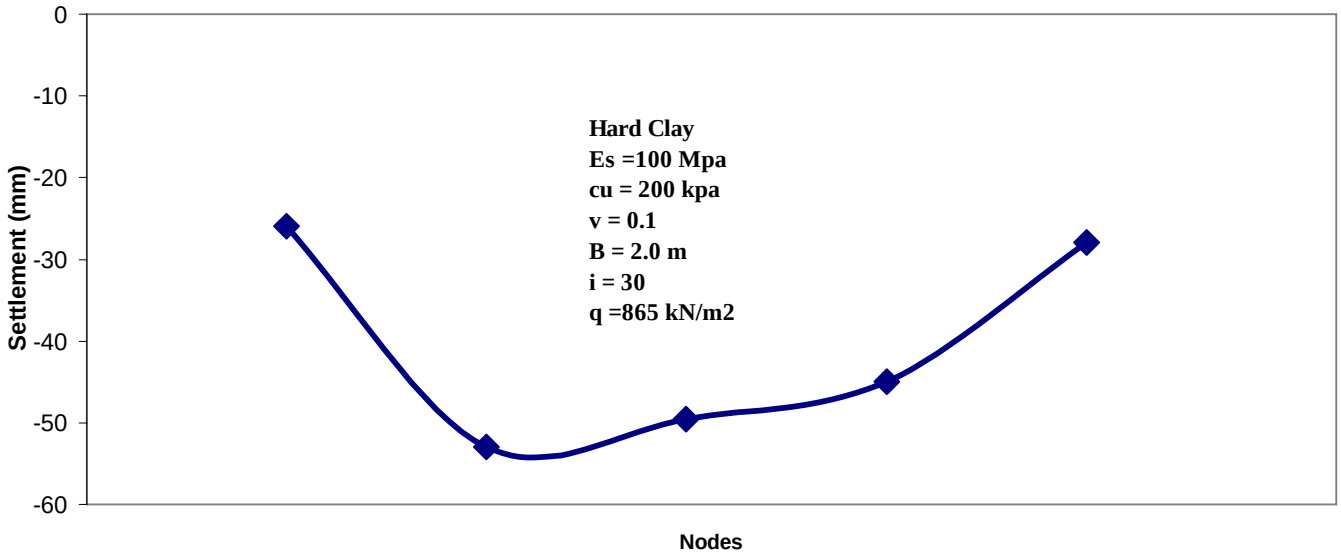

Figure 4.68 Settlement Prifile of Strip Footing under Centrally Applied Inclined Loading

However, the settlement profiles for the same strip footing on hard clay, when plotted for various load increments corresponding to load inclination i = 30^0, and i = 30^0, (Figure 4.42 a to 4.42 k) show that:

(i) Settlement profile is symmetric non-uniform

(ii) The profile is parabolic in shape for the first few load increments

(iii) The profile pattern for higher pressure increments no more remains parabolic, and gets distorted.

(iv) The maximum settlement occurs not below the point of application of inclined load, but the point at which maximum settlement occurs moves in the direction of the load inclination.

4.4.4 Comparison of N_c values

The bearing capacity factor, N_c corresponding to cohesion of the strip surface footing resting on clay ($\Phi = 0$) and carrying the inclined load has been obtained by dividing the ultimate load at soil bearing failure by the corresponding value of undrained cohesion c_u. The values N_c for various inclinations of loading and clay consistency can be seen in Table.4.2. The values of N_c

Under vertical load (i = 0) range from 5.000 to 4.144. These well compared with Prandtl Theory (N_c = 5.14), Meyerhof Theory (N_c = 5.14), Skempton Theory (N_c = 5.14), or Teraghi Theory (N_c = 5.14). The values obtained by using this elasto-plastic finite element analysis are little on the lesser side.

It can be seen that the N_c values for the values of i >0 decreases with the increase in the load inclination. These values and tendency are agree with the results obtained from experiments results by Saran and Agrawal, 1986. The values obtained from experimental results for inclined loading (e/B = 0, $\Phi = 0$) are:

for $i = 10^0$ $N_c = 5.00$

for $i = 20^0$ $N_c = 3.33$

for $i = 30^0$ $N_c = 3.077$

The values obtained in present study are lesser for $i = 10^0$, and somewhat bigger for $i > 10^0$.

Table 4.2 Values of Bearing Capacity and N_c Values Obtained

$i = 0^0$

Consistency of Clay	**Hard**	**Very Stiff**	**Stiff**	**Medium**	**Soft**	**Very Soft**
C_u (Kpa)	200	150	75	37.5	18.75	10
$q_{failure}$(kN/m^2)	1060	795	400	205	100	53
$q_{ultimate}$ (kN/m^2)	1025	750	385	192	94	50
N_c factor	5.125	5	5.133	5.12	5.013	5

$i = 10^0$

Consistency of Clay	**Hard**	**Very Stiff**	**Stiff**	**Medium**	**Soft**	**Very Soft**
C_u (Kpa)	200	150	75	37.5	18.75	10
$q_{failure}$(kN/m^2)	995	730	375	183	92.5	49.5
$q_{ultimate}$ (kN/m^2)	880	650	340	170	83	44
N_c factor	4.4	4.333	4.533	4.533	4.427	4.4

$i = 20^0$

Consistency of Clay	Hard	Very Stiff	Stiff	Medium	Soft	Very Soft
C_u (Kpa)	200	150	75	37.5	18.75	10
$q_{failure}$(kN/m^2)	925	700	365	173	86.5	46.5
$q_{ultimate}$ (kN/m^2)	810	625	325	159	80	42
N_c factor	4.05	4.167	4.333	4.24	4.267	4.2

$i = 30^0$

Consistency of Clay	Hard	Very Stiff	Stiff	Medium	Soft	Very Soft
C_u (Kpa)	200	150	75	37.5	18.75	10
$q_{failure}$(kN/m^2)	865	650	335	166	82	45.5
$q_{ultimate}$ (kN/m^2)	800	590	300	155	76	40
N_c factor	4	3.933	4	4.133	4.053	4

4.4.5 Influence of Load Inclination

It can be seen that as the inclination of load increases, the value o vertical settlement at the same level of pressure increases. This can be seen clearly in soil with low consistency, but in soil with

high consistency, this tendency can not be seen clearly. For the same inclination of loading, the settlement at the same level of pressure increases as the consistency of clay moves from higher consistency to lower consistency.

It can also be seen that as the load inclination increases, the horizontal displacement at failure is also increases.

4.5 CRITICAL COMMENTS

In general, it has been found that:

(i) The settlement profile of the strip footing is, in general, non-uniform and parabolic.

(ii) The strip footing on clay with different consistency behaves as a flexible footing.

(iii) As load inclination increases, the settlement profile becomes more unsymmetrical.

(iv) Ultimate load carrying capacity of the strip footing decreases with the increase in load inclination.

(v) The values of bearing capacity factor, N_c, lesser than those given by earlier investigators for $i \leq 10^0$, and somewhat bigger for $i > 10^0$.

CHAPTER-5
CONCLUSIONS

5.1 SUMMARY

The behavior of strip footing subjected to central loading has been studied by using elasto-plastic finite element analysis so as to obtain the ultimate bearing capacity, the pressure-vertical settlement characteristics the pressure-horizontal displacement characteristics, and the settlement profile. The investigation has been conducted for all states of clay consistency, and for various inclinations of load.

5.2 CONCLUSIONS

(i) Based on the results of analysis, the following conclusions have been drawn:
The ultimate bearing capacity of strip footing under inclined load decreases with load inclination .For the same inclination of load, the ultimate bearing capacity of soil decreases as the consistency of soil decreases.

(ii) By using the incremental elasto-plastic finite element analysis and the Von Mises criterion, the settlements of footing in every increment of load have been monitored and plotted. Typically, it has been found that the increase of vertical displacement is less at the low pressure intensity. But as the bearing failure of soil approaches, the displacements rapidly increase.

(iii) The bearing capacity factor, N_c value, decreases with increasing of load inclination. The N_c values from finite element analysis have been compared with experimental results of Saran and Agrawal (1986), and these values lesser for $i \leq 10^0$, and somewhat bigger for $i > 10^0$.

(iv) The profile of the settlement of the footing indicates that footing behaves as a flexible footing. At the 0^0 of loading the maximum value of displacement occurs in the centre point of footing. At the initial stage of loading, the settlement profile is smooth parabolic, and then finally becomes more asymmetric curve when the soil failure approaches.

5.3 SCOPE FOR FURTHER RESEARCH

(i) Finite element analysis can be carried our for other type of soil (non-cohesive soil) with other relevant yield criteria such as Mohr-Coulomb, Tresca Criteria and using the critical state model.

(ii) The analysis can also be done by taking the eccentricity of loading into account.

(iii) A more reliable model in the finite element analysis would be, the analysis of footing embedded in soil mass, and with the joint element between the footing and the soil. The interface behavior can alter the results. True interaction can be represented only when interface behavior is taken into account.

(iv) Further studies could be done on the strip footing resting on clay stabilized with geogrids.

REFRENCE

1. **Agrawal, R. K.** (1986); "Behaviour of Shallow Foundation Under Eccentric-Inclined Loads", *Ph.D. Thesis*, Civil Engineering, University of Roorkee, Roorkee.
2. **Brinch Hansen, J.** (1970). "A revised and extended formula for bearing capacity." *DGI Bull. No.* 28, Danish Geotech. Inst., 5-11.
3. **Duncan, J.M. and Chang, C.Y.** (1970) *"Nonlinear analysis of stress and strain in soils",* Proc. ASCE, Journal of the Soil Mechanics and Foundation Engineering Division, 96 (SM5): pp 1629-1653
4. **Dalia Youssef Abdel Masseh, Elias-Al-Hashem & Abdul Hamid Soulra**,(2005); "Bearing Capacity of Eccentrically or Obliquely Loaded Strip footing Over Two-layer Foundation Soil by Kinematical Approach", *VIII International Conference on Computational Plasticity*
5. **Gopal Ranjan; Rao, A. S.** (2000); "Basic and Applied Soil Mechanics" *New Age International Limited*, New Delhi, India.
6. **G.T Houlsby & A. M. Purzin**, (1998); "The Bearing Capacity of a Strip Footing on Clay Under Combined Loading", *The Royal Society*, Oxofrd University (U.K.)
7. **Jean-Louis Bariaud** (2005); "Spread Footings in Clay: Load Settlement Curve Approach", *Department of Civil Engineering*, Texas
8. **Meyerhof, G. G.** (1953); "The Bearing Capacity of Foundations Under Eccentric and Inclined Loads", *Proceedings 3rd International Conference Soil Mechanics and foundation Engineering, Zurich*, volume, pp (440-445).
9. **Patra, C. R.; Das, B. M.; Shin, E. C.** (1995); "Ultimate Bearing Capacity of Eccentrically Loaded Strip Foundation of Sand Reinforced with Geogrids", *Paper presented in Internatonal Symposium on Tsunami reconstruction with Geosynthetics*, Bangkok.
10. **Prakash, C.** (1975); "Behavior of Eccentrically Loaded Footing on Clay" , *M.E. Thesis* , Civil Engineering Department, University of Roorkee
11. **Prakash S, Gopal Ranjan & S Saran** (1979) "Analysis and Design of Foundation and Retaning Structures" *Sarita Prakashan Merrut*.
12. **Prandtl, L.** (1920) *Uber die harte plastischer korper.* Nachr. K. Ges. Wiss. Gott., Math-Phys. Kl., 74-85.

13. **Professor John Carter** et al(2001) ; “Foundation response”, *Research report,* University of Sydney
14. **Saran, Swami** (1996); “Analysis and Design of Substructures – Limit State Design” *Oxford & IBH publishing Co Pvt. Ltd, New Delhi,* India
15. **Salencon, J., and Peeker, A**. (1995a). "Ultimate bearing capacity of shallow foundations under inclined and eccentric loads. Part I: Purely cohesive soil." *Eun J.Mech. A/Solids*, 14(3), 349-375.
16. **Salencon, J., and Peeker, A**. (1995b). "Ultimate bearing capacity of shallow foundations under inclined and eccentric loads. Part II: Purely cohesive soil without tensile strength." *Eur*. J. *Mech. A/Solids, 14(3),*377-396.
17. **S. K. Bose & S. C. Das**, (1997); ”Nonlinear Finite Element Analysis of Stresses and Deformation Beneath Rigid Footing” *Journal of Computers & Structures*, Volume 62, No. 3 PP 482 -492
18. **Terzaghi, K**. (1943). *Theoretical soil mechanics.* John Wiley & Sons, Inc.,New York, N.Y.
19. **Vesic, A. S**. (1975). "Bearing capacity of shallow foundations." *Foundation engineering handbook,* H. F. Winterkorn and H. Y. Fang, eds., Van Nostrand Reinhold, New York, N.Y., 121-145.
20. **Zienkiewicz**, **O. C**. (1983). *The finite element method.* McGraw-Hill Book Co., Inc., New York, N.Y